Die Rolle von Serin-Threonin-Kinasen für epitheliale Transportvorgänge
The role of serine-threonine-kinases in epithelial transport

DISSERTATION

der Fakultät für Chemie und Pharmazie
der Eberhard-Karls-Universität Tübingen

zur Erlangung des Grades eines Doktors
der Naturwissenschaften

2008

vorgelegt von

Rexhep Rexhepaj

Tag der mündlichen Prüfung: 12 Februar 2008

Dekan:	Prof. Dr. L. Wesemann
1. Berichterstatter	Prof. Dr. F. Lang
2. Berichterstatter	Prof. Dr. M. Duszenko

…….familjes sime!

Contents

1 Introduction 1

1.1 Proteins 1

1.1.1 Membrane proteins involved in solute transport 1

1.2 Protein Kinases 2

1.2.1 Phosphoinositide 3-kinases - PI3-Kinase 2

1.2.2 SGKs belong to a family of serine/threonine kinases 3

1.2.3 SGK1 Regulation of Epithelial Sodium Transport 4

1.3 Transepithelial transport 6

1.3.1 PI3 kinase a regulator of intestinal nutrient transport 8

1.3.2 Impact of PDK1 on transport of amino acids in the intestine 8

1.3.3 SGK3 participates in epithelial transport regulation 9

1.3.4 Transepithelial potential and amiloride-sensitive short circuit current 9

1.3.5 Aims of the studies 10

2 Materials and Methods 11

2.1 Materials 11

2.1.1 Equipment 11

2.1.2 Chemicals 11

2.1.3 Kits 13

2.1.4 Animals 14

2.1.4.1 PDK1 hypomorphic mice 14

2.1.4.2 Sgk1/ Sgk3 KO mice 14

2.1.4.3 Standard diet 15

2.2 Methods 16

2.2.1 Transepithelial Measurements using - the Ussing Chamber 16

2.2.2 Ussing chamber experiments in small intestine 17

2.2.3 Terminal uridine deoxynucleotidyl transferase nick - end labeling TUNEL staining 18

2.2.4 Glucose load and glucose excretion 19

2.2.5 Food intake, fecal weight and electrolyte composition 19

2.2.6 Collection and preparation of feces 20

2.2.7 Electrogenic glucose and amino acid transport in isolated perfused proximal straight tubules 20

2.2.8 Preparation of Brush Border Membrane Vesicles (BBMV) 21

2.2.9 In situ Hybridisation 22

2.2.10 Quantitative real-time PCR measurements 23

2.2.11 *In situ* hybridization of SGK3 mRNA 24

2.2.12 Dexamethasone, DOCA and low salt treatment 25

2.2.13 Plasma aldosterone measurements 25

2.2.14 Intestinal NHE3 activity. 25

2.2.15 Statistics 27

3 Results 28

3.1 PI3-kinase-dependent glucose and amino acid transport 28

3.1.1 Glucose and amino acid transport 28

3.1.2 PDK1-dependent glucose transport 33

3.1.3 PDK1-dependent amino acid transport 39

3.1.4 SGK3-dependent regulation of SGLT1 45

3.1.5 Quantitative RT-PCR 51

4 Discussion 59

4.1 Effect of PI3 kinase inhibitors on electrogenic transepithelial transport of glucose 59

4.2 Intestinal and renal glucose transport 60

4.3 Intestinal and renal transport of amino acids 62

4.4 Role of Sgk 3 gene knock-outon glucose transport 64

4.5 Mineralocorticoids and glucocorticoids enhance the SGK1 transcript levels in distal colon 66

5 Summary 68

6 Zusammenfassung 70

7 Abbreviations 72

8 References 74

9 Publications 84

10 Acknowledgements 87

11 Akademische Lehrer 88

12 Lebenslauf 90

1 Introduction

1.1 Proteins

Proteins constitute most of the cell dry mass. When a cell is observed under a microscope or when its electrical or biochemical activity is analysed, we in essence observe proteins. They are not only the cellular building blocks, but they also execute nearly all cell functions.

Proteins embedded in the plasma membrane form channels, transporters and pumps that control the passage of small molecules in und out of the cell. Other proteins carry messages from one cell to another or act as signal integrators that relay sets of signals inward from the plasma membrane to the cell nucleus, for example the family of serine/threonine kinases.

1.1.1 Membrane proteins involved in solute transport

The vast majority of solutes cross membranes with the help of membrane proteins. Special membrane transport proteins are responsible for transfering lipophobe solutes across cell membranes. These proteins occur in many forms and in all types of biological membranes. Each protein transports only a particular class of molecules such as ion, sugars or aminoacids and often their transport characteristics are very specific and restricted to few members of each class.

Transporters and channels are the two major classes of membrane transport proteins. Tranporters bind the specific solute and undergo a series of conformational changes to transfer the bound solute accros the membrane. Channel proteins in contrast, do not interact with the transported solute. All channels and many transporters allow solutes to cross the membrane only passively – a process called passive transport. In the case of transport of a single uncharged molecule, it is simply the difference of its concentration on the two sides of the membrane – its concentration gradient – that drives passive transport and determines its direction. If the solute carries a net charge however, both its concentration gradient and the electrical potential difference across the membrane, influence its transport. Cells require transport proteins that will actively pump certain solutes across the membrane against their electrochemical gradient; this process, known as active transport, is mediated by pumps. Thus, transport by carriers can be either active or passive, whereas transport by channel proteins is always passive.

One of the best understood pumps is the Na^+/K^+ ATPase. The sodium-potassium pump is probably the single most important transport protein in animal cells because it maintains the concentration gradient of Na^+ and K^+ across the cell membrane. The transporter is situated on the basolateral side of the cell membrane and pumps $3Na^+$out of the cell and $2K^+$ into the cell for each ATP consumed.

The energy for the active transport comes either directly or indirectly from the high-energy phosphate bond of ATP.

1.2 Protein Kinases

A protein kinase is an enzyme that modifies other proteins by chemically adding phosphate groups to them a process called phosphorylation. Phosphorylation usually results in a functional change of the target protein (substrate) by changing enzyme activity, cellular location, or association with other proteins.

Protein phosphorylation involves the enzyme – catalyzed transfer of the terminal phosphate group of an ATP molecule to the hydroxyl group of a serine or threonine side chain of a protein This reaction is catalyzed by a protein kinase, and the reaction is essentially unidirectional because of the large amount of free energy released when the phosphate –phosphate bond in ATP is broken to produce ADP.

The different protein kinases in a eucaryotic cell are organized into complex networks of signalling pathways which help to coordinate cell activites, drive the cell cycle, and relay signals into the cell from their environment

Serine/threonine protein kinases phosphorylate the OH^- group of serine or threonine (which have similar sidechains). The activity of these protein kinases can be regulated by specific events (e.g. DNA damage), as well as numerous chemical signals, including e.g. cAMP/cGMP.

1.2.1 Phosphoinositide 3-kinases - PI3-Kinase

The PI3- kinase enzymes are a group of ubiquitously expressed proteins that were shown to be essential for a plethora of biological responses including cell survival, cell proliferation, glucose and aminoacids transport, actin polymerisation and membrane ruffling.

The PI3 kinase family of enzymes is recruited upon growth factor receptor activation and produces 3' phosphoinositide lipids. The lipid products of PI3K act as second messengers

by binding to and activating diverse cellular target proteins. These events constitute the start of a complex signaling cascade, which ultimately results in the mediation of cellular activities such as proliferation, differentiation, chemotaxis, survival, trafficking, or glucose homeostasis. Therefore, PI3Ks play a central role in many cellular functions. The factors that determine which cellular function is mediated are complex and may be partly attributed to the diversity that exists at each level of the PI3K signaling cascade, such as the type of stimulus, the isoform of PI3K, or the nature of the second messenger lipids. Numerous studies have helped to elucidate some of the key factors that determine cell fate in the context of PI3K signaling. Transgenic and knockout mouse studies where either PI3K or its signaling components are modified have helped to build a picture of the role of PI3K in physiology and indeed there have been a number of surprises.

Phosphoinositide 3-kinases generate specific inositol lipids that have been implicated in the regulation of cell growth, proliferation, survival, differentiation and cytoskeletal changes. One of the best characterized targets of PI3K lipid products is the protein kinase Akt or protein kinase B (PKB). In quiescent cells, PKB resides in the cytosol in a low-activity conformation. Upon cellular stimulation, PKB is activated through recruitment to cellular membranes by PI3K lipid products and phosphorylation by PDK1 (1).

Upon phosphorylation of PI3,4,5-P3 by PI3-kinase, the PH-containing phosphoinositide depedent protein kinase (PDK)-1 and 2 are recruited to the plasma membrane. Translocation to the membrane coincides with their activation, respectively. Interestingly, PDK1 has been described as a governing point for the activation of a number of different other kinases such as Akt/PKB, SGK isoforms and PKC?.

1.2.2 SGKs belong to a family of serine/threonine kinases

Serum and glucocorticoid-inducible kinases (SGKs) belong to a family of serine/threonine kinases that are regulated at both the transcriptional and posttranslational levels by external stimuli. SGKs are members of the AGC subfamily that includes the PKC isoforms, cyclic-AMP-dependent PKA and p90RSK. There are 3 isoforms, SGK1, SGK2 and SGK3. The transcriptional regulation of the two closely related isoforms, SGK2 and SGK3, are not well understood. So far it is known that both can be activated by phosphorylation and that SGK3 has some role in the IL-3 mediated survival of hematopoietic cells. SGK1 contains a catalytic domain that is ~45-55% homologous to the catalytic domains of PKA, PKB, PKC-? and rat p70S6K/p85 S6K kinases which propagate cell signalling cascades associated with the control of cell growth,

differentiation and cell survival. The availability and function of SGK1 is regulated at three distinct levels of cellular control. First, SGK1 gene expression is strongly stimulated by hormonal and non hormonal stimuli. Second, like PKB, SGK1 is phosphorylated and enzymatically activated as a downstream component of the PI 3-kinase signalling cascade that mediates the mitogenic and cell survival responses to many growth factors and insulin. Finally, the subcellular localization of SGK1 is controlled by the cell cycle and exposure to specific hormones and environmental stress stimuli. SGK1 plays an important role in activating certain potassium, sodium and chloride channels, suggesting an involvement in the regulation of membrane transport (2-4).

SGK1 is subject to complex regulatory mechanisms. Cross-talk among these signaling pathways may play an important role in the pathogenesis of hypertension associated with hyperinsulinemia, obesity, and insulin resistance (5).

1.2.3 SGK1 Regulation of Epithelial Sodium Transport

Epithelial ion transport in vertebrates is regulated by a variety of hormonal and non-hormonal factors, including mineralocorticoids, insulin, and osmotic differences. SGK1 has been established as an important convergence point for multiple regulators of Na^+ transport. Unlike most other serine-threonine kinases, SGK1 is under dual control: protein levels are controlled through effects on its gene transcription, while its activity is dependent on PI3 -Kinase. Aldosterone is the most known regulator of SGK1 protein level in ion transporting epithelia, while insulin and other activators of PI3K are key regulators of its activity. Activated SGK1 regulates a variety of ion transporters, the best characterized of which is the epithelial sodium channel (ENaC). The apical targeting of ENaC is controlled by the ubiquitin ligase Nedd4-2, and SGK1. SGK1 acts, at least in part, through phosphorylation-dependent inhibition of Nedd4-2. This effect of SGK1 requires physical association of Nedd4-2 with both SGK1 and ENaC. Moreover, direct physical association between SGK1 and ENaC may also be implicated in the formation of a tertiary complex. Osmotic shock is likely the most important non-hormonal regulator of SGK1 expression, and surprisingly, SGK1 expression can be induced by hypotonic or hypertonic stress in a cell-type dependent fashion. The SGK family represents an ancient arm of the serine-threonine kinase family, present in all eukaryotes that have been examined, including yeast. SGK1 appears to have been implicated in membrane trafficking and possibly in the control of ion transport and cell volume in early single cell eukaryotes. In metazoan epithelia, it seems likely that SGK1 was adapted to the regulation

of ion transport in response to hormonal and osmotic signals (6).

SGKs activate ion channels (e.g., ENaC, TRPV5, ROMK, Kv1.3, KCNE1/KCNQ1, GluR1, GluR6), carriers (e.g., NHE3, GLUT1, SGLT1, EAAT1-5), and the Na^+-K^+-ATPase. They regulate the activity of enzymes (e.g., glycogen synthase kinase-3, ubiquitin ligase Nedd4-2, phosphomannose mutase-2) and transcription factors (e.g., forkhead transcription factor FKHRL1, beta-catenin, nuclear factor kappaB). SGKs participate in the regulation of transport, hormone release, neuroexcitability, cell proliferation, and apoptosis. SGK1 contributes to Na^+ retention and K^+ elimination of the kidney, mineralocorticoid stimulation of salt appetite, glucocorticoid stimulation of intestinal Na^+/H^+ exchanger and nutrient transport, insulin-dependent salt sensitivity of blood pressure and salt sensitivity of peripheral glucose uptake, memory consolidation, and cardiac repolarization. A common (prevalence approximately 5%) SGK1 gene variant is associated with increased blood pressure and body weight. SGK1 may thus contribute to the metabolic syndrome. SGK1 may further participate in tumor growth, neurodegeneration, fibrosing disease, and the sequelae of ischemia. SGK3 is required for adequate hair growth and maintenance of intestinal nutrient transport and influences locomotive behavior. In conclusion, the SGKs cover a wide variety of physiological functions and may play an active role in a multitude of pathophysiological conditions. There is little doubt that further targets will be identified that are modulated by the SGK isoforms and that further SGK-dependent physiological functions and pathophysiological conditions will be defined.(7)

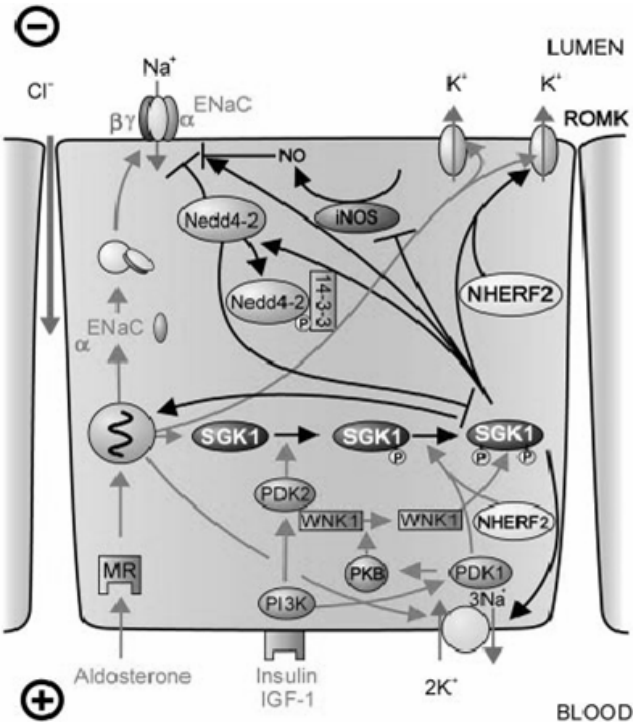

Figure 1. Model for the Serum- and Glucocorticoid-inducible Kinase-1 (SGK1)-dependent regulation of Na^+ reabsorption and K^+ secretion in the aldosterone-sensitive distal nephron. Aldosterone binds to mineralocorticoid receptors (MR) and stimulates the expression of SGK1, **a**-epithelial Na^+ channel (**a** ENaC), renal outer medullary K^+ channel (ROMK), and the Na^+-K^+-ATPase. (7)

1.3 Transepithelial transport

All the transport processes described in the previous sections deal with the movement of molecules across a single membrane, that of the cell. Molecules cross the first membrane when they move into an epithelial cell from the external enviroment and cross the second when they leave the epithelial cell to enter the extracellular fluid. Movement across epithelial cells, transepithelial transport, uses a combination of active and passive transport mechanisms. The transporting epithelium of the intestine is specialized to selectively transport molecules into and out of the body. The surface of the epithelial cell that faces the lumen of an organ is called the apical membrane. It is often folded into microvilli that increase its surface area. Transporting epithelial cells are said to be polarized because their apical and basolateral membranes have different properties. Certain transport proteins such as the Na^+-K^+-ATPase, are almost (always) found only on the basolaterale membrane, whereas other like the Na^+ - glucose symporter are localized to the apical membrane.

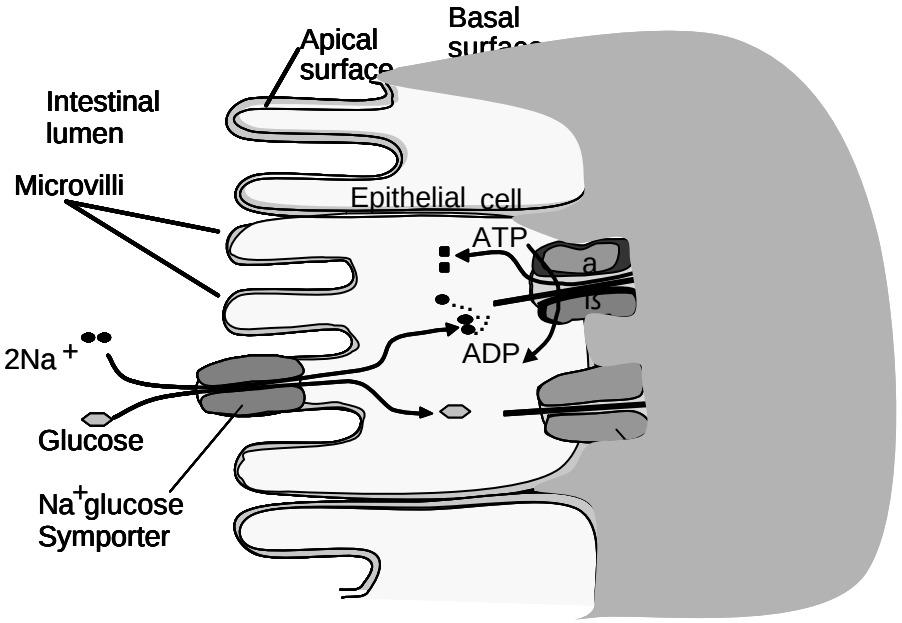

Figure 2: Glucose transport in intestinal epithelial cells.

The glucose/Na^+ symport uses the energy stored in the Na^+ gradient (produced by the Na^+/K^+ ATPase) to transport glucose against its concentration gradient.

Glucose transport is of fundamental importance for energy metabolism. The maintenance of a relatively constant blood glucose concentration to sustain cerebral metabolism and the delivery of glucose to peripheral tissues for storage and utilization are key metabolic processes. In many situations, transport of glucose across cell membranes plays a key role in its regulation and control.(8).

Glucose enters eucaryotic cells via 2 different types of membrane associated carrier proteins, the Na^+-coupled glucose transporters (SGLT) and the glucose transporter facilitators (GLUT). Three members of the SGLT family function as sugar transporters (SGLT1 and SGLT2) or sensors (SGLT3). The human GLUT family consists of 14 members, of which 11 have been shown to catalyze sugar transport (9).

Intestinal and renal transport of glucose is accomplished by Na+-coupled uptake across the apical cell membrane. Little is known about the cellular mechanisms mediating the regulation of glucose transport. Recently, a novel mechanism of transport regulation was described for the renal epithelial Na^+ channel ENaC. The ubiquitin ligase neuronal cell expressed evelopmentally downregulated neuronal cell expressed developmentally downregulated 4-2 (Nedd4-2) (10); ubiquitinates the channel protein, thereby inducing the subsequent clearance of the channel protein from the cell membrane (11;12). Nedd4-2 is phosphorylated and inactivated by the serum- and glucocorticoid-dependent kinase 1

(SGK1) (13).In vitro experiments have revealed the ability of SGK1 to stimulate intestinal Na^+-coupled glucose cotransporter 1 (SGLT1) and intestinal Na^+/H^+ exchanger 3 (NHE3).

1.3.1 PI3 kinase a regulator of intestinal nutrient transport

According to in vitro coexpression studies in Xenopus oocytes, protein kinase B/Akt (11;12) and the SGK1(2), SGK2 (14) and SGK3 (14) Kinases upregulate a variety of channels and transporters, (4;15;16) including the electrogenic glucose transporter SGLT1 (13), the glutamine transporter SN1 (17), and the glutamate transporters EAAT1 (17), EAAT2 (18), EAAT3 (19), EAAT4 (20)and EAAT5 (21).

The PKB and SGK isoforms are activated through the PI3 - Kinase and PDK1 (3;22-27). Thus, PI3 kinase may be a regulator of intestinal nutrient transport.

The present experiments have been performed to explore whether pharmacological inhibiton oder gene knock-out of serine/threonine kinases interferes with electrogenic glucose and/or amino acid transport.

1.3.2 Impact of PDK1 on transport of amino acids in the intestine

PKB and SGKs are activated by IGF1 and insulin through the PI3 - Kinase and PDK1 (3;22-28). The PI3 kinase pathway is an integral element of growth factor, insulin and interferon signalling (29-33). Its pleotropic functions include the regulation of cell survival (34;35) and cell proliferation (36-39). Moreover, inactivation of PDK1 by the phosphatase PTEN is abrogated by oxidation and thus, PDK1 participates in the signaling of oxidative stress (40). In view of its influence on the PKB and SGK isoforms, PDK1 may be a master switch in the growth factor, insulin and stress dependent regulation of amino acid transport.

The PDK1-knockout-mouse is not viable (41), highlighting the functional importance of this kinase. Mice with suppressed PDK1 activity to of up to ~ 20 % ($pdk1^{hm}$) are significantly smaller than their age and sex matched wild type littermates ($pdk1^{wt}$) (41). The smaller weight of the animals appeared to be primarily due to decreased cell volumes and not cell number (41). Among the determinants of cell volume is the concentrative cellular uptake of amino acids (42-44).

Several amino acid transport systems contribute to the intestinal absorption or renal proximal tubular reabsorption of amino acids in mammals (45-47). Neutral amino acids are mainly transported by the Na^+-dependent system B^0 and IMINO encoded by the B^0AT1 (SLC6A19) and SIT (SLC6A20) (47-50). Accordingly, mutations in B^0AT1 are

responsible for Hartnup disease, characterized by the impaired transport of neutral amino acids in the intestine and renal proximal tubule (51;52), . Anionic amino acids are transported in a Na^+- and K^+-dependent manner by the system X^-_{AG} EAAC1/ EAAT3 (SLC1A1) transporter, whereas cationic amino acids and cystine are transported by the dimeric b^0, +AT/rBAT (SLC7A9/ SLC3A1) transporter. Mutations in either b^0,+AT or rBAT cause cystinuria with reduced transport of these amino acids both in intestine and kidney, (46;53). Up to date, little to nothing is known about the regulation of these transport systems in vivo.

1.3.3 SGK3 participates in epithelial transport regulation

The serum and glucocorticoid inducible kinase SGK1 was originally cloned as a glucocorticoid inducible gene (2;54;55). Homology screening led to the discovery of the isoforms SGK2 and SGK3, (14;56) which appear not to be transcriptional targets of glucocorticoids or serum (4). SGK3 has independently been discovered as "cytokine independent survival kinase" CISK (31). All three kinases are activated by IGF1 and insulin through the phosphatidyl-inositol 3 (PI3) kinase and phosphoinositide-dependent kinase PDK1 (3;22-24;26-28).

The ability of SGK3 to regulate transport mechanisms in heterologous expression systems raises the question whether SGK3 participates in epithelial transport regulation in vivo. As shown recently, gene targeted mice lacking functional SGK3 ($sgk3^{-/-}$) gain weight after birth slightly slower than their wild type littermates ($sgk3^{+/+}$) (57), which could point to some impairment of intestinal absorption.

1.3.4 Transepithelial potential and amiloride-sensitive short circuit current

SGK1 was originally cloned as a glucocorticoid inducible gene (2;55). It was subsequently shown to be upregulated by mineralocorticoids (58-60). The human SGK1 was discovered as a cell volume-sensitive gene up-regulated by cell shrinkage (61). SGK1 was shown to participate in the regulation of renal Na^+ (58-60;62-64). and K^+ (65) excretion. SGK1 transcription is up-regulated by mineralocorticoids (58-60).

In Xenopus oocytes expressing the a, ß, ?-subunits of ENaC, coexpression of SGK1 results in a marked up-regulation of Na^+-channel activity (58;66-70). Similarly, SGK1 has been shown to stimulate ENaC activity in cortical collecting duct cells (71;72) and A6 cells (73;74).

Under regular salt intake, gene targeted mice lacking SGK1 ($sgk1^{-/-}$) excrete similar

amounts of NaCl as their wild-type littermates ($sgk1^{+/+}$) (64).Thus, lack of SGK1 does not lead to the severe phenotype of mice lacking functional aENaC (75;76), ßENaC (77), ?ENaC (78) or the mineralocorticoid receptor (79). The defective regulation of renal Na^+ excretion only becomes apparent following exposure to salt deficient diet which unmasks the limited ability of the ($sgk1^{-/-}$) mice to decrease their urinary Na^+ output (64). Perfusion of isolated collecting ducts disclosed that the impaired renal Na^+ retention was paralleled by decreased transepithelial voltage and amiloride sensitive current in this nephron segment (61;64).

At least in theory, the regulation of ENaC in colon may similarly involve SGK1. Conflicting data have been reported on the colonic regulation of SGK1 by mineralocorticoids. In one study, the abundance of SGK1 in the distal colon did not change significantly after sodium depletion or after a single dose of aldosterone (80). Other studies, however, reported that SGK1 mRNA levels (60;81;82) and protein levels (81) were significantly elevated in the distal colon in response to aldosterone.

Hitherto, nothing is known about the functional role of SGK1 in colonic epithelium.

1.3.5 Aims of the studies

The aim of the present study was to assess the function and regulation of intestinal transport by different protien kinases using sensitive inhibitors of tubular function and epithelium transporters. Special emphasis was applied on PI3K sig., Pdk1, Sgk1, Sgk3. For that purpose experiments were carried out with following objectives:

To elucidate the regulation of intestinal glucose and amino acid transport activity by the serum and glucocortikoid inducible kinase isoforms SGK1, SGK3, protein kinase B and other PI3-kinases.

To identify the role of SGK3 in upregulation of a variety of transport systems including the sodium depedent glucose transporter SGLT1.

To assess the Sgk1 mediated influence of mineralocorticoids on ENaC activity in the colon.

2 Materials and Methods

2.1 Materials

2.1.1 Equipment

Aida Image Analyzer software, Raytest, Germany.

Camera Proxitronic, Bensheim, Germany.

Eppendorf Centrifuge 5415R Hinz GmbH, Hamburg, Germany.

Eppendorf Pipets 1000µl, 200µl, 20µl, 10µl,Eppendorf, Hamburg, Germany.

Flame photometry, AFM 5051, Eppendorf, Hamburg, Germany.

Fluorescence microscope (Axiovert, Zeiss, Jena, Germany).

Fluorescence Microscopy low lightCCD camera/NIR/UV, Proxitronic Bensheim Germany.

Glucometer Accutrend, Roche, Mannheim, Germany

Lambda 10-2 Sutter Instrument Company, Novato, USA.

Lamp ebx 75 isolated Leika, Jena Germany.

MagNa Lyser (Roche Diagnostics, Mannheim, Germany)

Mastercycler gradient Eppendorf, Hamburg, Germany.

Metabolic cages ,Tecniplast, Hohenpeissenberg, Germany.

Microflow Biological Safety, Cabinet Nalge Nunc Wiesbaden-Bierbach Germany.

Microscope Zeiss Axiovert 135, Oberkochen, Germany.

Microscope Zeiss Stemi 2000, Oberkochen, Germany.

Milli-Q, MILLIPORE S.A. Molsheim France.

Na-Heparine disposable capillaries

Petridishes ,Greiner Bio-one, Frickenhausen, Germany.

pH Meter 646,Carl Zeiss, Oberkochen, Germany.

Preparation material, F.S.T. Heildelberg, Germany.

Vortex ,Labnet Abimed, Langenfeld, Germany..

2.1.2 Chemicals

Amiloride	Sigma, Taufkirchen, Germany
BaCl2x2H2O	Carl Roth, Karlsruhe, Germany.
Buffer –formamide	Sigma, Taufkirchen, Germany.

BSA bovine serum albumine Sigma	Sigma, Taufkirchen, Germany.
CaCl2x2H2O	Carl Roth, Karlsruhe, Germany.
Ca-Gluconate	Sigma, Taufkirchen, Germany.
Carbogen mixture 95% O2 and 5% CO2	Air Liquide Düsseldorf Germany.
Deoxycorticosterone acetate DOCA	Sigma, Taufkirchen, Germany.
Dextran sulfate	Sigma, Taufkirchen, Germany.
Diethyl ether	Carl Roth, Karlsruhe, Germany.
DOCA pellets ,50 mg,	Innovative Research of America, Sarasota, FL, USA.
EDTA Ethylenediamine tetraacetic acid	Sigma, Taufkirchen, Germany.
Ethanol absolute (99%)	Sigma-Aldrich; Hannover, Germany.
Forskolin	Sigma, Taufkirchen, Germany.
Glucose	Carl Roth Karlsruhe Germany.
HCl	Sigma, Taufkirchen, Germany.
HEPES	Sigma, Taufkirchen, Germany.
Indomethacin	Sigma, Taufkirchen, Germany.
K gluconate	Sigma, Taufkirchen, Germany.
K2HPO4x2H20	Sigma, Taufkirchen, Germany.
Kaiser's gelatine	Merck, Darmstadt, Germany.
Kaiser's solution	Merck, Darmstadt, Germany.
KCl	Carl Roth Karlsruhe Germany.
KH2PO4	Sigma, Taufkirchen, Germany.
L-Alanin	Carl Roth, Karlsruhe, Germany.
L-Arginin	Carl Roth, Karlsruhe, Germany.
L-Cystein	Carl Roth, Karlsruhe, Germany.
L-Glutamin	Carl Roth, Karlsruhe, Germany.
L-Leucine	Carl Roth Karlsruhe, Germany.
L-Lysine	Carl Roth Karlsruhe, Germany.
L-Methionin	Carl Roth, Karlsruhe, Germany.
L-Methionine	Carl Roth Karlsruhe, Germany.
L-Phenylalanine	Carl Roth, Karlsruhe, Germany.
L-Prolin	Carl Roth, Karlsruhe, Germany.
L-Tryptophan	Carl Roth Karlsruhe, Germany.
L-Valine	Carl Roth Karlsruhe, Germany.
LY-294,002 Hydrochloride	Sigma, Taufkirchen, Germany.

Mannitol	Sigma, Taufkirchen, Germany.
MgCl2 x 6H2O	Sigma, Taufkirchen, Germany.
MgSO4	Sigma, Taufkirchen, Germany.
Na - Pyruvat	Sigma, Taufkirchen, Germany.
NaCl	Sigma, Taufkirchen, Germany.
Na-lactate	Sigma, Taufkirchen, Germany.
Nitric acid	Carl Roth, Karlsruhe, Germany.
Nitroblue tetrazolium salt (NBT)	Sigma, Taufkirchen, Germany
N-Methyl-d-glucamine (NMDG)	Sigma, Taufkirchen, Germany.
Paraformaldehyde	Carl Roth, Karlsruhe, Germany.
Phloridzin	Sigma, Taufkirchen, Germany.
PFA- Paraformaldehyd	Merck, Darmstadt, Germany.
Saline 0.9%	Fresenius Kabi Bad Homburg Germany.
phosphate buffered DAPI (4'-6-Diamidino-2-phenylindole)	Sigma, Taufkirchen, Germany
Sodium bicarbonate	Sigma, Taufkirchen, Germany.
Sterilium	Carl Roth, Karlsruhe, Germany.
TEA buffer triethanolamine acetic anhydride	Sigma, Taufkirchen, Germany.
Tris buffer,	Sigma, Taufkirchen, Germany.
Wortmannin	Sigma, Taufkirchen, Germany.
5-bromo-4-chloro-3-indolyl phosphate (X-phosphate),	Sigma, Taufkirchen, Germany.

2.1.3 Kits

Aanti-DIG antibody	Roche, USA
CDP Star kit	Roche, USA.
Creatinine kit enzymatic colorimetric method,	Lehmann, Berlin, Germany.
Death Detection Kit	Roche Applied Sciences, Mannheim, Germany.
Detection Kit	Roche Applied Sciences, Mannheim, Germany.
DIG nucleic acid detection kit	Roche, Basel Schwitzerland.
DIG-labeling kit	Roche, Molecular Biochemicals, Mannheim, Germany.
ELISA kit	dsl, Webster, USA.
Glucose kit: gluco-quant®,	Roche Diagnostics, Mannheim, Germany.
GoTaq® Green Master Mix	Promega, Madison, USA.
PTH Elisa kit,	Immunotopics, CA, USA.

PCR purification kit	Qiagen, Hilden, Germany.
Photometric kit	Roche Manheim Germany.
Plasma leptin ELISA kit,	Linco, St. Charles, USA.
Primer mix	Search LC, Heidelberg, Germany.
rabbit anti-B0AT1	Alpha Diagnostics, San Antonio, TX, USA.
rabbit anti-EAAC1/ EAAT3	Alpha Diagnostics, San Antonio, TX, USA.
rabbit anti-SIT	Alpha Diagnostics, San Antonio, TX, USA.
RIA kit, Demeditec	Kiel, Germany.
RNAeasy Mini Kit	Qiagen, Hilden, Germany.
Superscript II reverse transcriptase	Invitrogen, Karlsruhe, Germany.
Trizol reagent Invitrogen	Karlsruhe, Germany.

2.1.4 Animals

All animal experiments were conducted according to the guidelines of the American Physiological Society and the German law for the care and welfare of animals and were approved by local authorities.

2.1.4.1 PDK1 hypomorphic mice

Generation and basic properties of PDK1 hypomorphic mice have been described (41). Genotyping was made by PCR on tail DNA using PDK1 and neo-R-specific primers as previously described (41;83). Intestinal segments were obtained from 3-8 month old wild-type mice of a mixed Sv129J/C56Bl/6 background, to reduce the impact of a specific genetic background. Comparisons have always been made within the same mouse to avoid any bias by variability of mice. Prior to removal of the organ, the animals had free access to standard mouse diet, mice had free access to standard mouse diet (C1310, Altromin, Langen, Germany) and tap water.

2.1.4.2 Sgk1/ Sgk3 KO mice

Mice deficient in SGK1 ($sgk1^{-/-}$) and SGK3 ($sgk3^{-/-}$) were generated as described previously (61;84).Genotyping was made by PCR on tail DNA using SGK3 and neo-R-specific primers as previously described (57). Mice have always been reproduced by heterozygous crossing. Therefore, the genetic background of the animals was a mix of

Sv/J129 and C57BL/6. Mice had free access to a standard mouse diet (C1310 Altromin, Heidenau, Germany) and tap water.

2.1.4.3 Standard diet

Standard diet C1310/1314 [0.24% Na^+, 0.71% K^+, 0.95% Ca^{2+} (wt/wt)] Altromin, Heidenau, Germany.

Control diet C1000 [0.24% Na^+, 0.71% K^+, 0.95% Ca^{2+} (wt/wt)] Altromin, Germany

2.2 Methods

2.2.1 Transepithelial Measurements using - the Ussing Chamber

Hans Ussing worked out the following concept to measure transepithelial transport in 1957: With a piece of epithelium the measurement chamber is divided into two halves. One can separately supply each half of the chamber with experimental solutions. Thereby one can distinguish between basolateral and apical effects, because the epithelium (still intact) continues transporting water and ions. The short circuit current which occurs during this procedure can be measured directly. To do that, one clamps the voltage above the epithelium to zero and measures the necessary current I_{sc} by an external measuring circuit. Alternatively one can clamp the current to zero and can then calculate the equivalent I_{sc}. This is less harmful for the epithelium. The latter „open circuit" configuration is the method that we used in our experiments. For this purpose an impulse generator (Dr. F.Grahammer, Physiologisches Institut Tübingen/Freiburg) generates the injection current (I_0) at prespecified intervals via Ag-Ag-Cl-electrodes. Depending on the resistance of the epithelium the injection current then causes a voltage drop ($?V_{te}$) over the epithelium. The measurement of V_{te} and $?V_{te}$ occurres via two Ag-Ag-Cl-agar bridges with a highly resistant voltmeter that is switched parallel to the epithelium. During the intervals without a current impulse the voltmeter registered the spontaneous transepithelial potential V_{te} which is built up through the active transport of ions. When there is a current injection then the voltmeter registers $?V_{te}$. Both are recorded using the computer program *chart 4.2* (Microsoft) and data are evaluated later after data transferinto *excel* (Microsoft). The resistence of the empty chamber was subtracted from the resistance of the epithelium, and the voltage zero was averaged before and after the experiment. With these data one can calculate the transepithelial resistance

$R_{te} = ?V_{te}/I_0$

and the equivalent short-circuit current $I_{sc} = V_{te}/ R_{te}$ by the means of Ohm's law.

Only tissue samples with a transepithelial resistance > 10 $?*cm^2$ were taken for data analysis. We used a modified and perfused miniature Ussing chamber (85;86) for our measurements. We could use extremely small tissue samples, because the opening of the chamber had a surface of only 0.00769 cm^2. The biopsates were clamped on the chamber application with a screw by lowering a drilled metal plate. This construction was then inserted in the actual chamber. The volume of the chamber was 3.80 ml and was continuously perfused with 5-6 ml/min. The solution and the chamber were both

thermostated at 37 °C. The injection current of 1 µA was applied every 6 s for 1 s.

Figure 3 Schematic construction of the miniature Ussing chamber.

A screw clamps the jejunum/colon mucosa on the chamber application (1) which is inserted into the chamber (4). Both sides of the epithelium are continuously perfused with experimental solution. The current I_0 is injected via electrodes of silver filament (3). The voltage drop ? V_{te}

is then recorded by a agar bridge with 1 M KCl-solution and a dipped Ag-AgCl-electrode (2).

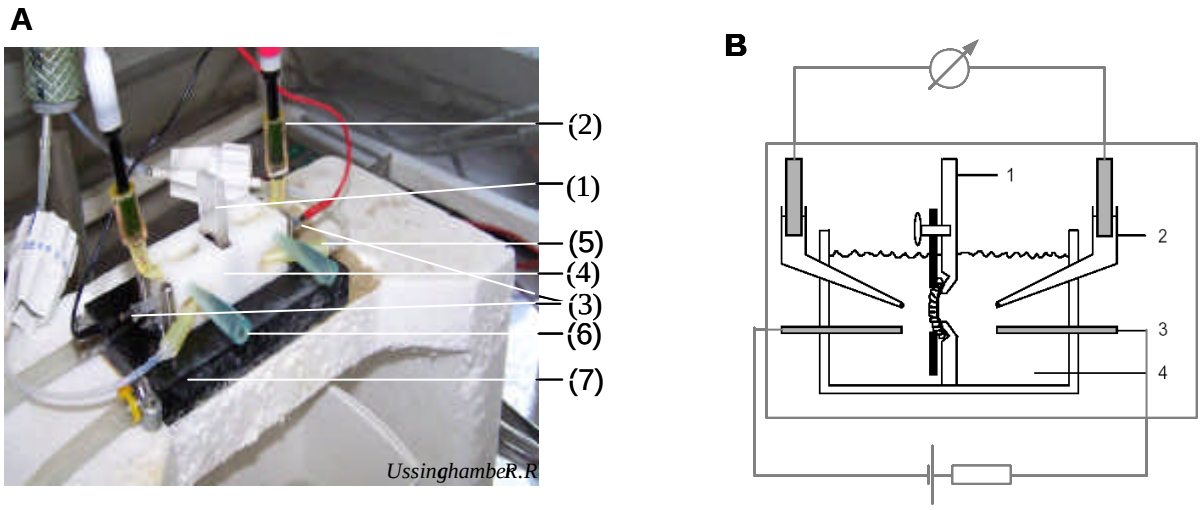

Figure 3. Miniature ussing chamber.

A. Original photograph of Ussing Chamber. **B.** Schematic structure of the miniature Ussing Chamber.

(1) Tissue holder, (2) Agar Electrode, (3)Ag/AgCl Electrode, (4) Half Chamber, (5) Inflow, (6) Outflow, (7) heated socket.

2.2.2 Ussing chamber experiments in small intestine

For analysis of electrogenic intestinal glucose and amino acid transport, animals were sacrificed, the abdomen opened and the intestine was quickly removed. Two adjacent jejunal segments (5 to 10 cm post pylorus) were mounted onto two identical custom-made mini-Ussing chambers with an opening diameter of 0.99 mm and an opening area of 0.00769 cm^2 allowing simultaneous measurements of potential difference and resistance. Both chambers were first perfused with control solution from both the serosal and the luminal side. The perfusate contained (in mM): 115 NaCl, 2 KCl, 1 $MgCl_2$, 1.25 $CaCl_2$, 0.4 KH_2PO_4, 1.6 K_2HPO_4, 5 Na pyruvate, 25 $NaHCO_3$, 20 Mannitol. All solutions were gassed with 95% O_2 / 5%CO_2 for at least 60 min until usage in the experiment. The pH of the perfusates, determined immediately prior to the experiments, was 7.4. The small size of the chamber favored an underestimation of the transepithelial resistance (87), yielding

values lower than those reported previously (88). The present study addressed relative changes of currents, which were not affected by this bias. After stabilization of the tissues in the chamber, one chamber was incubated with the PI3-Kinase inhibitor Wortmannin (1 µM) or LY294002 (50 µM) by continuous perfusion from the serosal side for 15 - 60 min. The other chamber was perfused with control solution.

To test for electrogenic transport of glucose or amino acids, D-glucose, L-phenylalanine, L-cysteine, L-glutamine or L-proline (20 mM, all from Roth, Karlsruhe, Germany) were added to the luminal perfusate at the expense of mannitol in both chambers. Substrates were simultaneously and repeatedly administered over the next 40 min allowing paired comparison between the responses in the two chambers.

2.2.3 Terminal uridine deoxynucleotidyl transferase nick - end labeling TUNEL staining

Cryosections of jejunum were analyzed for apoptotic cells by transferase (TdT)-mediated deoxyuridine-triphosphate (dUTP) nick-end labeling (TUNEL) method with the In Situ Cell Death Detection Kit (Roche Applied Sciences, Mannheim, Germany). Jejunal tissues were fixed in para-formaldehyde solution (4% PFA in phosphate buffered saline) for 30 min and frozen in O.C.T. compound (Tissue-Tek; Sakura Finetek, Heppenheim, Germany). Sections of 12 µm thickness were sliced on a freezing microtome, mounted on silane coated slides (2 % 3-aminopropyltriethoxy-silane (Sigma, Taufkirchen, Germany) in acetone), and dried at room temperature for 1 h. After washing in PBS for 30 min, tissue was fixed again in 4 % PFA for 20 min. Afterwards, tissues were incubated with proteinase K solution (10 µg/ml in Tris buffer, Roche) for 15 min at room temperature and permeabilized with 0.1 % sodium citrate/0.1 % Triton-X-100 (Sigma) for 2 min on ice. For the positive control sections were treated with DNase I solution (10 µg/ml in 50 mM Tris-HCl/1mg/ml BSA, pH 7.5, Sigma) for 30 min at 37°C. After washing with PBS, slides were incubated with only one-fourth of the manufacturer's recommended concentration of enzyme labeling solution for 1 h at 37°C. For the negative control transferase enzyme solution was omitted. After washing with PBS, slides were additionally stained with phosphate buffered DAPI (4'-6-Diamidino-2-phenylindole) solution (1 µg/ml, Sigma) for 10 min. Afterwards, slides were washed three times in PBS, briefly rinsed in distilled water, dried and coverslipped with Kaiser's gelatine (Merck, Darmstadt, Germany). Representative areas were photographed with an inverted

fluorescence microscope (Axiovert, Zeiss, Jena, Germany).

2.2.4 Glucose load and glucose excretion

For determination of glucose tolerance and renal glucose excretion unfasted mice were injected with 3 mg/g bw glucose in a volume of 30 µl aqua ad iniectabilia/g bw intraperitoneally (i.p.). Control experiments in both genotypes were performed injecting 30 µl 0.9 % NaCl / g bw. Blood glucose was measured from tail-vein blood using a glucometer (Accutrend, Roche, Mannheim, Germany) before and at 30, 60 and 120 minutes after the injection of glucose. Throughout the experiment mice were placed in individual metabolic cages (Tecniplast, Hohenpeißenberg, Germany) for the collection of a spot urine sample after injection over the next 3 hours yielding 0.1-1.8 ml urine. Urinary glucose and creatinine concentrations were determined utilizing commercial enzymatic kits: gluco-quant®, Roche Diagnostics, Mannheim, Germany, based on the hexokinase method and creatinine PAP, Labor & Technik, Berlin, Germany, based on the creatininase method. For quantitative analysis of glucosuria the ratio between glucose and creatinine concentration was calculated (in mg glucose/ mg creatinine) to adjust for differences in urinary dilution.

2.2.5 Food intake, fecal weight and electrolyte composition

Mice were placed in individual metabolic cages (Tecniplast, Hohenpeißenberg, Germany). After a training period of two days food and fluid intake as well as urinary and fecal output were determined under control conditions (Control diet C1000 Altromin, Germany) over two consecutive 24 h periods. Results were averaged for each animal. The inner wall of the metabolic cages was siliconized and urine was collected under water-saturated oil to allow for quantitative measurements. Before and at the end of the metabolic cage experiments about 150 µl blood was withdrawn into heparinized capillaries by puncturing the retro-orbital plexus. Haematocrit was determined after centrifugation. Plasma was separated for further analysis. Serum IGF 1 was measured using an ELISA kit according to the manufacturer instructions (DSL-10-2900, dsl, Webster, USA).

To determine amino acid concentrations in urine, mice were individually placed in metabolic cages and urine was collected quantitatively over 24 h. To prevent bacterial growth and hence metabolism and breakdown of amino acids 5 µl of concentrated acetic

acid was added into the urine collectors beneath the mineral oil. Amino acid concentrations in urine and serum were measured by HPLC as described before (15). Urinary creatinine concentrations were determined utilising a commercial enzymatic kit (Labor und Technik, Berlin, Germany).

After a training period of two days food and fluid intake as well as urinary and fecal output were determined over three consecutive 24h periods and results were averaged for each animal. Feces were dried for 3h at 80°C, weighed and suspended in 0.75 N nitric acid. Over two days this mixture was alternately put on a shaker at room temperature or into a 50°C water bath for 12h. After centrifugation Na^+ and K^+ content was determined in the supernatant with a flamephotometer (Eppendorf FCM 6341, Germany). Phosphorus (Pi) concentration was determined using a photometric kit (Roche) following the manufacturer's manual.

2.2.6 Collection and preparation of feces

For the analysis of fecal Na^+ and K^+ excretion feces was collected in metabolic cages (Tecniplast, Hohenpeissenberg, Germany). Before the collection, the standard mouse diet was switched to a control diet for 1 week (C1000, measured Na^+ content 120µmol/g food, Altromin, Heidenau, Germany) and the animals were placed individually in metabolic cages for 24 hour feces collection.

To investigate the effects of salt depletion, feces was collected for two days under the control diet and access to distilled water preventing compensatory sodium intake by tap water (Na^+ content 1mM). After switching the animals to the low salt diet (C1036, Altromin, Heidenau, Germany), a second feces collection was made on the fourth and fifth day. For final data analysis the average of the two days under the respective diet was taken.

To investigate the effects of a 4 day treatment with dexamethasone (10µg/g bw) on fecal Na^+ and K^+ excretion, feces was collected 1 day before treatment and on the 4th day of treatment under control diet (C1000) and tap water.

2.2.7 Electrogenic glucose and amino acid transport in isolated perfused proximal straight tubules

Experiments were performed in proximal straight tubules. Segments of 0.2 to 0.4 mm length were dissected and perfused following principally the method of Burg et al. (89).

Modifications of the technique concerning track system, pipette arrangement and use of dual channel perfusion pipettes have been described in detail previously (90;91). The luminal perfusion rate was < 10 nl/min. The bath was continuously perfused at a rate of 20 ml/min and thermostated with a dual channel feedback system (Hampel, Frankfurt, Germany). The bath temperature was kept constant at 38 ^{0}C. The potential difference across the basolateral cell membrane (PD_{bl}) was determined utilizing Ling-Gerard electrodes (100-200 MΩ) pulled from filament capillaries (1.5 o.d., 1.0 i.d., Hilgenberg, Malsfeld; Germany). The electrodes were connected to a high impedance electrometer (FD223, WPI, Science Trading, Frankfurt, Germany) via an Ag/AgCl half cell. An Ag/AgCl reference electrode was connected with the bath. Entry of positive charge by electrogenic transport is expected to depolarize the basolateral cell membrane. The magnitude of the depolarization depends on the magnitude of the induced current on the one hand and on the resistances of cell membranes and shunt on the other. PD_{bl} was continuously recorded with and without Glucose, L-phenylalanine, L-glutamine or L-proline (20 mM each) in the luminal perfusate to stimulate electrogenic reabsorption as described (92). The bath and luminal perfusates were composed of (all numbers mM): 110 NaCl, 5 KCl, 20 $NaHCO_3$, 1.3 $CaCl_2$, 1 $MgCl_2$, and 2 Na_2HPO_4. In the bath, (in mM) 18 mannitol, 1 glucose, 1 glutamine and 1 Na-lactate and in the lumen 20 mannitol and 1 Ba^{2+} were added. Where indicated, 20 mM mannitol were replaced by 20 mM of the respective amino acid in the luminal perfusate. The bath solution was constantly gassed with a mixture of 95% O_2 and 5% CO_2 resulting in a pH of 7.4.

2.2.8 Preparation of Brush Border Membrane Vesicles (BBMV)

BBMV were prepared from whole mouse kidney using the Mg^{2+}- precipitation technique as described previously (93) After measurement of the total protein concentration (Biorad Protein kit), 20 µg of brush border membrane protein were solubilized in Laemmli sample buffer, and SDS-Page was performed on 10 % polyacrylamide gels. For immunoblotting, proteins were transferred electrophoretically from unstained gels to PVDF-membranes (Immobilon-P, Millipore, Bedford, MA, USA). After blocking with 5 % milk powder in Tris-buffered saline/0.1% Tween-20 for 60 min., the blots were incubated with affinity purified rabbit anti-B^0AT1 (SLC6A19), rabbit anti-SIT (SLC6A20) (50), rabbit anti-EAAC1/ EAAT3 (SLC1A1) (Alpha Diagnostics, San Antonio, TX, USA), rabbit anti-b0,+AT1 (SLC7A9) (Pfeiffer et al. 1999 antibodies (1:1000) and mouse monoclonal anti-actin (42 kDa, Sigma) 1: 500 either for 2 h at room temperature or overnight at 4 °C. After

washing and subsequent blocking, blots were incubated with secondary antibodies conjugated with alkaline phosphatase or horse radish peroxidase (goat anti-rabbit 1: 5000 and donkey anti-mouse 1: 5000 (Promega)), for 1 h at room temperature. Antibody binding was detected with the enhanced chemiluminescence kit (Pierce) in the case of HRP-linked antibodies and with the CDP Star kit (Roche, USA) for AP linked antibodies before detection of chemiluminescence with the Diana III Chemiluminescence detection system. Bands were quantified with the Aida Image Analyzer software (Raytest, Germany).

2.2.9 In situ Hybridisation

DIG-labeled, SGK3-specific, antisense and sense RNA probes were generated from RT-PCR derived templates by in vitro transcription. Total cellular RNA was prepared from adult mouse hippocampus by using Trizol reagent (Invitrogen, Karlsruhe, Germany). After treatment with RNase-free DNase, the first-strand oligo (dT)-primed cDNA was synthesized with Superscript II reverse transcriptase (Invitrogen). Afterwards, PCR amplification of a 470-bp specific DNA fragment of SGK3 sequence was performed with following primers: SGK3 forward: 5' CAGAAAACAGCCCTATGACAACAC 3'; SGK3 reverse: 5' GAGGGGCGTAAGAAAAACCAACA 3'. PCR was carried out under following conditions: 95 °C for 10 min, 35X (95 °C for 30 s, primer annealing at 58 °C for 45 s, 72 °C for 45 s) and 72 °C for 10 min. AmpliTaq DNA polymerase and PCR reagents were purchased from Applied Biosystems (Lincoln, USA). In order to produce a DNA template for the generation of antisense and sense RNA probes by in vitro transcription, T7 RNA polymerase promoter sequence was added to the 5' end of PCR product by a further PCR reaction under the same PCR conditions, described above. Primer sequences are shown below, whereby promoter sequences are underlined: For generation of sense probe: T7_SGK3 forward: 5' GCAGTAATACGACTCACTATAGGGCAGAAAACAGCCCTATGACAACAC 3'; SGK3 reverse: 5' GAGGGGCGTAAGAAAAACCAACA 3'; For production of antisense probe: SGK3 forward: 5' CAGAAAACAGCCCTATGACAACAC 3'; SGK3_T7 reverse: 5' GCAGTAATACGACTCACTATAGGGGAGGGGCGTAAGAAAAACCAACA 3'. Afterwards, PCR fragments were purified with a PCR purification kit (Qiagen, Hilden, Germany). In vitro transcription was performed with the DIG-labeling kit (Roche Molecular Biochemicals, Mannheim, Germany) by using 100 ng template DNA. After ethanol precipitation, labeled RNA probe was quantified by dot blot according to the

protocol of the DIG-labeling kit.

2.2.10 Quantitative real-time PCR measurements

To test whether colonic SGK1 transcription is up-regulated by dexamethasone and DOCA, wild-type mice underwent a four day treatment with dexamethasone (10µg/g bw s.c.) or a seven day treatment with DOCA (1.5mg/day in 50µl DMSO). To obtain colonic tissue treated and untreated wildtype animals were deeply anesthetized with diethylether and killed by cervical dislocation and the abdomen was opened. The intestine was quickly removed and carefully flushed with 4°C control buffer to remove remaining food particles. Specific intestinal segments were rapidly frozen in liquid nitrogen. Automated disruption and homogenization of frozen tissue was performed using the MagNa Lyser Instrument (Roche Diagnostics, Mannheim, Germany). For each sample one-way special tubes containing ceramic beads were filled with 20-30 mg of frozen tissue and 600 µl of RLT-buffer (Qiagen, Hilden, Germany). Cleared cell lysate was transferred for further RNA purification (RNAeasy Mini Kit, Qiagen, Hilden, Germany). Subsequently 1 µg of total RNA was reverse transcribed to cDNA utilizing the reverse transcription system (Bioscience, USA) with oligo (dT) primers according to the manufacturer's protocol. To determine mSGK1 mRNA levels, quantitative real-time PCR with the LightCycler System (Roche Diagnostics, Mannheim, Germany) was established. PCR reactions for mSGK1 were performed in a final volume of 20 µl containing 2 µl cDNA, 2.4 µl $MgCl_2$ (3 µM), 1 µl primermix (0.5 µM of both primers), 2 µl cDNA Master SybrGreen I mix (Roche Molecular Biochemicals, Mannheim, Germany) and 12.6 µl DEPC treated water. The transcript levels of the housekeeping gene mGAPDH were also determined for each sample using a commercial primer kit (Search LC, Heidelberg, Germany). PCR reactions for *GAPDH* were performed in a final volume of 20 µl containing 2 µl cDNA, 2 µl primer mix (Search LC, Heidelberg, Germany), 2 µl cDNA Master Sybr Green I mix (Roche Molecular Biochemicals, Mannheim, Germany) and 14 µl DEPC treated water.

Amplification of the target DNA was performed during 35 cycles of 95°C for 10s, 68°C for 10s and 72°C for 16s, each with a temperature transition rate of 20°C/s and a secondary target temperature of 58°C with a step size of 0.5°C. Melting curve analysis was performed at 95°C 0s, 58°C 10s, 95°C 0s to determine melting temperatures of primer dimers and the specific PCR products. Melting curve analysis confirmed the amplified products, which were then separated on 1.5% agarose gels to confirm the expected size (406 bp). Finally, results were calculated as a ratio of the target vs. house

keeping gene transcripts.

The following primers for mSGK1 (Gene bank No.: NM_011361) were used:

mSGK1 sense:5'-TGT CTT GGG GCT GTC CTG TAT G-3'

mSGK1 antisense:5'-GCT TCT GCT GCT TCC TTC ACA C-3'

2.2.11 *In situ* hybridization of SGK3 mRNA.

Adult mice (C57/BL6 wild type and $SGK3^{-/-}$) were deeply anesthetized with ketamine/xylazine. Large and small intestine were removed, immediately frozen in 25°C cold isopentane and sliced on a freezing microtome at 12 µm thickness. Sections were subsequently mounted on silane coated slides (2% 3-aminopropyltriethoxy-silane (Sigma, Taufkirchen, Germany) in acetone), dried at 60 °C for 30 s and fixed with 4% phosphate buffered paraformaldehyde for 20 min. After three washes with phosphate buffered saline (PBS, 0.1 mM, pH 7.4), slides were incubated with TE buffer (100 mM Tris, 50 mM EDTA, pH 8) containing 2 µg/ml proteinase K for 10 min at room temperature and rinsed again three times with PBS. In order to reduce nonspecific background, slides were acetylated with TEA buffer (0.1 M triethanolamine, pH 8.0) containing 0.25% (v/v) acetic anhydride (Sigma) twice for 5 min. After pre-hybridization with hybridization buffer (50% formamide (Sigma), 10 % dextran sulfate, 5 mM EDTA, 20 mM Tris pH 8, 10 mM DTT, 1X Denhardt's solution, 0.05 % tRNA, 300 mM NaCl) for 1 h at 62 °C, sections were incubated with fresh hybridization buffer containing the denatured DIG-labeled sense or antisense probe (200 ng/ml) overnight at 62 °C. After hybridization, slides were briefly rinsed in 2X SSC at room temperature and 3 times in 0.1X SSC for 15 min at 62 °C. Detection of DIG-labeled RNA probe was performed according to the protocol of the DIG nucleic acid detection kit (Roche, Basel Schwitzerland). The tissues were blocked for 30 min with blocking buffer (1% blocking reagent (Roche) in maleic acid buffer (0.1 M maleic acid, 0.15 M NaCl, pH 7.5) and then incubated with alkaline phosphatase-conjugated antibody solution (anti-DIG antibody (1:2500 Roche) in blocking buffer containing 0.1% Triton® X 100) for 1 h. Following 4 washes with maleic acid buffer for 15 min, slides were equilibrated for 5 min in Tris buffer pH 9.5 (0.1 M Tris, pH 9.5, 0.1 M NaCl, 50 mM $MgCl_2$). The colour development was carried out with freshly prepared substrate solution (nitroblue tetrazolium salt (NBT) and 5-bromo-4-chloro-3-indolyl phosphate (X-phosphate) (Roche) in Tris buffer pH 9.5). After 3 washes with PBS, slides were rinsed in distilled water, dried, and coverslipped with Kaiser's solution (Merck, Darmstadt, Germany).

2.2.12 Dexamethasone, DOCA and low salt treatment

For analysis of glucocorticoid effects on colonic ENaC activity, $sgk1^{+/+}$ and $sgk1^{-/-}$ mice (3-12 months old, both genders) were injected subcutaneously with dexamethasone phosphate disodium salt (Sigma, Taufkirchen, Germany; dissolved in 0.9% saline) at a dose of 10µg/g BW for four consecutive days at 8 pm. $sgk1^{-/-}$ and $sgk1^{+/+}$ mice injected with 0.9% saline alone served as controls. This regimen had previously shown marked up-regulation of intestinal SGK1 (94) but was tolerated by the mice seemingly well. Mice had free access to a standard mouse diet (C1310, Altromin, Heidenau, Germany) and tap water.

For analysis of mineralocorticoid effects, $sgk1^{+/+}$ and $sgk1^{-/-}$ mice were treated with intraperitoneal injections of DOCA (Sigma, Taufkirchen, Germany) at a dose of 1.5mg per day dissolved in 50µl DMSO for seven consecutive days. This dose was adapted according to a previous study (95)and was tolerated by the mice seemingly well. Again, mice had free access to a standard mouse diet (C1310, Altromin, Heidenau, Germany) and tap water.

To analyze the effects of salt depletion, the standard mouse diet (C1310, measured Na^+ content 82 µmol/g, Altromin, Heidenau, Germany) was replaced by low salt diet (C1036, measured Na^+ content 7.3 µmol/g food, Altromin, Heidenau, Germany). Animals were sacrificed for Ussing chamber experiments after 7 days of treatment.

2.2.13 Plasma aldosterone measurements

Blood specimens were obtained during light anesthesia with diethylether (Roth, Karlsruhe, Germany) and approximately 150 µl of blood was drawn into heparinized capillaries by puncturing the retro-orbital plexus. Plasma aldosterone concentrations were measured using a commercial RIA kit (Demeditec, Kiel, Germany).

2.2.14 Intestinal NHE3 activity.

For isolation of ileal villi, animals were fasted for 6 h before experiments. After the death of the animals, the terminal 2 cm of the ileum were removed and cut longitudinally. After being washed with standard HEPES solution, the intestine was sliced into 0.3-cm^2 sections. The tissues were transferred onto the cooled stage of a dissecting microscope,

and individual villi were detached from the intestine by snapping off the ileal base with sharpened microdissection tweezers. Care was taken not to damage the apical part of the villi. The villi were attached to a glass coverslip precoated with Cell-Tak adhesive (BD Biosciences, Heidelberg, Germany). For quantitative digital imaging of intracellular pH (pHi), isolated individual villi were incubated in a HEPES-buffered Ringer solution containing10 µM 2',7'-bis-bis(2-carboxyethyl)-5(6)-carboxyfluorescein (BCECF)-AM (Molecular Probes, Leiden, The Netherlands) for 15 min at 37°C. After being loaded, the chamber was flushed for 5 min with Ringer solution to remove any deesterified dye sticking to the outside of the villi. The perfusion chamber was mounted on the stage of an inverted microscope (Zeiss Axiovert 135, Oberkochen, Germany), which was used in the epifluorescence mode with a 40 oil-immersion objective (Zeiss Neoplan, Oberkochen, Germany). BCECF was successively excited at 490 ± 10 and 440 ± 10 nm, and the resultant fluorescent signal was monitored at 535 ±10 nm via an intensified charge-coupled device camera (Proxitronic, Bensheim, Germany) and specialized computer software (Metafluor, Universal Imaging, Downingtown, PA). Individual regions of interest at the tip of the villi were outlined and monitored during the course of the measurement. Intensity ratio data (490/440) were converted into pH values by the high-K /nigericin calibration technique (96).

The solutions, flow lines, and perfusion chamber were maintained at 37°C by a thermostatically controlled heating system. The volume of the perfusion chamber was 600 µl and the flow rate was 4 ml/min for all solutions. For acid loading, cells were transiently exposed to a solution containing 20 mM NH_4Cl leading to marked initial alkalinization of pHi due to entry of NH_3 and binding of H^+ to form NH_4^+ (97). The acidification of pHi upon removal of ammonia allowed us to calculate the mean intrinsic buffering power (ß) of the cells (97), assuming that NH_4^+ and NH_3 are in equilibrium in cytosolic and extracellular fluid and that ammonia leaves the cells as NH_3:

$ß = ?[NH_4^+]_i / ? pH_i$

where ?pHi is the decrease of pHi after ammonia removal and $?[NH_4^+]$ i is the decrease of cytosolic NH_4^+ concentration, which is identical to the concentration of NH_4^+ immediately before the removal of ammonia. Given the pK for NH_4^+ /NH3 of 8.9 (98), an extracellular pH (pH_0) of 7.4 and an NH_4^+ concentration in extracellular fluid ($[NH_4^+]_0$) of 19.37 $[20/(1 +10^{pHo- pK})]$, then $[NH_4^+]i =19.37 \times 10^{pHo- pK}$.

For some experiments, the selective NHE_3 inhibitor S3226 (Aventis, Frankfurt, Germany) was added to all solutions at a concentration of 10µM.The solutions were composed of the

following (in mM): for standard HEPES, 115 NaCl, 5 KCl, 1 $CaCl_2$, 1.2 $MgSO_4$, 2 NaH_2PO_4, 10 glucose and 32.2 HEPES; for sodium-free HEPES, 132.8 NMDG, 3 KCl, 1 $CaCl_2$, 1.2 $MgSO_4$, 2 KH_2PO_4, 32 HEPES, 10 mannitol, and 10 glucose; for sodium-free ammonium chloride, 15 NMDG-Cl and 10 mannitol were replaced by 20 mM NH_4Cl; and for calibration, 105 KCl, 1 $CaCl_2$, 1.2 $MgSO_4$, 32.2 HEPES, and 10 mannitol (5 M nigericin). The pH of the solutions was titrated to 7.4 or 7.0 with HCl-NaOH, HCl-NMDG, and HCl-KOH, respectively, at 37°C. All substances were from Sigma (Taufkirchen, Germany) or Roth (Karlsruhe, Germany). SDS-PAGE and Western blot analysis.

2.2.15 Statistics

Data are provided as means ± SEM, n represents the number of independent experiments. All data were tested for significance using paired or unpaired Student´s t-test with or without Welch´s correction or Mann-Whitney test where applicable, and only results with $P < 0.05$ were considered statistically significant.

3 Results

3.1 PI3-kinase-dependent glucose and amino acid transport

3.1.1 Glucose and amino acid transport

To determine PI3-kinase-dependent glucose and amino acid transport in wild-type mice, segments of jejunum were mounted onto mini-Ussing chambers for electrophysiological analysis. Simultaneous measurements with one control chamber and one chamber incubated with the PI3 kinase inhibitor Wortmannin. allowed paired comparison between control and treatment. In the absence of luminal substrates, the transepithelial potential difference (V_{te}) of all studied jejunal segments (n = 22) amounted to -0.39 ± 0.10 mV and the transepithelial resistance (R_{te}) approached 6.1 ± 0.3 O cm^2. The values allowed the calculation of the basal short circuit current (I_{sc}), which approached -55 ± 15µA/cm².

Neither transepithelial potential difference (-0.50 ± 0.12 mV) nor transepithelial resistance (5.8 ± 0.4O cm^2) were significantly altered 55 minutes after the application of 1 µM Wortmannin (n = 22). Accordingly, I_{sc} was similarly not significantly affected by the PI3-kinase inhibitors (-90 ± 24 µA/cm²).

The isoosmotic replacement of mannitol by glucose generated a lumen-negative shift of the transepithelial potential difference (? V_{glc}) without significantly altering the transepithelial resistance (Fig. 4.) The ? V_{glc} and R_{te} allowed the calculation of the glucose-induced current (I_{glc}), which approached -1353 ± 216 µA/cm^2 under control conditions, i.e. in the absence of Wortmannin (Fig. 4, n=5). Throughout the course of the experiment I_{glc} remained constant in the control chamber. In contrast, I_{glc} gradually declined in segments incubated with 1µM Wortmannin. Within 40 min I_{glc} was only 61 ± 12 % of the control value (Fig. 4).

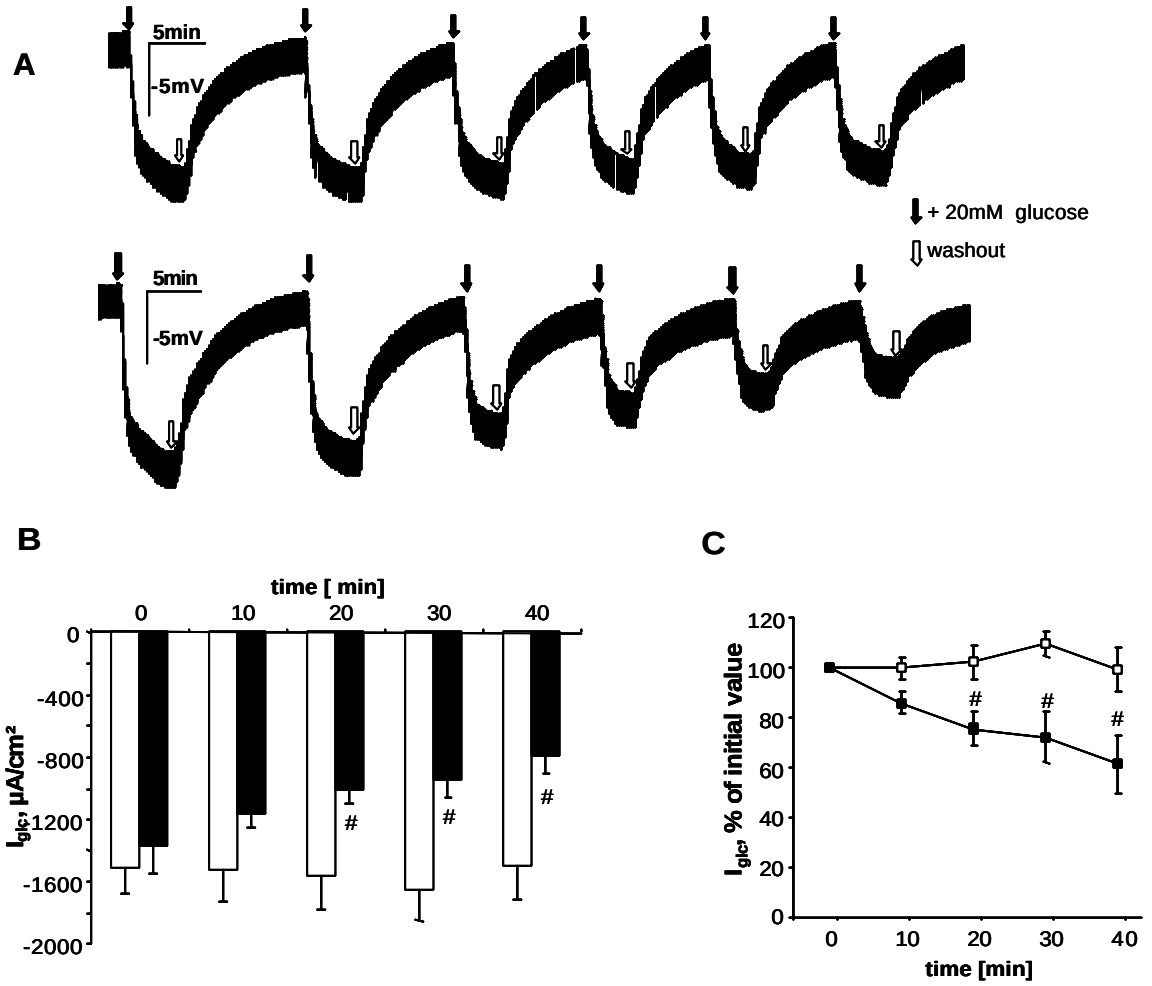

Figure 4. Effect of Wortmannin on glucose-induced current in jejunal segments. Alterations of transepithelial voltage (?V_{glc}) and glucose-induced currents (I_{glc}) in proximal segments of jejunal tissue with or without ncubation with Wortmannin (1 µM).

A Original tracings illustrating the effect of 20 mM glucose on the transepithelial potential difference in the absence (upper panel) and presence (lower panel) of Wortmannin.
B Arithmetic means±SEM (n=5) of glucoseinduced currents (µA/cm^2) following exposure to perfusate with Wortmannin (closed bars) or without Wortmannin (open bars).
#Significant difference between presence and absence of Wortmannin.
C Arithmetic means ± SEM (n=5) of glucoseinduced current, in percent of the currents in the beginning of the experiment, following exposure to perfusate with Wortmannin (closed symbols) or without Wortmannin (open symbols).
#Significant difference between presence and absence of Wortmannin

Similar to glucose, the amino acids phenylalanine, cysteine, glutamine or proline generated a lumen-negative shift of the transepithelial potential difference (? V_{aa}) without significantly altering the transepithelial resistance. The ? V and R_{te} allowed the calculation of the amino acid induced current (Fig. 5, table 1).

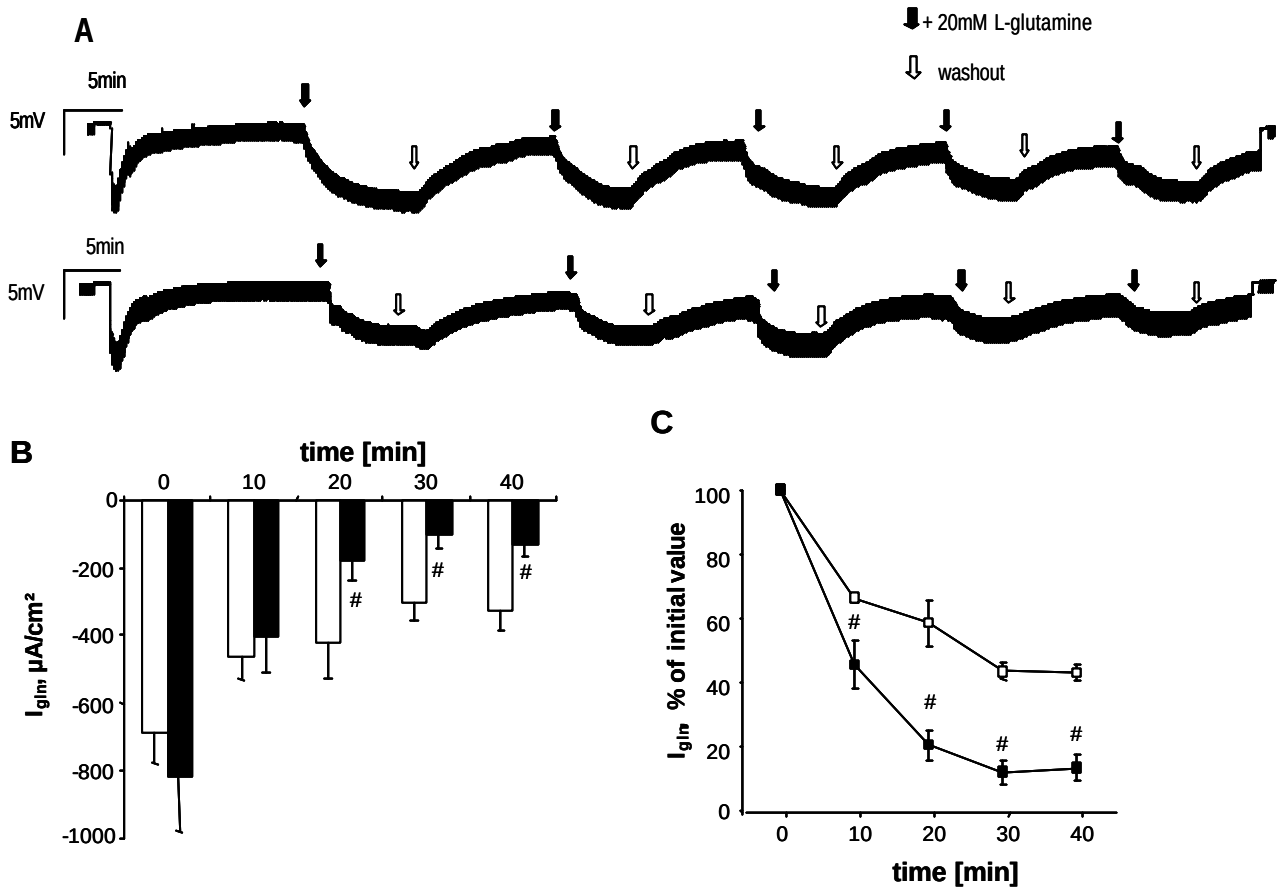

Figure 5 Effect of Wortmannin on glutamine-induced current in jejunal segments. Alterations of transepithelial voltage (? V_{gln}) and glutamine induced currents (I_{gln}) in proximal segments of jejunal tissue with or without incubation with Wortmannin (1 µM).

A Original tracings illustrating the effect of 20 mM glutamine on the transepithelial potential difference in the absence (upper panel) and presence (lower panel) of Wortmannin.
B Arithmetic means ±SEM (n=4) of glutamineinduced currents in jejunum following exposure to perfusate with Wortmannin (closed bars) or without Wortmannin (open bars).
Significant difference between presence and absence of Wortmannin.
C Arithmetic means ±SEM (n=4) of glutamine-induced current, in percent of the currents in the beginning of the experiment, following exposure to perfusate with Wortmannin (closed symbols) or without Wortmannin (open symbols).
Significant difference between presence and absence of Wortmannin

Table 1.Amino acid-induced currents following a 40 min treatment with 1 µM Wortmannin

	Control chamber		Chamber incubated with Wortmannin	
	initial value	after 40min	initial value	after 40min
Phenylalanine (n=4)	1046 ± 163	541 ± 137	1013 ± 77	174 ± 59 #
Glutamine (n=4)	689 ± 88	327 ± 59	821 ± 158	131 ± 36 #
Cysteine (n=6)	549 ± 91	201 ± 75	528 ± 89	57 ± 47 #
Proline (n=3)	815 ± 20	443 ± 134	1089 ± 181	208 ± 179 #

Substrate-induced currents (µA/cm^2) in the control chamber as well as in the chamber incubated with Wortmannin. # indicates significant difference between presence and absence of Wortmannin.

The amino acid-induced currents significantly decreased in the control chamber even in the absence of Wortmannin. This decrease was, however, significantly accelerated in the presence of Wortmannin. Within 40 min I_{phe} declined by 70 ± 7%, I_{gln} by 69 ± 8%, I_{cys} by 67 ± 8 %, and I_{pro}l by 79 ± 12%, as compared to the respective currents in the control chamber (Fig. 5, table 1).

As shown for glucose-induced currents, the PI3 kinase inhibitor LY294002 was similarly effective as Wortmannin. Following a 15 min preincubation with a luminal fluid containing 50 µM LY294002, I_{glc} gradually declined to 46 ± 9% of the original value within 40 min (Fig. 6, n=6).

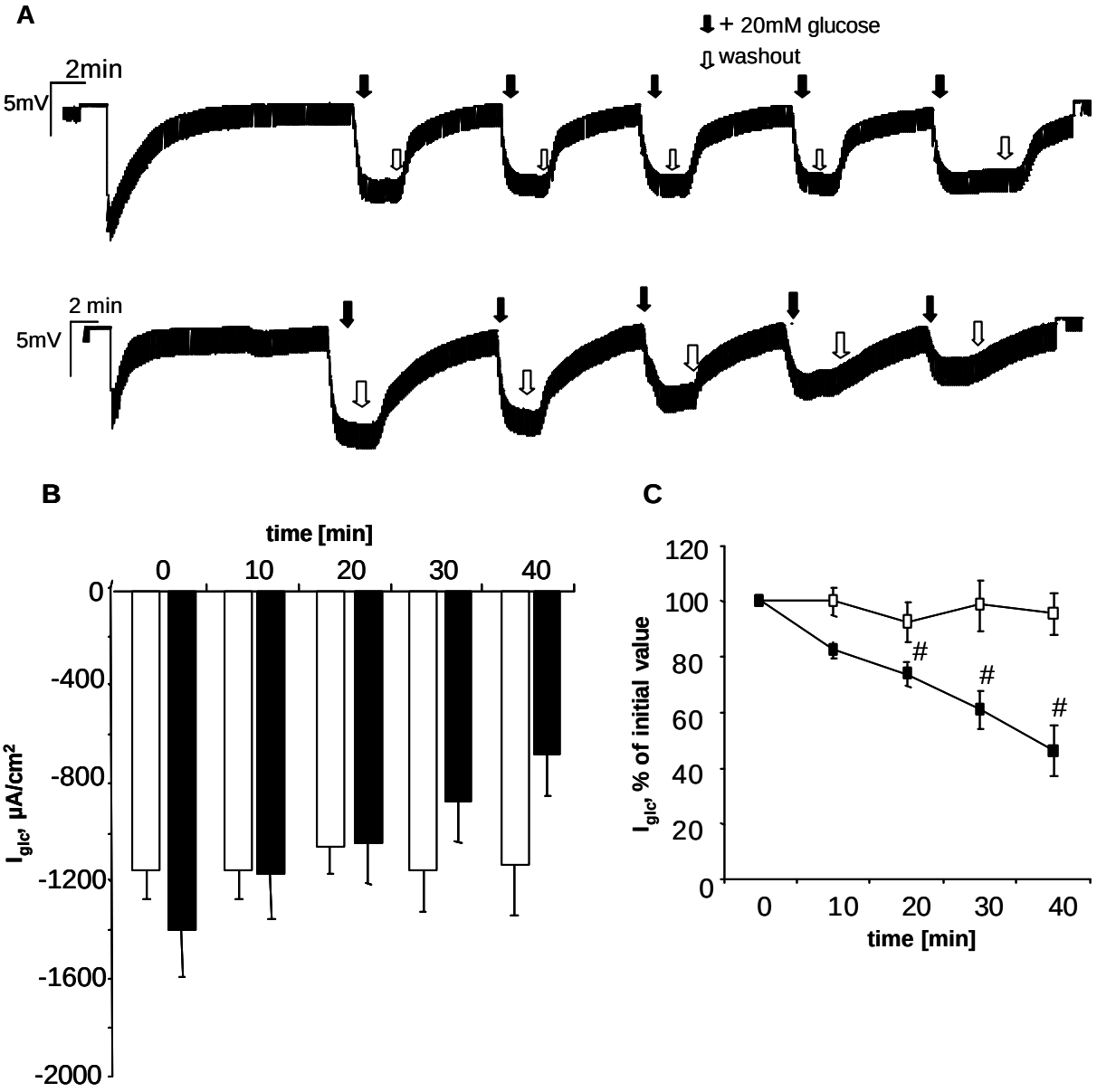

Figure 6 A Effect of LY294002 on glucose-induced current in jejunal segments. Alterations of transepithelial voltage (?V_{glc}) and glucose-induced currents (I_{glc}) in proximal segments of jejunal tissue with or without incubation with LY294002 (50 µM).

A Original tracings illustrating the effect of 20 mM glucose on the transepithelial potential difference in the absence (upper panel) and presence (lower panel) of LY294002.

B Arithmetic means ±SEM (n=5) of glucose-induced currents in jejunum following exposure to perfusate with Wortmannin (closed bars) or without Wortmannin (open bars).
#Significant difference between presence and absence of LY294002.
C Arithmetic means±SEM (n=5) of glucoseinduced currents, in percent of the currents at the beginning of the experiment, following exposure to perfusate with Wortmannin (closed symbols) or without Wortmannin (open symbols).
Significant difference between presence and absence of LY294002.

Additional experiments have been performed to test for forskolin-induced currents. Following a 15 minute treatment, the forskolin-induced current was similar in Wortmannin treated (701 ± 155 µA/cm^2) and solvent treated (700 ± 176 µA/cm^2) intestine. After 60 minutes treatment, the forskolin-induced currents decreased in both, Wortmannin treated (107 ± 27 µA/cm^2) and solvent treated (294 ± 55 µA/cm^2) intestine. After 60 minutes the current was significantly lower in Wortmannin-treated intestine.

To explore whether the decline of current was the result of tissue injury, additional experiments have been performed to elucidate the appearance of apoptosis. As shown in Fig. 7, apoptosis was similarly low following a 15 minute treatment of intestine with Wortmannin as in untreated time controls.

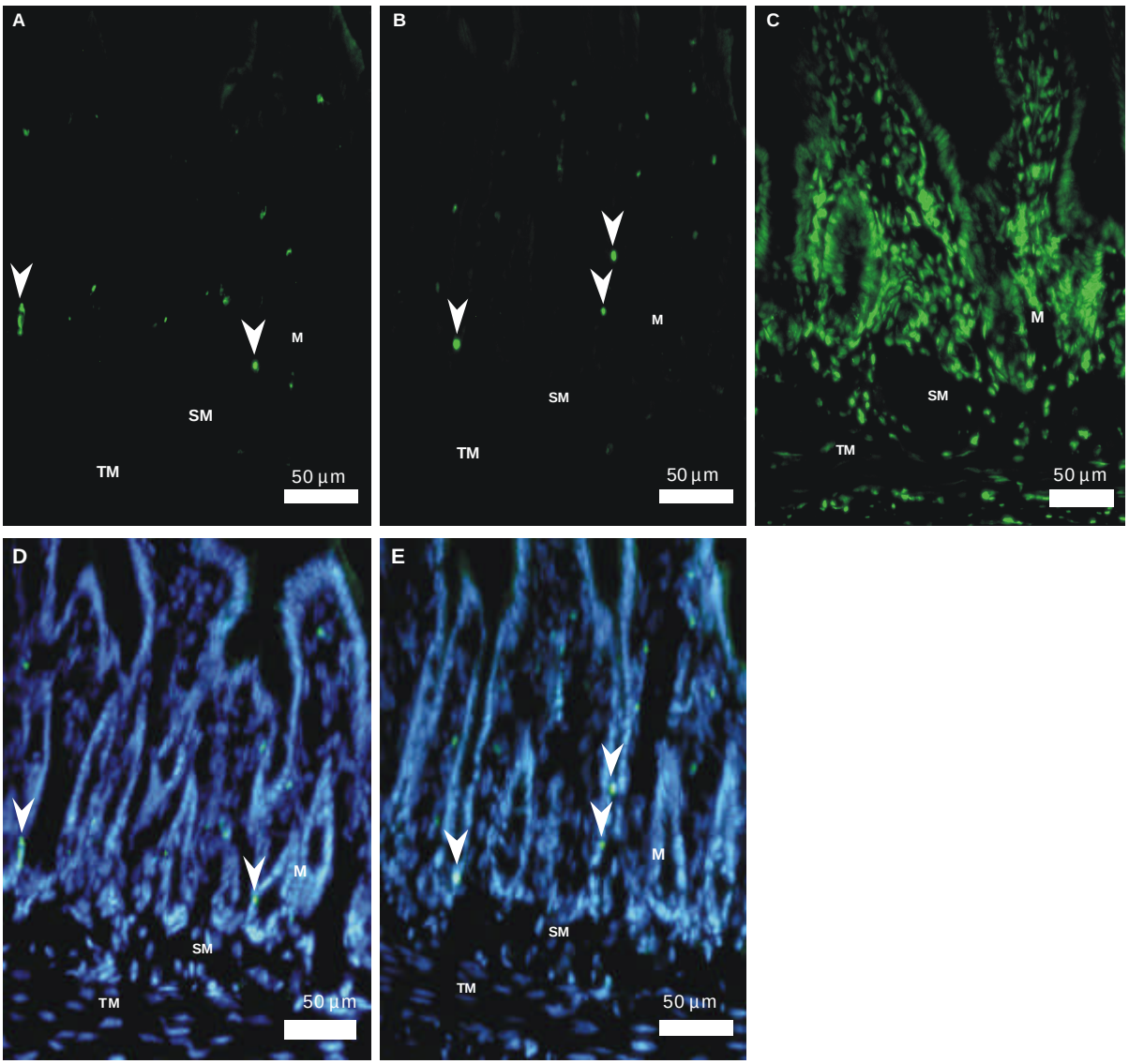

Figure 7. Apoptosis in jejunum in absence and presence of Wortmannin. TUNEL staining of representative jejunal gut sections. Only few apoptotic cells (*arrowheads*) were observed in the control tissue (**a** and **d**) and in the tissue treated with 1 µM Wortmannin for 15 min (**b** and **e**). **a**, **b** TUNEL-positive nuclei (*arrowheads*) of untreated (**a**) and treated tissue (**b**), respectively. c Sections of positive control treated with DNase I. All nuclei of intestinal tissue were TUNEL-positive.The strongly reduced DAPI staining of positive control caused by the DNase I treatment is not shown. **d**, **e** Fluorescence co-staining for DAPI (*blue*) and TUNEL-positive nuclei (*green*) of the same area shown in **a** and **b**. Scale bars=50 µm.

Abbreviations: *TM* tunica muscularis, *SM* submucosa, *M* mucosa

In contrast, strong TUNEL staining was observed following treatment of the tissue with DNase.

3.1.2 PDK1-dependent glucose transport

To determine PDK1-dependent glucose transport, segments of jejunum from $pdk1^{hm}$ and $pdk1^{wt}$ mice were mounted into mini-Ussing chambers and electrogenic glucose transport was determined utilizing electrophysiological analysis (Fig. 8).

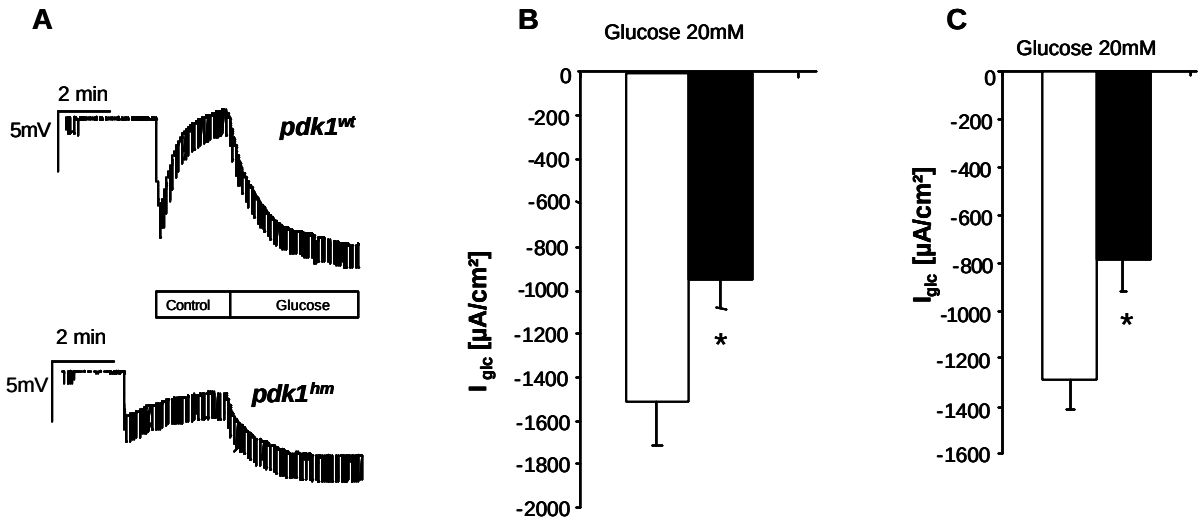

Figure 8. **Glucose-induced voltage deflections and currents in jenunal segments**. Glucose-induced alterations of transepithelial voltages and currents (Iglc) in proximal segments of jejunal tissue from phosphoinositide-dependent kinase-1 (PDK-1) hypomorphic ($pdk1^{hm}$) mice and wild-type littermates ($pdk1^{wt}$) are shown. Glucose (20 mM) was added, replacing 20 mM mannitol.

A: original tracings illustrating the effect of glucose on the transepithelial potential difference (PD). Arithmetic means SE of Iglc in proximal (**B**) and distal (**C**) jejunum from pdk1hm [solid bars, n 10 (**B**) and 11 (**C**)] and $pdk1^{wt}$ [open bars, n 13 (**B**) and 12 (**C**)] mice. *Statistically significant (P 0.05) difference between $pdk1^{hm}$ and $pdk1^{wt}$ mice.

The isoosmotic replacement of mannitol by glucose generated a lumen-negative shift of the transmural potential difference (? V_{glc}) without significantly altering the transmural resistance. The ? V_{glc} and R_{te} allowed the calculation of the glucose induced current I_{glc}. In proximal segments of $pdk1^{hm}$ I_{glc} amounted to -943 ± 139 µA/cm^2 (n = 10) for 20 mM glucose. In proximal segments of $pdk1^{wt}$ mice I_{glc} approached -1507 ± 210 µA/cm^2 (n = 13). As demonstrted in Fig. 8B, the currents were significantly smaller in proximal jejunum obtained from $pdk1^{hm}$ than in the proximal jejunum of $pdk1^{wt}$ mice.

Similar observations were made in distal jenunal segments. In distal segments of $pdk1^{hm}$ I_{glc} amounted to -785 ± 133 µA/cm^2 (n = 11) for 20 mM glucose. In distal segments of pdk^{1wt} mice I_{glc} approached -1291 ± 127 µA/cm^2 (n = 12). Again, the currents were significantly smaller in $pdk1^{hm}$ than in $pdk1^{wt}$ mice (Fig. 8*C*).

According to intracellular impalements, the potential difference across the basolateral cell membrane (PDbl) of isolated perfused straight proximal tubules (i.e. late aspects of proximal tubule) was in the absence of glucose was not different between $pdk1^{hm}$ (-54.6 ± 1.3 mV, n = 7) and $pdk1^{wt}$ (-54.9 ± 2.4 mV, n = 6) mice (Fig. 9).

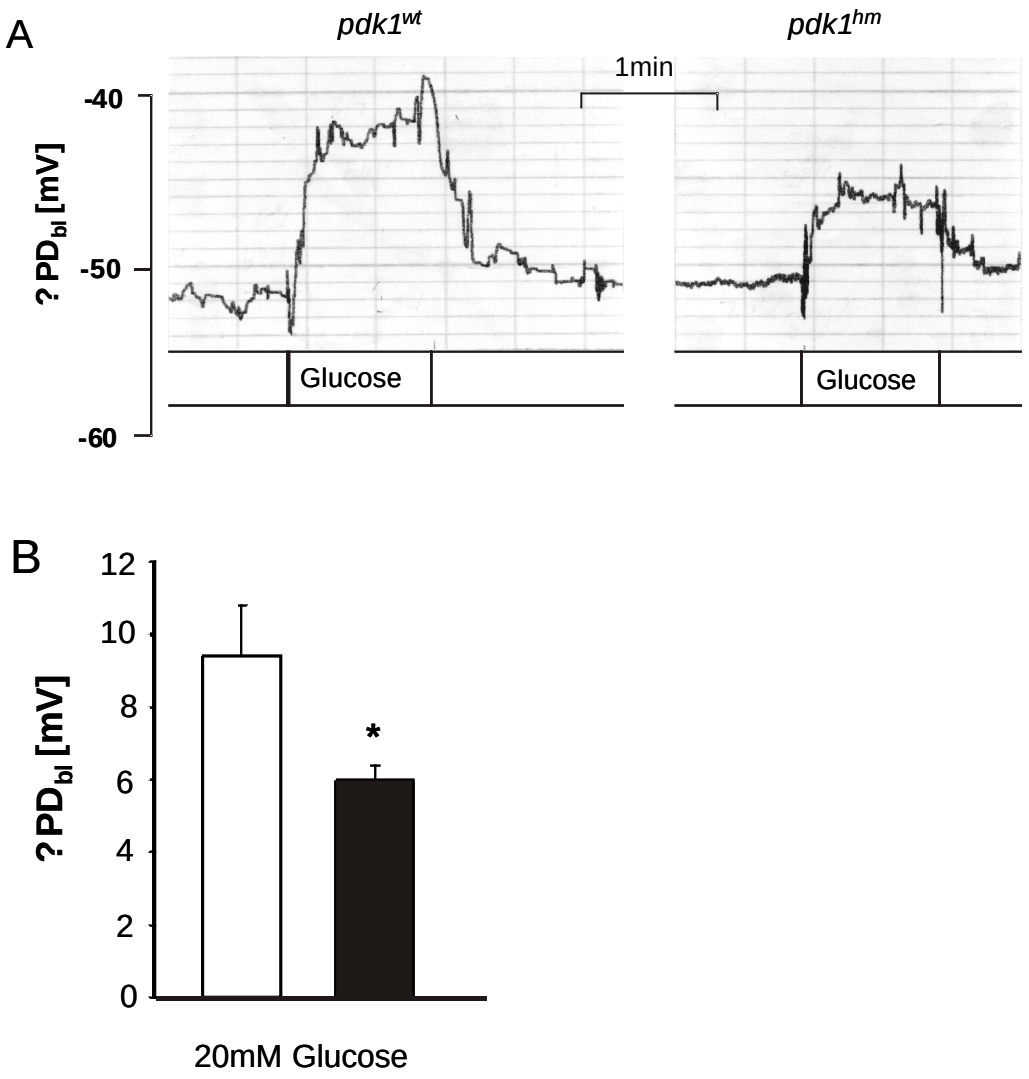

Figure 9. Effect of glucose on the PD across the basolateral cell membrane of straight proximal tubules.
A: original tracings illustrating the effect of glucose on the PD across the basolateral cell
B: arithmetic means SE of the glucose-induced depolarization of the basolateral cell membrane from *pdk1*^{hm} (solid bar, *n* 7) and *pdk1*^{wt} (open bar, *n* 6) mice.
*Statistically significant (*P*< 0.05) difference between *pdk1*^{hm} and *pdk1*^{wt} mice.

Addition of 20 mM glucose to the luminal fluid replacing mannitol significantly decreased PDbl in both, pdk1^{hm} and pdk1^{wt} mice, an effect, however, significantly smaller in pdk1^{hm} than in pdk1^{wt} mice (Fig. 9).

PDK1 could regulate electrogenic glucose transport by enhancing expression and/or by increasing the activity of expressed protein. To explore the effect of PDK1 on SGLT1 expression, immunoblotting was performed in brush border membranes of the proximal tubule, jejunum and ileum. No significant difference in SGLT1 protein abundance could be detected in the brush border membrane fraction obtained from kidney, jejunum, and ileum from pdk1hm and pdk1wt mice (n = 5 for each genotype, (Fig. 10).

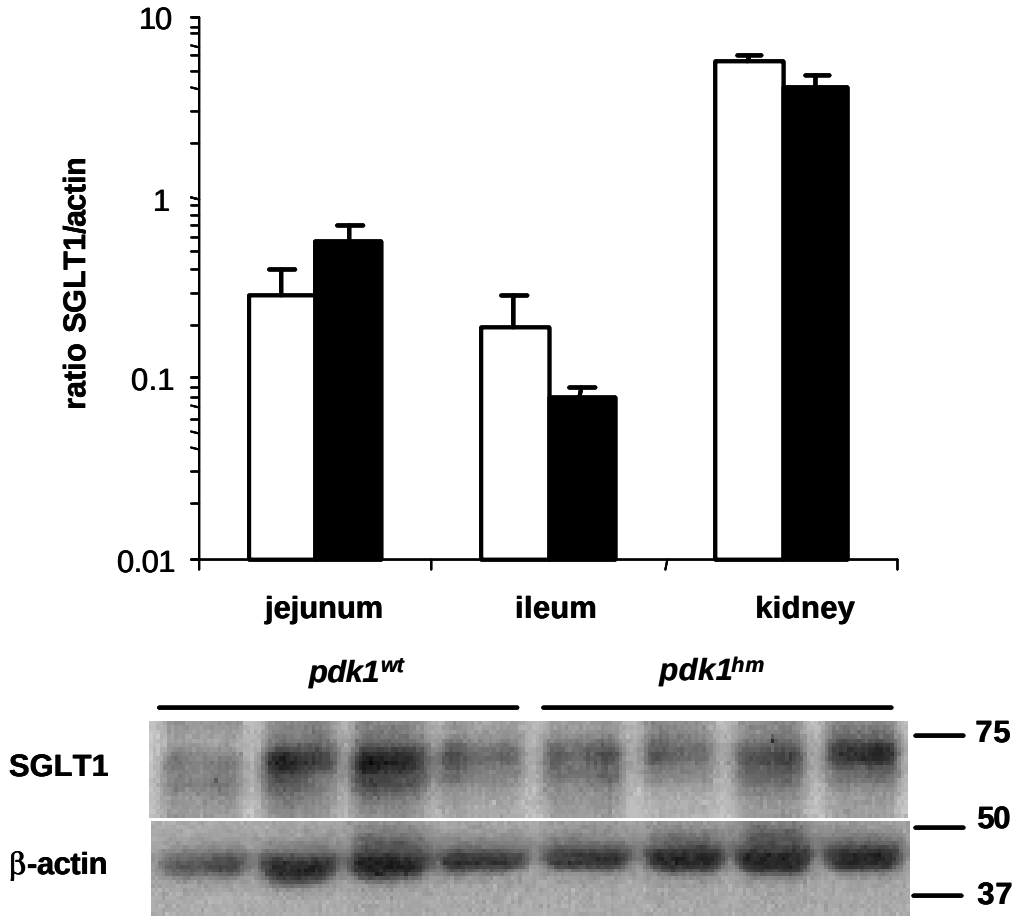

Figure 10 Abundance of sodium-dependent glucose transporter-1 (SGLT-1) in the brush-border membrane in kidney, jejunum, and ileum.
Top: arithmetic means SE of SGLT-1 expression normalized for ß-actin in brush-border membranes obtained from kidney, jejunum, and ileum of *pdk1*^{hm} and *pdk1*^{wt} mice (*n* 5 each). *Bottom*: original Western blots of SGLT-1 and -ßactin.

Further experiments were performed to elucidate the plasma concentrations and renal excretion of glucose prior to and following a glucose load of 3 g/kg bw. As illustrated in (Fig. 9), intraperitoneal injection of glucose led to a transient increase of plasma glucose concentration approaching similar values in pdk1^{hm} and pdk1^{wt} mice.

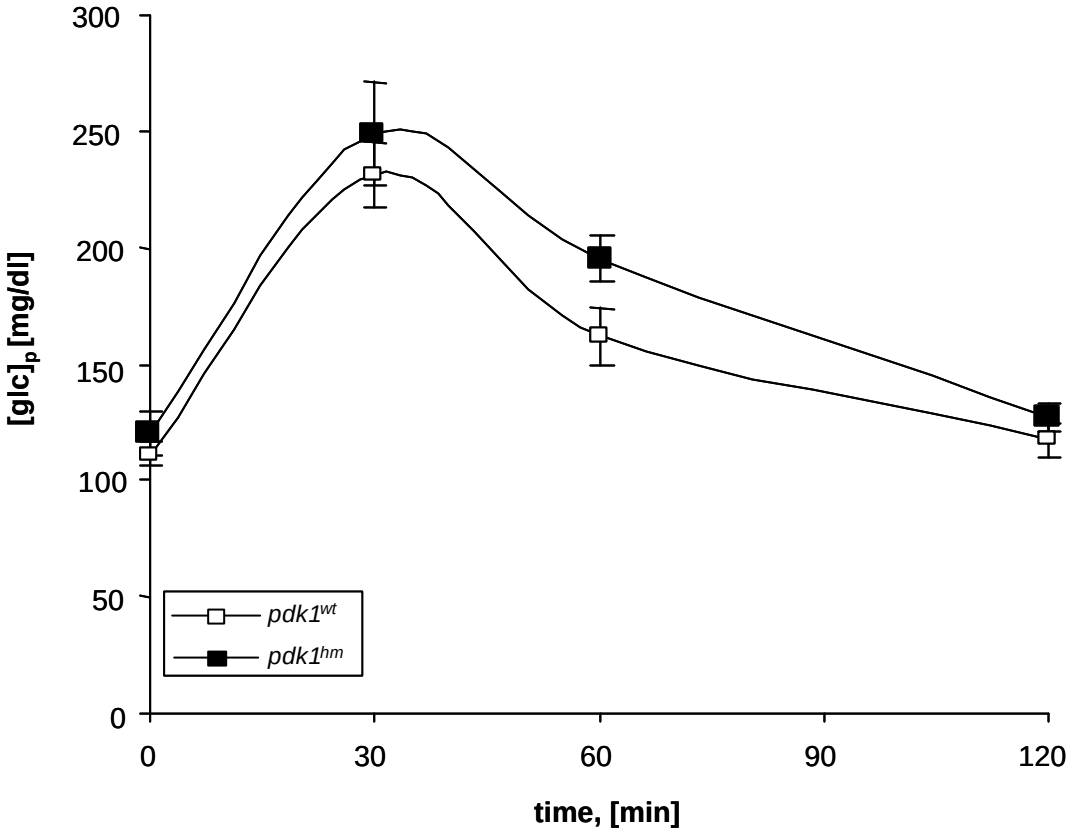

Figure 11. Plasma glucose concentrations ([glc]p) following intraperitoneal glucose injection.
Values are arithmetic means SEM (*n* 10–12) of [glc]p following intraperitoneal injection of 3 g/kg body wt glucose in $pdk1^{hm}$ (solid bar) and $pdk1^{wt}$ (open bar).

The peak glucose concentration tended to be higher and the subsequent decline of plasma glucose concentration tended to be slower in pdk1hm than in pdk1wt mice, a difference, however, not statistically significant. To explore whether the filtered glucose load during the intraperitoneal glucose injection exceeded the maximal renal tubular glucose reabsorption, mice were placed in metabolic cages and urinary glucose concentration was determined. To account for individual variations of urinary flow rate, the urinary excretion of glucose was divided by the respective creatinine excretion. As shown in (Fig. 12 and Table 2), intraperitoneal glucose administration led to a transient glucosuria which was markedly higher in $pdk1^{hm}$ than in $pdk1^{wt}$ mice.

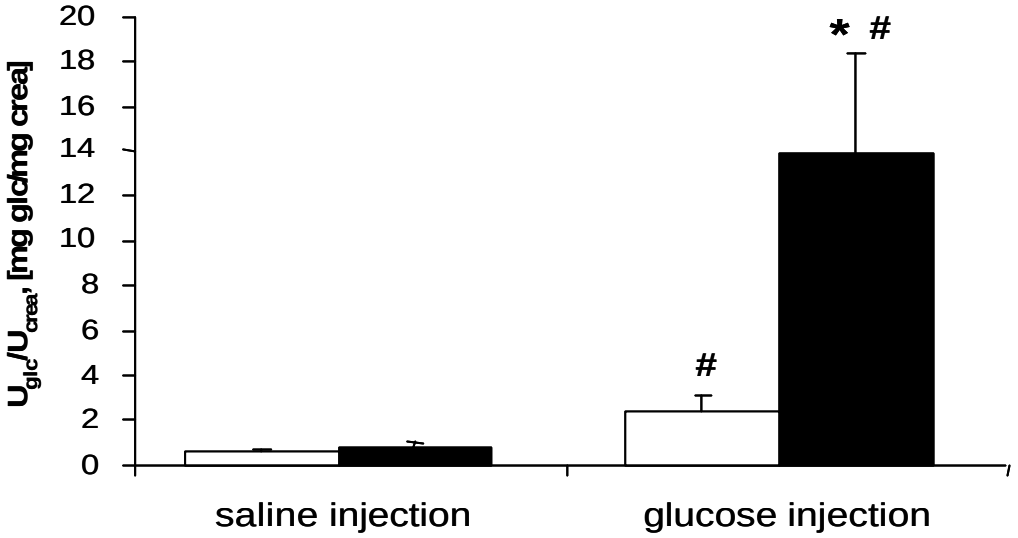

Figure 12 Urinary glucose excretion following an intraperitoneal glucose injection.Values are arithmetic means SE (*n* 9–12) of urinary glucose over creatinine concentration [U_{glc}/U_{crea}] following the intraperitoneal injection of 3 g/kg body wt glucose in *pdk1*^{hm} (solid bar) and *pdk1*^{wt} (open bar) mice.
*Statistically significant ($P < 0.05$) difference between *pdk1hm* and *dk1*^{wt} mice.
#Statistically significant ($P < 0.05$) increase following glucose injection.

Table 2.Renal excretion of glucose prior to or following a saline or a glucose load of 3 g/kg bw i.p

	Saline injection		Glucose injection	
	pdk1^{wt}	pdk1^{hm}	pdk1^{wt}	pdk1^{hm}
BW (g)	28.5 ± 1.0 (12)	21.1 ± 1.0 (12) *	26.6 ± 1.1 (12) $^{\#}$	19.1 ± 1.0 (12) *
V_u (ml/3h)	0.78 ± 0.13 (12)	0.40 ± 0.10 (12)	0.35 ± 0.05(12) $^{\#}$	0.18 ± 0.04 (10) *
U_{crea} (mg/dl)	11.2 ± 1.6 (12)	12.4 ± 1.9 (12)	15.0 ± 3.4 (12)	12.4 ± 2.5 (9)
UV_{crea} (mg/3h/g BW)	2.59 ± 0.29 12)	1.79 ± 0.27 (11)	1.35 ± 0.18 (12) $^{\#}$	0.84 ± 0.12 (10) $^{\#}$
U_{glc} (mg/dl)	6.71 ± 0.88 12)	8.38 ± 0.89 (12)	18.07 ± 5.66 (12)	96.62 ± 28.0 (10) *
UV_{glc} (mg/3h/g BW)	1.69 ± 0.33 12)	1.27 ± 0.18 (12)	2.79 ± 1.41 (12)	9.19 ± 4.06 (10)
U_{glc}/U_{crea} (mg glc /mg crea)	0.67 ± 0.09 12)	0.82 ± 0.15 (12)	2.38 ± 0.78 (12) $^{\#}$	13.81 ± 4.56 (10) *

BW = body weight, V_u = urinary volume U_{crea} = urinary creatinine concentration, UV_{crea} = urinary creatinine excretion, U_{glc} = urinary glucose concentration, UV_{glc} = urinary glucose excretion
# statistically significant ($p<0.05$) difference between saline and glucose injection * statistically significant ($p<0.05$) difference between pdk1hm and pdk1wt mice.

3.1.3 PDK1-dependent amino acid transport

As reported earlier, at the same age (32-36 weeks) body weight was significantly smaller in pdk1^{hm} mice (22.5 ± 0.9 g, n = 12) than in pdk1^{wt} mice (32.7 ± 1.3 g, n = 12). Despite lower body weight of pdk1^{hm} mice, food and water intake were similar in pdk1hm mice (3.8 ± 0.2 g/24h and 4.4 ± 0.4 ml/24h, respectively) as in pdk1^{wt} mice (3.2 ± 0.1 g/24h and 4.2 ± 0.5 ml/24h, respectively). Consequently, if expressed per g body weight, food and water intake were significantly larger in pdk1^{hm} than pdk1^{wt} mice (Fig. 13).

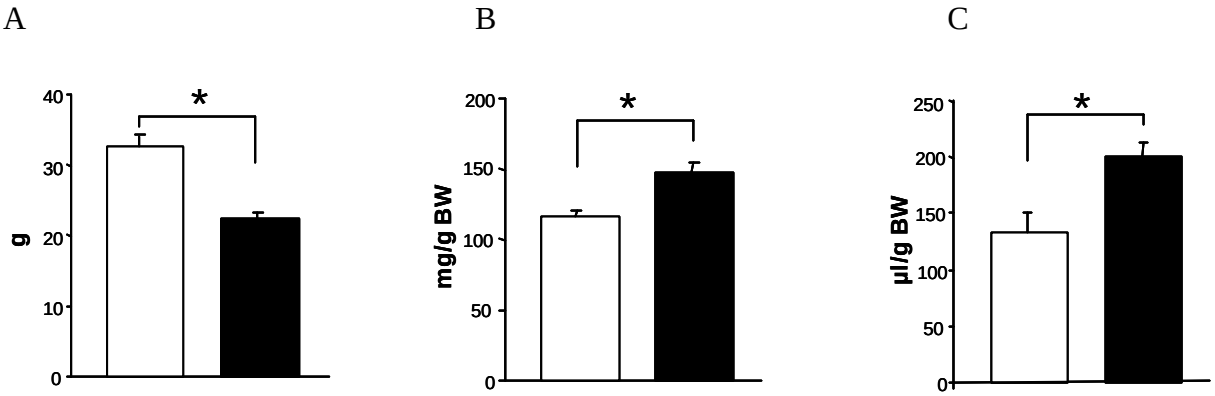

Figure 13. Body weight, food and water intake (per 24h) in *pdk1*^{hm} and *pdk1*^{wt} mice. Arithmetic means ± SE (n=12) of body weight, food and water intake of PDK1 hypomorphic mice (pdk1^{hm}, filled columns) and WT littermates (pdk1^{wt}, open columns).
*Statistically significant difference between pdk1hm and pdk1wt

In theory, growth retardation could result from defective release of growth hormone leading to decreased formation of IGF1. To explore this possibility, we determined plasma IGF-1 concentrations in both, weaning (18 days) and adult (4 months) animals. The respective values were, however, not significantly different between pdk1^{hm} mice (338 ± 43 ng/ml and 454 ± 44 ng/ml, respectively, n=7-9) and pdk1^{wt} mice (332 ± 13 ng/ml and 483 ± 64 ng/ml, respectively, n=7-9).

Further experiments were performed to determine whether altered weight was paralleled by altered intestinal transport. To determine PDK1-dependent amino acid transport, corresponding segments of jejunum from pdk1hm and pdk1wt mice were mounted into mini-Ussing chambers and electrogenic amino acid transport was determined utilizing electrophysiological analysis (Fig. 14).

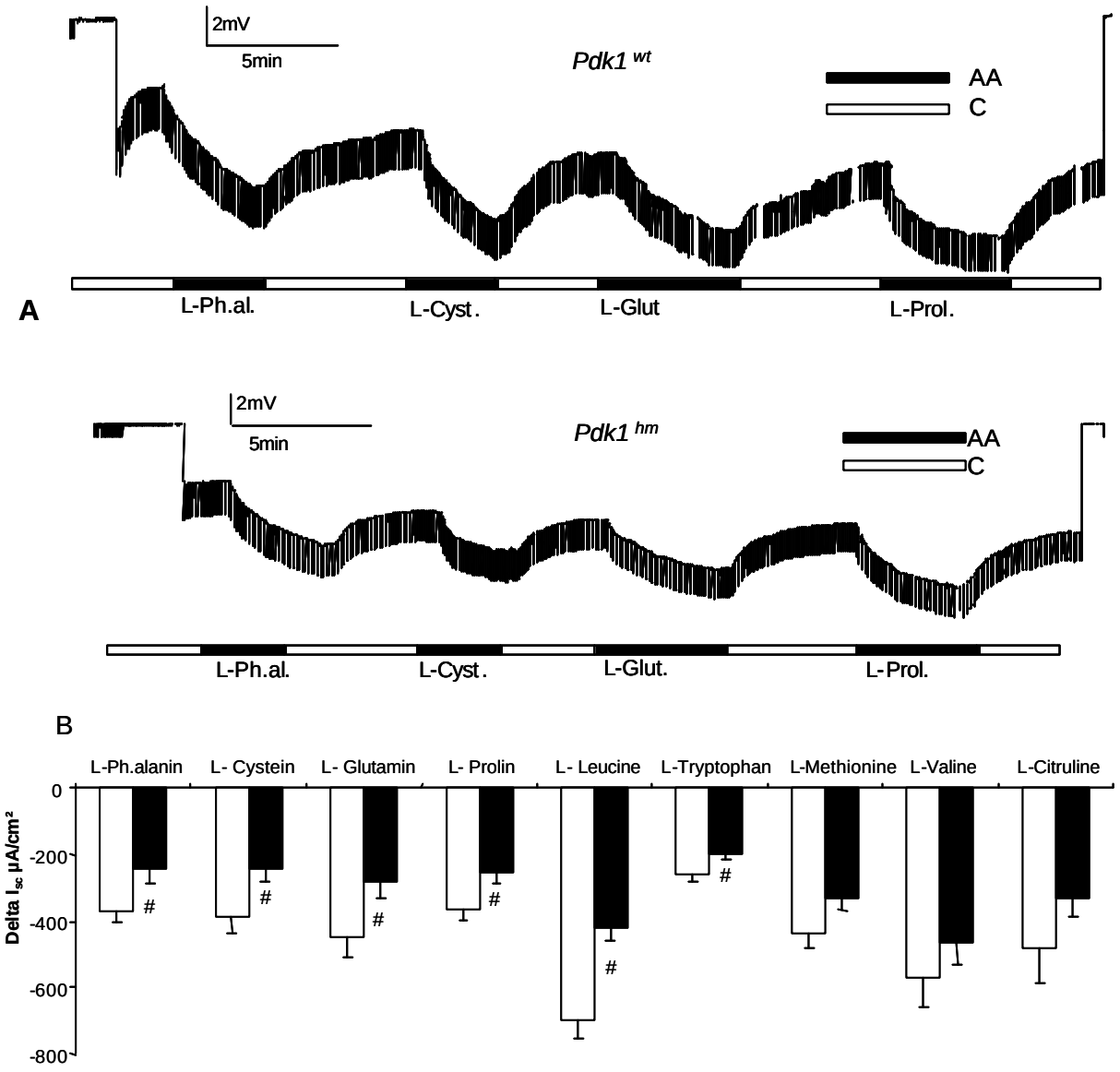

Figure 14. Amino acid-induced short circuit current ($I_{sc, aa}$) in proximal jenunal segments. Alterations of transepithelial voltages (ΔV_{aa}) and induced short circuit currents ($I_{sc,aa}$) in proximal segments of jejunal tissue from PDK1 hypomorphic mice (*pdk1*^{hm}) and WT littermates (*pdk1*^{wt}) before and after addition of phenylalanine (Phe), cysteine (Cys), glutamine (Gln), proline (Pro), leucine (Leu), tryptophan (Try), methionine (Met), valine (Val), and citrulline (Cit).
A) Original tracings illustrating the effect of amino acids on the transepithelial potential difference.
B) Arithmetic means ± SE (*n*13–14) of amino acid-induced short circuit currents in jejunum from *pdk1*^{hm} mice (open columns) and *pdk1*^{wt} mice (filled columns).
*Statistically significant difference between *pdk1*^{hm} and *pdk1*^{wt} mice.

In the absence of luminal substrates, the transepithelial potential difference (V_{te}) of jejunal segments amounted to -4.17 ± 0.33 mV (n = 13) in pdk1^{hm} mice and to -4.11 ± 0.24 mV (n = 14) in pdk1^{wt} mice. The transepithelial resistance (R_{te}) approached 9.4 ± 0.7 O · cm2 (n = 13) in pdk1^{hm} mice and 8.3 ± 0.4 O cm^2 (n = 14) in pdk1^{wt} mice. Neither transepithelial potential difference nor transepithelial resistance were significantly different between pdk1^{hm} and pdk1^{wt} mice. Accordingly, calculated basal short circuit

current (I_{sc}, basal) was also not different between the two genotypes, reaching -472 ± 56 µA/cm^2 in pdk1^{hm} mice and -514 ± 46 µA/cm^2 in pdk1^{wt} mice, respectively.

The iso-osmotic replacement of mannitol by phenylalanine, cysteine, glutamine, proline or leucine created a lumen-negative shift of the transepithelial potential difference (? V_{aa}) without significantly altering the transepithelial resistance. The ? V_{aa} and R_{te} allowed the calculation of the amino acid induced short-circuit current ($I_{sc,aa}$). The $I_{sc,aa}$ was smaller in pdk1^{hm} than in pdk1^{wt} mice, a difference reaching statistical significance for phenylalanine, cysteine, glutamine, proline, leucine and tryptophan (Table 3, Fig. 14). The currents induced by methionine, valine and citrulline tended to be lower in pdk1^{hm} mice, a difference, however, not reaching statistical significance between the genotypes (Table 3, Fig. 14).

Table 3. Amino acid induced currents in jejunum.

Amino acid	Current in *pdk1^{wt}*	Current in *pdk1^{hm}*	n
phenylalanine	-373 ± 33	-245 ± 44*	13-14
cysteine	-389 ± 47	-243 ± 35*	13-14
glutamine	-447 ± 62	-284 ± 49*	13-14
proline	-367 ± 30	-254 ± 36*	13-14
leucine	-697 ± 57	-423 ± 35*	5
tryptophan	-260 ± 20	-196 ± 19*	6
methionine	-435 ± 44	-334 ± 35	6
valine	-568 ± 90	-462 ± 70	6
citrulline	-478 ± 110	-333 ± 56	6

Arithmetic means ± SEM of the currents (in µA/cm^2) generated by the respective amino acids (20 mM).

* statistically significant difference between pdk1hm and pdk1wt mice, n = number of mice studied.

Similar to intestine, proximal renal tubules display decreased electrogenic transport of amino acids. As illustrated in (Fig. 15), the potential difference across the basolateral cell membrane (PDbl) of isolated perfused straight proximal tubules (i.e. late parts of proximal tubule) was in the absence of amino acids not significantly different between pdk1hm mice (-51.4 ± 2.5, n = 13) and pdk1wt mice (-54.4 ± 1.5 mV, n = 14). Addition of 20 mM L-phenylalanine, L-glutamine or L-proline, respectively, to the luminal fluid significantly decreased PDbl in both, pdk1hm and pdk1wt mice, an effect, however, significantly smaller in pdk1^{hm} than in pdk1^{wt} mice (Fig. 15).

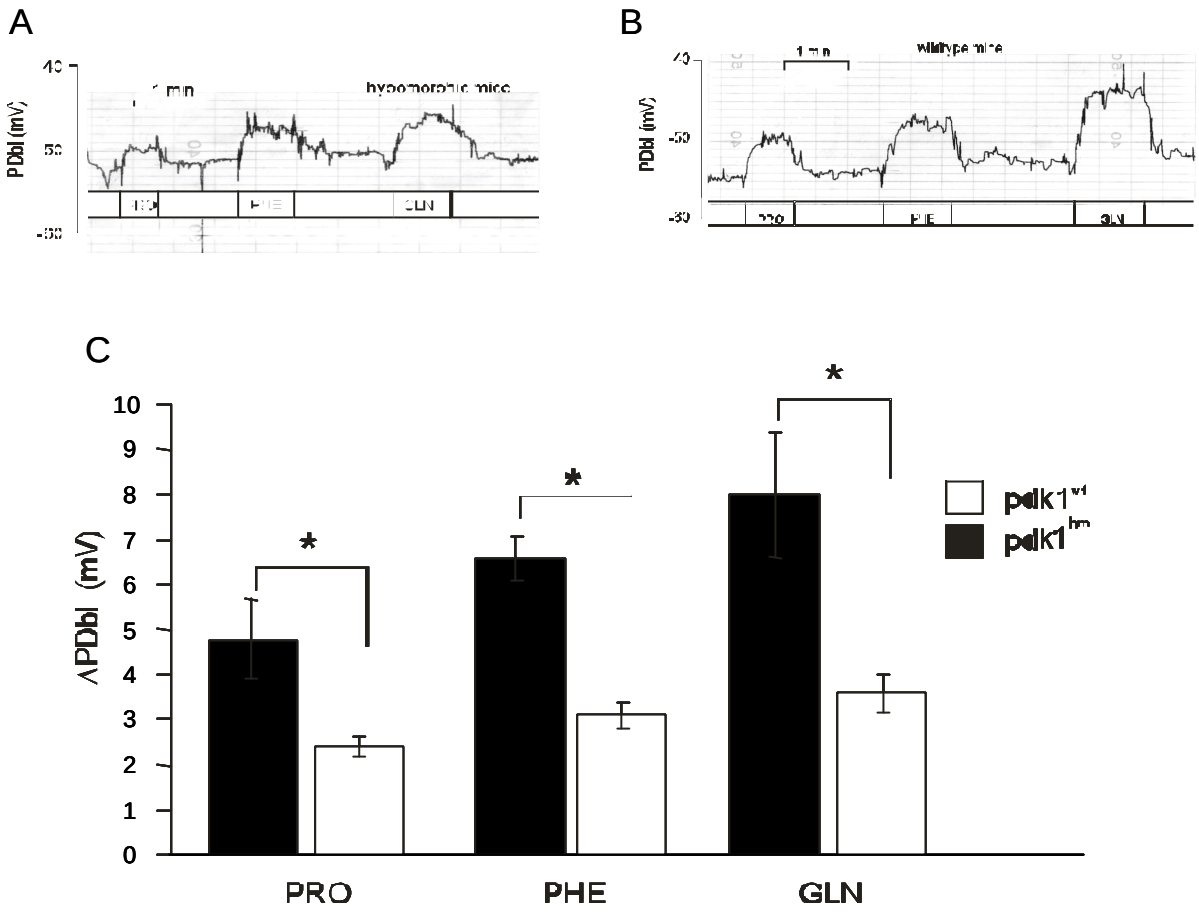

Figure 15. Effect of amino acids on the potential difference across the basolateral cell membrane of straight proximal tubules.

A, B) Original tracings illustrating the effect of the luminal application of 20 mM phenylalanine (Phe), glutamine (GLN), and proline (PRO) in the presence of the K channel blocker Ba^{2+} (1mM) on the potential difference across the basolateral cell membrane of straight proximal tubules (PD_{bl}) from PDK1 hypomorphic mice (*pdk1*^{hm}) and WT littermates (*pdk1*^{wt}).

C) Arithmetic means ±se of the depolarization of the basolateral cell membrane from *pdk1*^{hm} mice (open columns) and *pdk1*^{wt} mice (filled columns) following the luminal replacement of 20 mM mannitol with 20 mM phenylalanine (*n* 5 *pdk1*^{hm} and 6 *pdk1*^{wt}), glutamine (*n*5 *pdk1*^{hm} and 5 *pdk1*^{wt}) or proline (*n*3 *pdk1*^{hm} and 3 *pdk1*^{wt}).

*Statistically significant difference between *pdk1*^{hm} and *pdk1*^{wt} mice.

In order to assess the abundance of major amino acid transporter proteins expressed in the brush border membrane of the proximal tubule, immunoblotting was performed with isolated brush border membranes from kidney. A reduced abundance of the major renal Na^+-dependent amino acid transporter for neutral amino acids, B^0AT1 (SLC6A19), was found (Fig. 16).

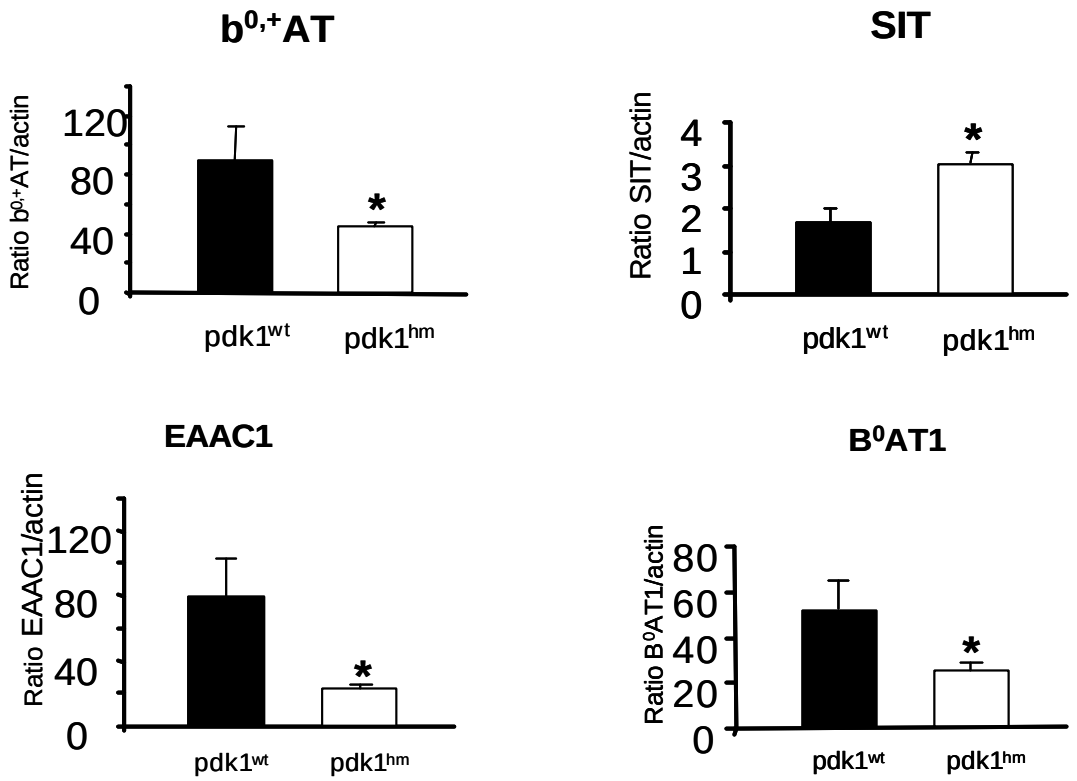

Figure 16. **Abundance of amino acid transporters in kidney brush border membrane. A***)* Immunoblots for b^0,AT (SLC7A9), SIT (SLC6A20), EAAC1 (SLC1A1), B^0AT1 (SLC6A19) amino acid transporters, and actin demonstrate the significant reduction in protein abundance of b^0,AT, EAAC1, B^0AT1, and increased expression of SIT amino acid transporters in the renal brush border membrane of *pdk1*^{hm} mice.
B*)* Bar graphs summarizing quantification of amino acid transporter abundance normalized for loading with actin (ratio transporter/actin).
*Statistically significant differences between *pdk1*^{wt} (open columns) and *pdk1*^{hm} (open columns) mice (*n*5 for each genotype).

In parallel, the abundance of the Na^+-dependent glutamate transporter EAAC1/ EAAT3 (SLC1A1) was decreased. Also expression of the $b^{0,+}$AT (SLC7A9) protein, the catalytic subunit of system $b^{0,+}$ responsible for the reabsorption of cationic amino acids and cystine, was reduced. The expression of the Na^+,proline cotransporter SIT (SLC6A20) was, however, enhanced in the pdk1hm kidney. Thus, at least in the kidney, decreased expression of several major renal amino acid transporters contributes to the impaired amino acid reabsorption in PDK1 hypomorphic mice.

Further experiments were performed to elucidate the plasma concentrations and renal excretion of the amino acids. As evident from Table 4, the plasma concentration of none of the amino acids was significantly different between *pdk1*^{hm} and *pdk1*^{wt} mice.

Table 4. Plasma concentrations of amino acids in pdk1^{hm}and pdk1^{wt} mice

	pdk1 ^{wt}	pdk1 ^{hm}
Glycine	275.4 ± 29.4	279.8 ± 32.7
Alanine	398.9 ± 64.7	375.7 ± 54.8
Aminobutyrate	23.2 ± 2.7	18.9 ± 1.6
Serine	38.7 ± 5.9	34.9 ± 5.4
Proline	53.2 ± 11.7	66.2 ± 16.1
Valine	223.2 ± 28.8	269.5 ± 36.5
Threonine	31.3 ± 6.0	37.3 ± 6.7
5-Oxoproline	15.9 ± 1.6	16.5 ± 1.3
Leucine+Isoleucine	216.0 ± 23.7	250.0 ± 32.8
Asparagine	34.2 ± 4.3	43.3 ± 5.6
Methionine	71.5 ± 11.1	83.2 ± 11.4
Histidine	33.9 ± 2.2	32.5 ± 1.7
Citrulline	53.4 ± 4.3	55.6 ± 4.5
Phenylalanine	110.8 ± 12.8	118.2 ± 16.7
Methylhistidine	44.3 ± 2.6	43.6 ± 2.3
Tyrosine	140.9 ± 21.2	138.2 ± 17.1
Aspartate	23.7 ± 3.7	24.7 ± 4.5
Glutamate/Glutamine	71.5 ± 8.1	60.3 ± 8.3
Tryptophan	20.1 ± 2.2	18.2 ± 2.2
Aminoadipate	5.1 0.9	6.8 ± 1.3
N-Acetylasparaginic acid	2.1 ± 0.4	1.6 ± 0.3
Ornithine	49.2 ± 6.4	70.4 ± 12.8

Arithmetic means ± SEM (n = 11) of the individual amino acid concentrations in plasma (µM) from PDK1 hypomorphic (pdk1^{hm}) mice and wild type littermates (pdk1^{wt}).

Table 5 shows the urinary excretion of creatinine and amino acids. The average daily urinary creatinine excretion was not significantly different between pdk1hm mice (17.6 ± 1.2 µg/24h/g BW) and pdk1wt mice (15.7 ± 0.7 µg/24h/g BW). To account for individual variations of urinary concentration, the daily urinary excretion of individual amino acids was divided by the respective daily creatinine excretion.

Table 5. Urinary excretion of amino acids in pdk1^{hm}and pdk1^{wt} mice.

	pdk1 ^{wt}	pdk1 ^{hm}
Glycine	496.3 ± 86.4	526.5 ± 110.7
Alanine	143.8 ± 22.9	208.9 ± 110.7
Proline	17.0 ± 2.7	34.3 ± 10.6 *
Valine	19.4 ± 2.3	27.5 ± 3.7 *
Guanidinoacetate	301.7 ± 32.3	414.6 ± 52.0 *
Leucine	153.5 ± 78.3	140.7 ± 73.2
Creatine	2286.5 ± 263.4	2476.4 ± 272.6
Ornithine	5.6 ± 1.4	6.4 ± 1.4
Lysine	21.3 ± 6.7	15.6 ± 5.0
Methionine	53.4 ± 8.4	94.1 ± 20.0 *
Histidine	8.2 ± 1.4	15.3 ± 6.7
Phenylalanine	11.1 ± 1.3	17.6 ± 2.5 *
Arginine	8.2 ± 2.3	11.8 ± 2.9
Citrulline	8.5 ± 1.9	14.2 ± 3.0 *
Tyrosine	28.9 ± 2.6	45.6 ± 10.7
Glutamine/glutamate	53.9 ± 7.6	105.3 ± 25.2 *
Tryptophan	4.4 ± 0.5	6.8 ± 1.5 *
5-Hydroxytryphtophane	0.4 ± 0.2	0.7 ± 0.2
Cystine	7.17 ± 1.5	9.1 ± 1.9
Homocystine	0.20 ± 0.1	0.26 ± 0.1

Arithmetic means ± SEM (n=12-14) of the urinary excretion of individual amino acid excretion (in mmol/mol creatinine) from PDK1 deficient (pdk1^{hm}) mice and wild type littermates (pdk1^{wt}). * statistically significant difference between pdk1^{hm} and pdk1^{wt} mice

As indicated in Table 5, renal excretions of several amino acids were larger in pdk1^{hm} than in pdk1^{wt} mice, differences reaching statistical significance for proline, valine, guanidinoacetate, methionine, phenylalanine, citrulline, glutamine/glutamate and tryptophan.

3.1.4 SGK3-dependent regulation of SGLT1

As reported previously (57), SGK3 knockout mice (sgk3$^{-/-}$) gain weight after birth slightly

slower than their wild type littermates ($sgk3^{+/+}$). However, at the age under study (5-7 months after birth) the weight was virtually identical in $sgk3^{-/-}$ (29.1 ± 0.9 g, n = 10) and $sgk3^{+/+}$ mice (29.4 ± 1.1 g, n = 10).

As evident from in situ hybridization (Fig. 17), SGK3 was expressed in small intestine.

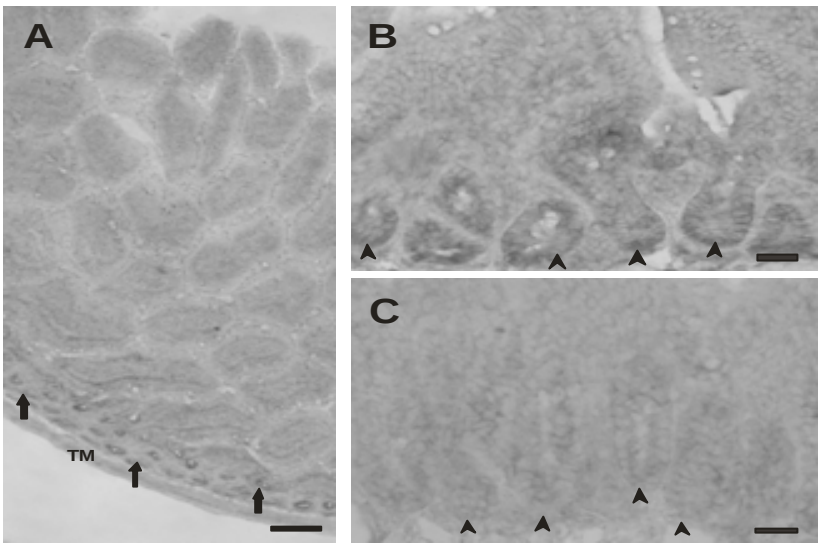

Figure 17. In situ hybridization for SGK-3 mRNA on cryostat sections of the adult jejunum
A: Overview of SGK-3 expression in the jejunum. *Arrows* point to stained crypts of Lieberkuhn; *TM*: tunica muscularis; *scale bar* 100 µm.
B: High magnification photomicrograph of SGK-3 expression in the jejunum. Note the expression of epithelial cells in the crypts (*arrowheads*), *scale bar*: 25 µm.
C: SGK-3 mRNA in situ hybridization of jejunum from $SGK3^{-/-}$ mouse. *Arrowheads* point to the base of crypts; scale bar: 25 µm.

Transcript levels were particularly high in crypts but are also detectable in more apical regions of the villi.

Food intake of $sgk3^{-/-}$ mice (4.62 ± 0.15 g/24h, n=10) was significantly ($p<0.003$) larger than food intake of $sgk3^{+/+}$ mice (3.71 ± 0.23 g/24h, n=10) while drinking volume was not significantly different between $sgk3^{-/-}$ mice (6.56 ± 0.32 ml/d, n = 10) and $sgk3^{+/+}$ mice (6.83 ± 0.39 ml/d, n = 10). Fecal weight was significantly ($p<0.027$) larger in $sgk3^{-/-}$ mice (37.80 ± 2.28 mg/g BW/24h, n=10) than in sgk3+/+ mice (28.50 ± 3.12 mg/g BW/24h, n=10). The difference in fecal weight was paralleled by significantly ($p<0.035$) larger fecal K+ excretion in $sgk3^{-/-}$ mice (6.99 ± 0.52 µmol/ g BW/24h, n=10) than in $sgk3^{+/+}$ mice (5.42 ± 0.46 µmol/g BW/24h, n=10). Fecal excretion of Na^+ and phosphorus (Pi) tended to be higher in $sgk3^{-/-}$ than in $sgk3^{+/+}$ mice (Fig. 18), a difference, however, not statistically significant ($p= 0.129$ and $p=0.057$ respectively).

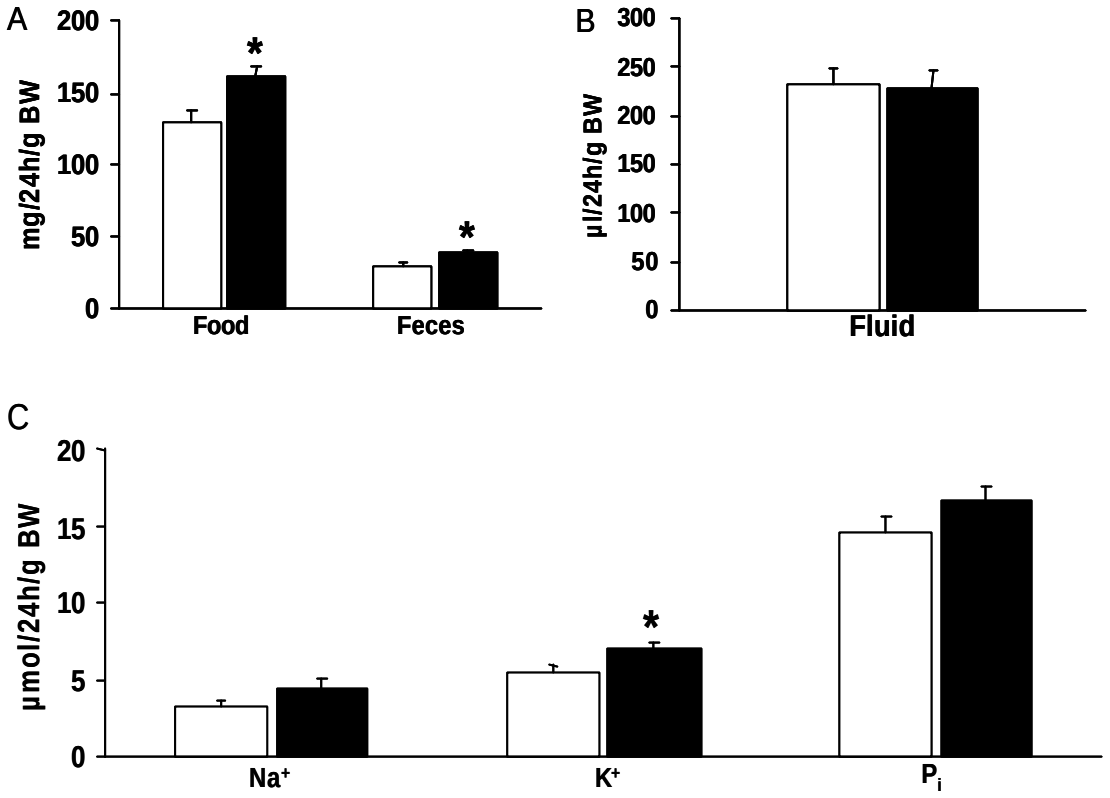

Figure 18. Food and water intake, fecal weight and fecal sodium, potassium and phosphorus.
Arithmetic means ± SEM (n = 10 each) of food and water intake, fecal weight (**A** and **B**) and fecal sodium, potassium and inorganic phosphorus content (**C**) in $sgk3^{+/+}$ mice (open columns) and $sgk3^{-/-}$ mice (closed columns).* Indicates statistically significant difference ($p<0.05$) between $sgk3^{+/+}$ and $sgk3^{-/-}$ mice.

To elucidate the in vivo significance of SGK3-dependent regulation of SGLT1, proximal and distal segments of jejunum from $sgk3^{-/-}$ and $sgk3^{+/+}$ mice were mounted into mini-Ussing chambers and Na^+ coupled glucose transport was determined utilizing electrophysiological analysis (Fig. 19).

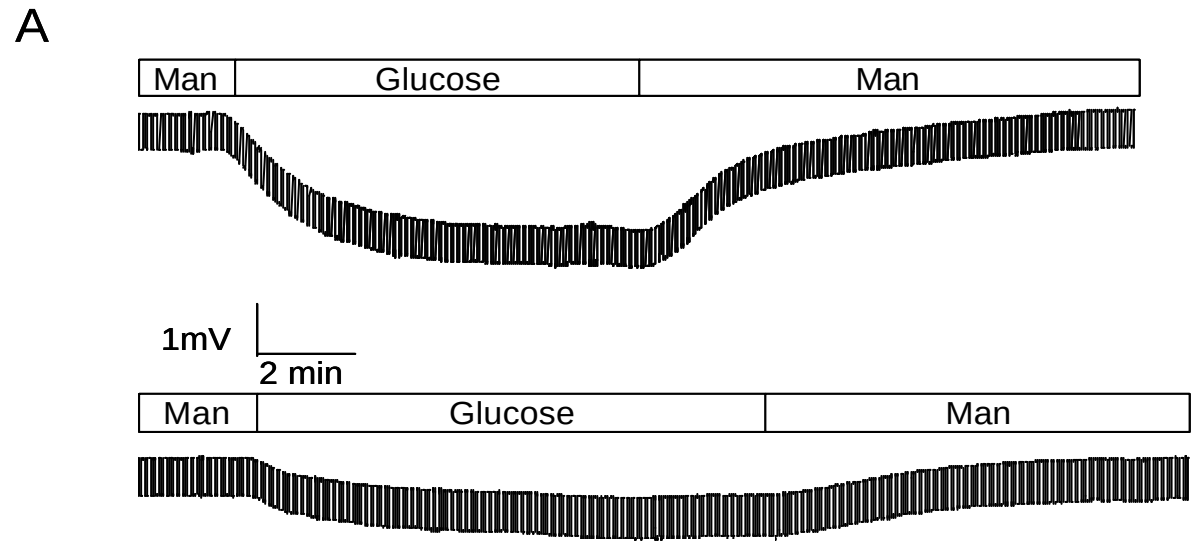

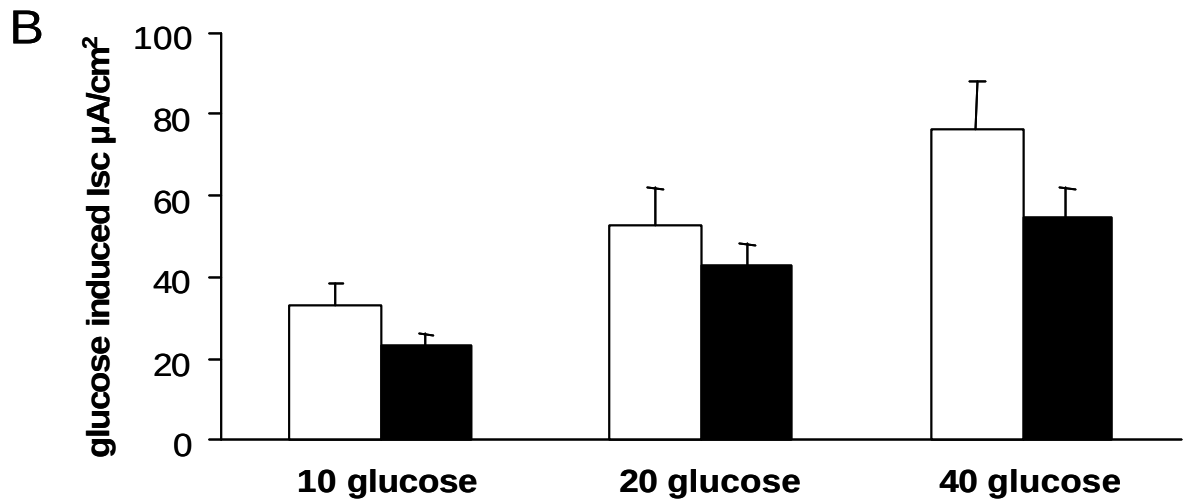

Figure 19. Glucose induced currents (Ig,p) in proximal intestinal segments
Glucose induced alterations of transepithelial voltages (**A**) and glucose induced currents (**B**) in proximal segments of jejunal tissue from *sgk3*$^{-/-}$ and *sgk1*$^{+/+}$ mice.
A: Original tracings illustrating the effect of 20 mM glucose replacing 20 mM mannitol (Man) on the transepithelial potential difference in *sgk1*$^{+/+}$ mice (upper panel) and *sgk3*$^{-/-}$ mice (lower panel). The voltage deflections are due to repetitive injections of test currents (1 µA).
B: Arithmetic means ± SEM (n = 15-19) of glucose induced currents in proximal jejunum from *sgk3*$^{+/+}$ mice (*open columns*) and *sgk3*$^{-/-}$ mice (*closed columns*).

In the absence of luminal substrates, the transepithelial potential difference ($V_{t,p}$) of proximal intestinal segments amounted to -0.61 ± 0.11 mV (n = 19) in untreated sgk3$^{-/-}$ mice and to -0.67 ± 0.12 mV (n = 15) in untreated sgk3$^{+/+}$ mice. The transepithelial resistance ($R_{t,p}$) approached 23.75 ± 2.02 O*cm^2 (n = 19) in sgk3$^{-/-}$ mice and 24.55 ± 1.86 O*cm^2 (n = 15) in sgk3$^{+/+}$mice. Neither transepithelial potential difference nor transepithelial resistance were significantly different between sgk3$^{-/-}$ and sgk3$^{+/+}$mice.
The partial isoosmotic replacement of mannitol by glucose created a lumen-negative shift of the transepithelial potential difference (?$V_{g,p}$) without significantly altering the transepithelial resistance (Fig. 20). In proximal jejunum the glucose induced current (Ig,p) at 10, 20 and 40 mmol/l glucose amounted to -23.35 ± 2.69 µA/cm^2; -42.65 ± 5.39 µA/cm^2 and -56.16 ± 7.08 µA/cm^2 (n=19) in sgk3 $^{-/-}$ mice and to -32.87 ± 5.56 µA/cm2, -52.71 ± 9.13 µA/cm^2 and -76.25 ± 12.02 µA/cm^2 (n=15) in sgk3$^{+/+}$mice. The increase in the proximal intestinal transepithelial potential difference following partial isosmotic replacement of mannitol by glucose tended to be smaller in sgk3$^{-/-}$ mice than in sgk3$^{+/+}$ mice, a difference, however, not reaching statistical significance (10 mM p =0.139, 20 mM p= 0.324, 40 mM p= 0.1404). In both genotypes the glucose induced currents did not saturate at high glucose concentrations which are well beyond the concentrations required for saturating SGLT1 (99;100). Presumably, unstirred layers lead to much lower concentrations at the carrier and thus to seemingly low affinity of transport.

The transepithelial potential difference ($V_{t,d}$) of distal intestinal segments in the absence of luminal glucose amounted to -1.00 ± 0.10 mV (n = 27) in untreated $sgk3^{-/-}$ mice and to -0.82 ± 0.09 mV (n = 27) in untreated $sgk3^{+/+}$ mice. The transepithelial resistance of distal intestinal segments ($R_{t,d}$) approached 33.21 ± 2.12 O*cm^2 (n = 27) in $sgk3^{-/-}$ mice and 29.20 ± 1.75 O*cm^2 (n = 27) in $sgk3^{+/+}$mice. (Fig.20).

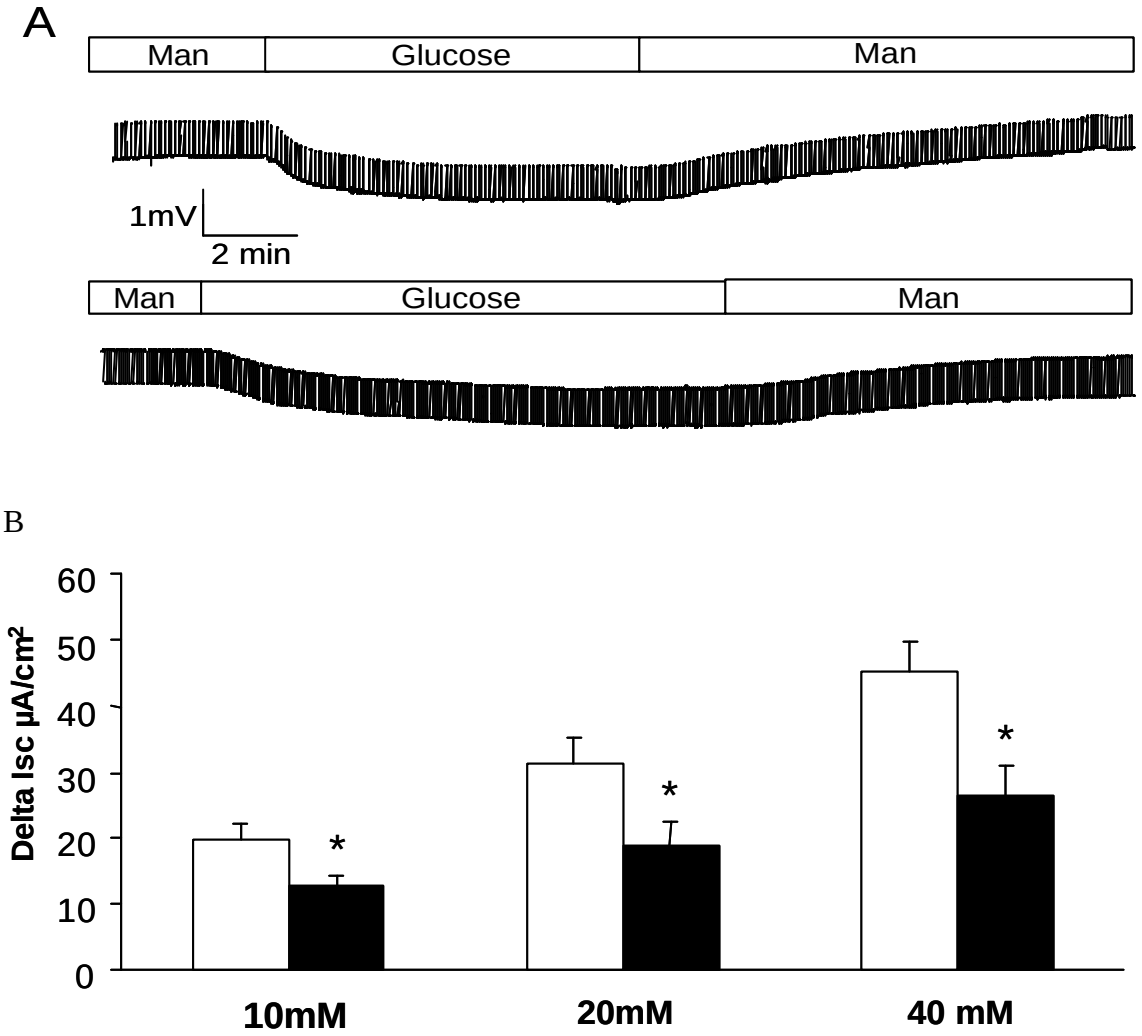

Figure 20.Glucose induced currents (Ig,d) in distal intestinal segments
Glucose induced alterations of transepithelial voltages (**A**) and glucose induced currents (**B**) in distal segments of jejunal tissue from SGK3 knockout mice ($sgk3^{-/-}$) and their wild type littermates ($sgk3^{+/+}$).
A: Original tracings illustrating the effect of 20mM glucose replacing 20 mM mannitol (Man) on the transepithelial potential difference in $sgk1^{+/+}$ mice (upper panel) and $sgk3^{-/-}$ mice (lower panel). The voltage deflections are due to repetitive injections of test currents (1 µA).
B: Arithmetic means ± SEM (n = 27) of glucose induced currents in distal jejunum from $sgk3^{+/+}$ (open columns) and $sgk3^{-/-}$ mice (closed columns).
*Indicates statistically significant difference ($p<0.05$) between $sgk3^{+/+}$ and $sgk3^{-/-}$ mice.

The transepithelial resistance of distal intestinal segments ($R_{t,d}$) approached 33.21 ± 2.12 O*cm^2 (n = 27) in $sgk3^{-/-}$ mice and 29.20 ± 1.75 O*cm^2 (n = 27) in $sgk3^{+/+}$ mice.

As in proximal intestinal segments, neither transepithelial potential difference nor transepithelial resistance were significantly different between $sgk3^{-/-}$ and $sgk3^{+/+}$mice. The

increase in the distal intestinal Ig,d following partial isoosmotic replacement of mannitol by glucose was at all three concentrations tested significantly smaller in $sgk3^{-/-}$ mice (-12.58 ± 1.61 µA/cm^2; -18.96 ± 3.54 µA/cm^2 and -26.36 ± 4.71 µA/cm^2, n=27) than in $sgk3^{+/+}$ mice (-19.95 ± 2.23 µA/cm^2, -31.22 ± 4.72 µA/cm^2 and -44.98 ± 4.72 µA/cm^2, n=27). Moreover, the current in the presence of 40 mmol/l glucose which was sensitive to the SGLT1 blocker phloridzin (200 µM) was significantly smaller in $sgk3^{-/-}$ mice (11.55 ± 1.81 µA/cm^2) than in $sgk3^{+/+}$ mice (21.81 ± 2.28 µA/cm^2).

Fasting plasma glucose concentrations were significantly ($p < 0.034$) lower in $sgk3^{-/-}$ mice (4.42 ± 0.28 mmol/l, n = 6) than in $sgk3^{+/+}$ mice (5.33 mmol/l ± 0.29, n=6).

To explore whether defective electrogenic glucose transport in $sgk3^{-/-}$ intestine is paralleled by a similar impairment of electrogenic amino acid transport, the currents induced by phenylalanine, cysteine, glutamine, and proline were determined in intestinal segments of $sgk3^{-/-}$ and $sgk3^{+/+}$ mice. No significant differences were observed between $sgk3^{-/-}$ and $sgk3^{+/+}$ mice in the currents of any of the amino acids tested (Fig. 21).

A

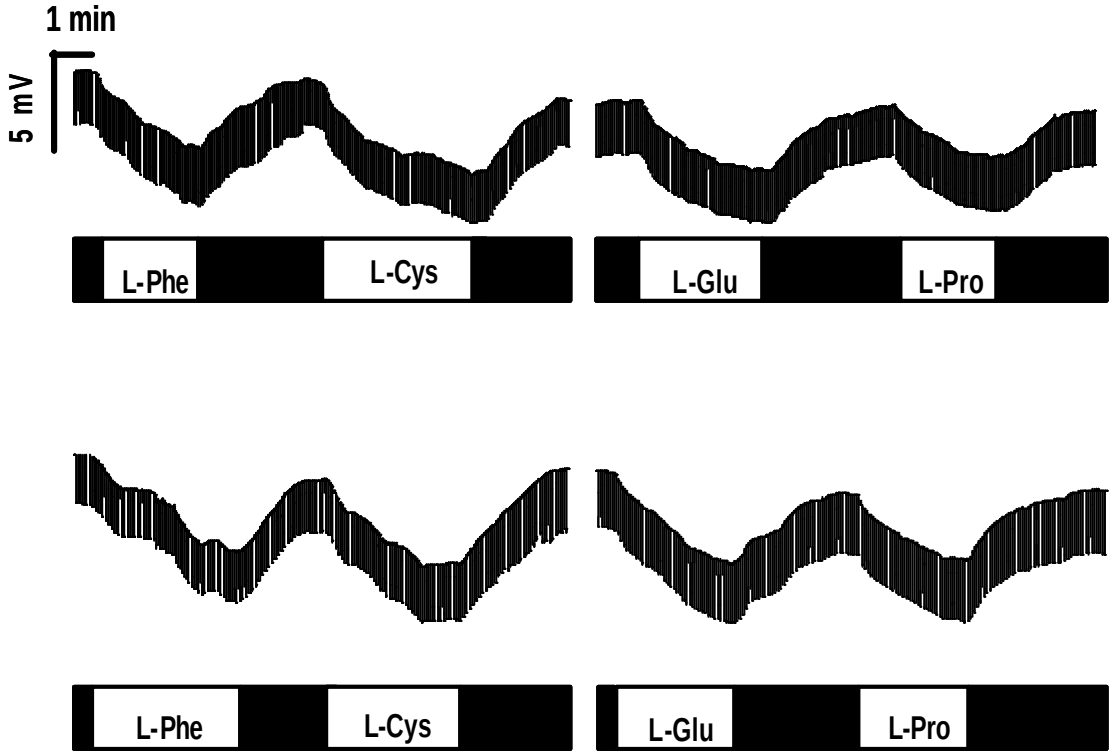

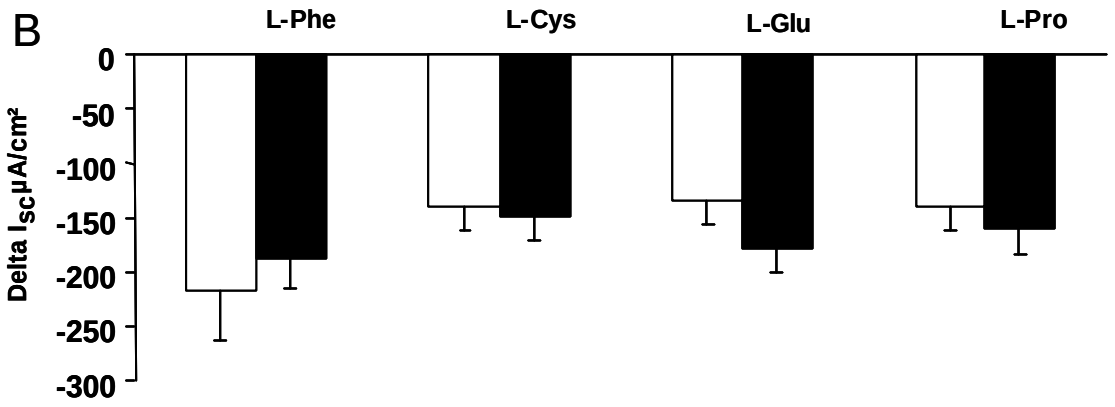

Figure 21. Amino acid induced currents (Iaa,d) in intestinal segments.
Alterations of transepithelial voltages. (A) and induced currents (B) in segments of jejunal tissue from *sgk3*$^{-/-}$ and *sgk3*$^{+/+}$ mice before and after addition of phenylalanine (Phe), cysteine (Cys), glutamine (Glu), and proline (Pro).
A: Original tracings illustrating the effect of amino acids on the transepithelial potential difference in *sgk1*$^{+/+}$ mice (upper panel) and *sgk3*$^{-/-}$ mice (lower panel). The voltage deflections are due to repetitive injections of test currents (1 µA).
.**B:** Arithmetic means ± SEM (n = 6-7) of amino acid induced currents in jejunum from *sgk3*$^{+/+}$ mice (*open columns*) and *sgk3*$^{-/-}$ mice (*closed columns*).

3.1.5 Quantitative RT-PCR

We used quantitative RT-PCR to test whether colonic SGK1 transcription is up-regulated by a four day treatment with dexamethasone or a seven day treatment with DOCA (Fig.22).

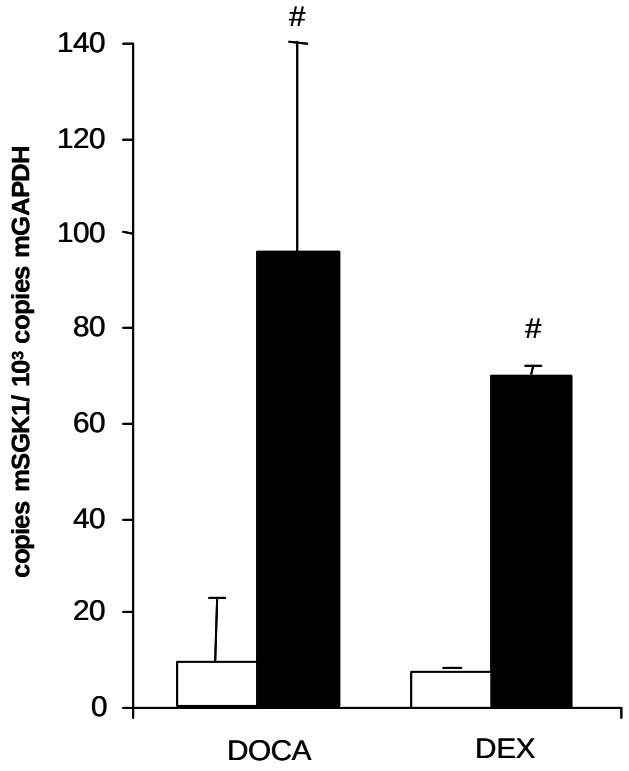

Figure 22. SGK1 expression
Arithmetic means ± SEM (n = 3-4 each) of SGK1 mRNA transcript levels in wild-type mice prior to (*open bars*) and following (*closed bars*) treatment with the mineralocorticoid DOCA or with the glucocorticoid dexamethasone (DEX).
# Indicates statistically significant difference between untreated and treated mice.

Following dexamethasone treatment the mSGK1/mGAPDH ratio increased in distal colon from 7.2 ± 0.4 (n = 3) to 69.6 ± 14.0 copies mSGK1/ 10^3 copies mGAPDH (n = 4). Following DOCA treatment the ratio increased in distal colon from 9.1 ± 2.1 (n = 3) to 95.6 ± 44.4 copies mSGK1/ 10^3 copies mGAPDH (n = 3). Hence, both, the glucocorticoid dexamethasone and the mineralocorticoid DOCA up-regulate SGK1 transcript levels. No SGK1 transcripts were detected in SGK1 knockout mice (SGK1/GAPDH ratio 0.0, n=4 in distal colon).

The potential difference across the colonic epithelium was determined to estimate ENaC activity. In untreated animals the transepithelial potential difference (V_{te}) across the colonic epithelium was significantly higher in untreated $sgk1^{-/-}$ mice than in untreated $sgk1^{+/+}$ mice (-6.8 ± 1.1 mV vs. -3.9± 0.5 mV, n=12-14 each).

A

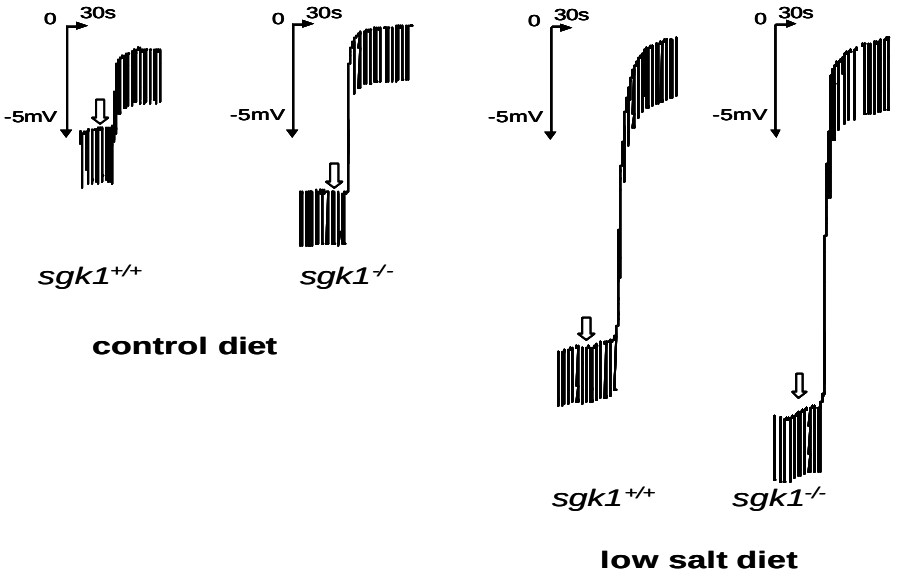

B

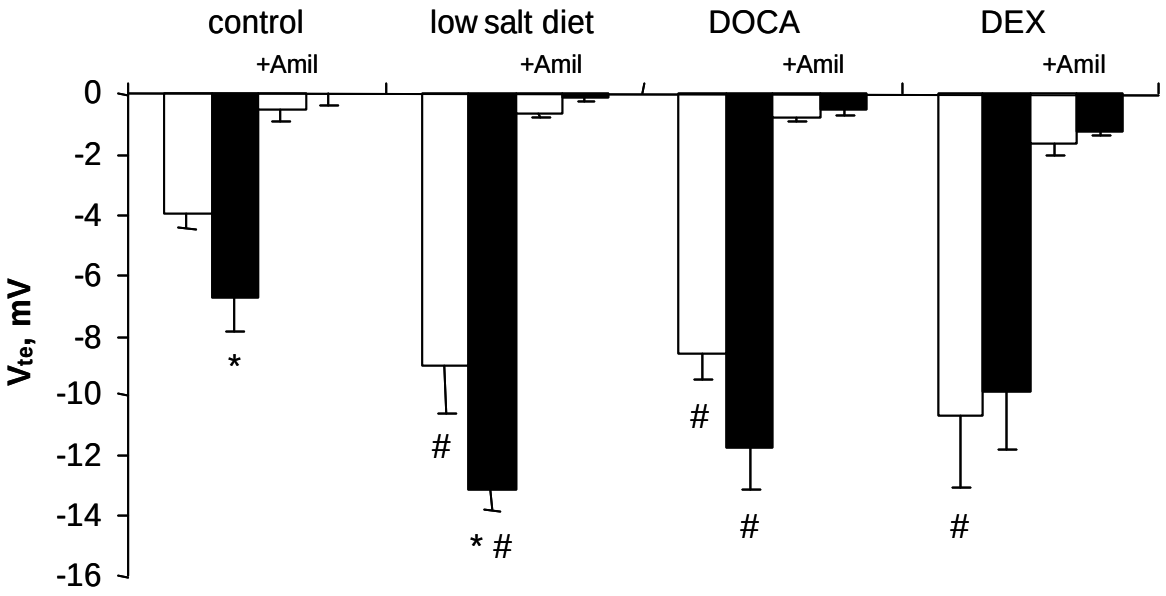

Figure 23. Amiloride-sensitive transepithelial potential in distal colon
A. Representative original tracings of the transepithelial colonic potential difference (V_{te}) in *sgk1*$^{+/+}$ mice and *sgk1*$^{-/-}$ mice under control diet (left) and low salt diet (right) before and after addition of 50µM amiloride (open arrow).
B: Arithmetic means ± SEM (n = 4-14) of transepithelial potential difference (V_{te}) across distal colonic epithelium in the absence and presence (+Amil) of amiloride (50 µM) in *sgk1*$^{+/+}$ mice (open bars) and *sgk1*$^{-/-}$ mice (closed bars) under control diet, low salt diet, treatment with the mineralocorticoid DOCA (1.5mg per day) or treatment with the glucocorticoid dexamethasone (DEX, 10µg/g BW).
# indicates statistically significant difference between control and the respective treatment,
* indicates statistically significant difference between *sgk1*$^{+/+}$ and *sgk1*$^{-/-}$ mice.

As shown in Fig. 23, addition of the Na^+ channel blocker amiloride (50 µM) decreased V_{te} to +0.1 ± 0.4 mV in sgk1$^{-/-}$ mice (n=14) and to -0.5 ± 0.4 mV in sgk1$^{+/+}$ mice (n=12). The lumen positive V_{te} in the presence of amiloride was not significantly different from zero and thus, V_{te} was fully dependend on amiloride sensitive ENaC activity. V_{te} and apparent R_{te} allowed the calculation of an apparent amiloride-sensitive equivalent short circuit current (I_{amil}) in distal colon. As illustrated in Fig.24 I_{amil} was significantly larger in untreated sgk1$^{-/-}$ mice (-595 ± 135 µA/cm^2, n=12) than in untreated sgk1$^{+/+}$ mice (-231 ± 33µA/cm², n=14).

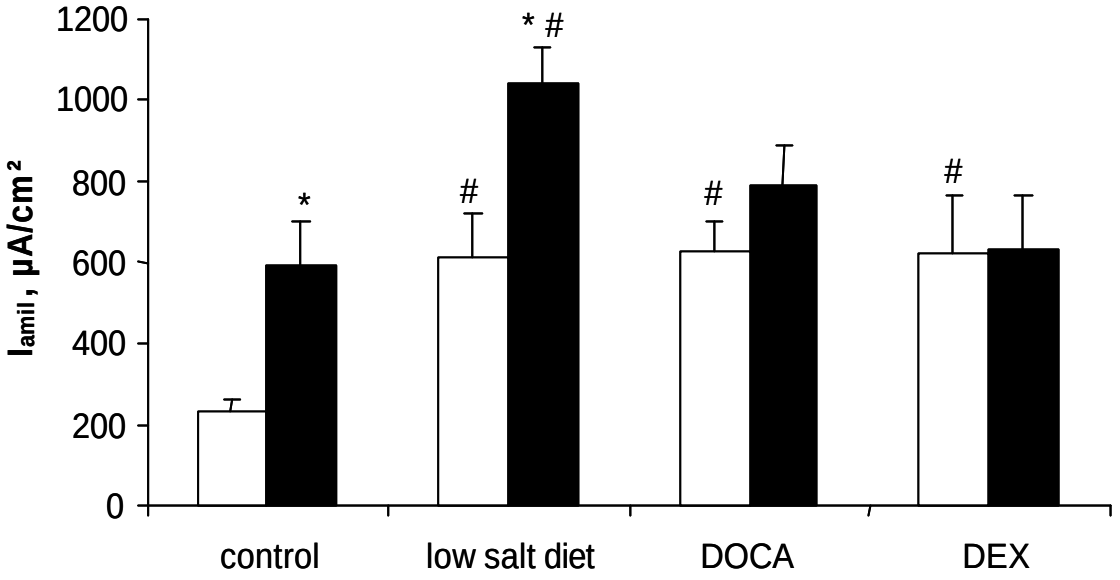

Figure 24. Amiloride-sensitive current in distal colon
Arithmetic means ± SEM (n = 4-14) of the amiloride-sensitive equivalent short circuit current (I_{amil}) in distal colon from *sgk1*$^{+/+}$ mice (open columns) and *sgk1*$^{-/-}$ mice (closed columns) under control diet, low salt diet, treatment with the mineralocorticoid DOCA (1.5mg per day) or treatment with the glucocorticoid dexamethasone (DEX, 10µg/g BW).
# indicates statistically significant difference between control and the respective treatment,
* indicates statistically significant difference between *sgk1*$^{+/+}$ and *sgk1*$^{-/-}$ mice.

The next series of experiments explored the influence of salt deficient diet, a maneuver increasing aldosterone release and thus increasing endogeneous mineralocorticoid stimulation of ENaC. A 7 day treatment with low salt diet significantly decreased body weight despite significant stimulation of fluid intake in both genotypes (Table 6).

Table 6. Arithmetic means ± SEM of the effects of 3 mM luminal Ba^{2+}

	Control diet (n=9 each)		Low salt diet (n=4 each)		DEX (n=8 each)		DOC (n=5 each)	
	sgk1$^{+/+}$	sgk1$^{-/-}$	sgk1$^{+/+}$	sgk1$^{-/-}$	sgk1$^{+/+}$	sgk1$^{-/-}$	sgk1$^{+/+}$	sgk1$^{-/-}$
? V_{te} , mV	-0.88 ± 0.13	-0.50 ± 0.13*	-0.32 ± 0.07$^{\#}$	-0.64 ± 0.11$^{\#}$	-0.46 ± 0.09$^{\#}$	-1.00 ± 0.03$^{\# *}$	-0.88 ± 0.09	-0.88 ± 0.12$^{\#}$

Arithmetic means ± SEM of the effects of 3 mM luminal Ba^{2+} on Vte in the presence of amiloride under control and low salt diet as well as after dexamethasone (DEX) and DOCA (DOC) treatment.
#indicates significant difference between control and respective treatment.
*indicates statistically significant difference between sgk1$^{+/+}$ and sgk1$^{-/-}$ mice

Salt deficient diet increased the absolute value of V_{te} and I_{amil} in both, sgk1$^{-/-}$ and sgk1$^{+/+}$ mice (Fig. 22 and 24, n=4 each). Under low salt diet V_{te} and I_{amil} remained significantly

higher in sgk1$^{-/-}$ than in sgk1$^{+/+}$ mice. Thus, lack of SGK1 does not blunt the effect of salt depletion on colonic transepithelial potential difference.

To elucidate the cause for the higher V_{te} and Iamil in sgk1$^{-/-}$ mice under control conditions and low salt diet we examined plasma aldosterone levels in both genotypes (Fig. 25).

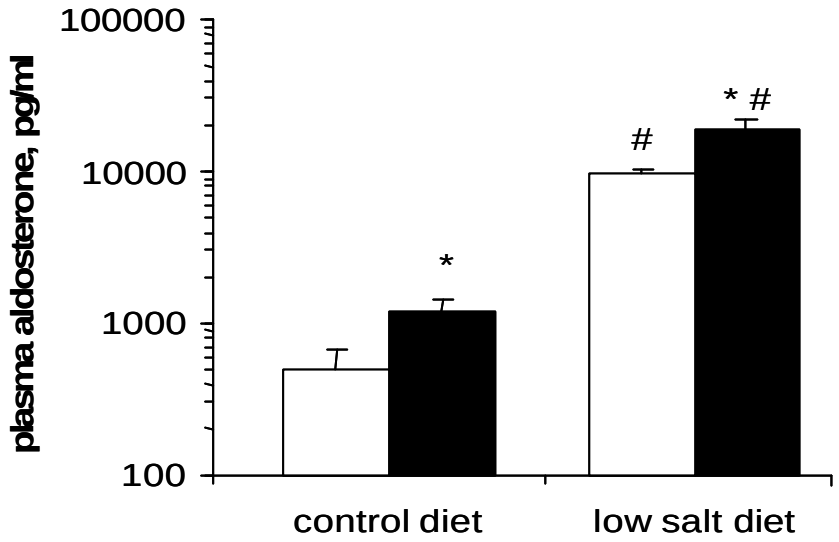

Figure 25. Plasma aldosterone concentrations
Arithmetic means ± SEM of plasma aldosterone concentrations in *sgk1*$^{-/-}$ (closed columns) and *sgk1*$^{+/+}$ mice (open columns, n = 12 each) under control diet (left) and low salt diet (right). # indicates statistically significant difference between diets,
* Indicates statistically significant difference between *sgk1*$^{+/+}$ and *sgk1*$^{-/-}$ mice.

Aldosterone plasma levels were significantly higher in sgk1$^{-/-}$ mice (1.2 ± 0.3 ng/ml, n=12) than in sgk1$^{+/+}$ mice (0.5 ± 0.2 ng/ml, n=12). Under low salt diet plasma aldosterone levels were strongly enhanced in both genotypes and remained significantly higher in the sgk1$^{-/-}$ mice (18.7 ± 3.3 ng/ml, n = 12) than in in sgk1$^{+/+}$ mice (9.6 ± 0.3 ng/ml, n=12).

Additional experiments have been performed to explore whether the up-regulation of SGK1 by the glucocorticoid dexamethasone (n=7-8 each) or the mineralocorticoid DOCA (n=7-8 each) participates in the regulation of the potential difference across the colonic epithelium. A 4 day dexamethasone treatment (10µg/g BW) significantly increased V_{te} and I_{amil} in sgk1$^{+/+}$ mice (Fig. 24). In sgk1$^{-/-}$ mice V_{te} tended to increase as well, an effect, however, not reaching statistical significance. Thus, following dexamethasone treatment V_{te} and I_{amil} were not significantly different between sgk1$^{-/-}$ than sgk1$^{+/+}$ mice. Similarly, a 7 day treatment with DOCA (1.5mg/day) significantly increased V_{te} and I_{amil} in sgk1$^{+/+}$ mice (Fig. 24).

In sgk1$^{-/-}$ mice V_{te} tended to increase as well, an effect, however, again not reaching

statistical significance (p=0.07). Thus, the increase of transepithelial potential difference following glucocorticoid or mineralocorticoid treatment is blunted in $sgk1^{-/-}$ mice.

To assess the contribution of K^+ channels to measured V_{te}, Ba^{2+} was added to the luminal perfusate in the presence of amiloride. As shown in Table 6, Ba^{2+} had only little effect on V_{te} suggesting that most of the V_{te} reflected amiloride-sensitive ENaC activity.

For the analysis of the fecal Na^+ and K^+ excretion feces was collected over 24 h with free access to control diet and distilled drinking water (Table 7).

Table 7.Arithmetic means ± SEM of body weight, food and fluid intake

	Control diet		Low salt diet	
	$sgk1^{+/+}$	$sgk1^{-/-}$	$sgk1^{+/+}$	$sgk1^{-/-}$
Body Weight (g)	26.0 ± 1.3	25.4 ± 1.4	23.7 ± 1.2 #	22.5 ± 1.2 #
Food intake (g/24h)	3.2 ± 0.2	3.0 ± 0.1	2.5 ± 0.2 #	2.2 ± 0.2 #
Fluid Intake (ml/24h)	3.8 ± 0.4	3.3 ± 0.2	8.9 ± 1.8 #	8.6 ± 1.0 #
Calculated Na^+ intake (µmol/24h)	379 ± 26	356 ± 16	18.3 ± 1.3 #	16.3 ±1.1 #
Fecal Na^+ excretion / Na^+ intake (%)	13.3 ± 1.4	12.8 ± 1.0	191 ± 20 #	179 ± 25 #
Fecal Na^+ excretion (µmol/24h)	48.4 ± 4.7	44.6 ± 3.2	33.9 ± 3.4 #	29.9 ± 4.9 #
Calculated K^+ intake (µmol/24h)	2022 ± 139	1900 ± 83	1607 ± 117 #	1427 ± 97 #
Fecal K^+ excretion (µmol/24h)	37.0 ± 4.0	42.5 ± 6.5	62.6 ± 5.3 #	45.5 ± 3.8
Fecal K^+ excretion / K^+ intake (%)	1.87 ± 0.18	2.21± 0.27	4.02 ± 0.37 #	3.22 ± 0.20 #

Arithmetic means ± SEM of body weight, food and fluid intake, calculated Na^+ and K^+ intake, fecal weight as well as fecal Na^+ and K^+ excretion in $sgk1^{+/+}$ and $sgk1^{-/-}$ mice treated with control diet or salt depleted diet and distilled water for 5 days (n = 12 each).
# indicates significant difference between control and low salt diet.

Under control conditions fecal Na^+ excretion was similar in $sgk1^{+/+}$ mice (48.4 ± 4.7 µmol/24h, n=12) and in $sgk1^{-/-}$ mice (44.6 ± 3.2 µmol/24h, n=12). Under low Na^+ diet fecal Na^+ excretion was similarly decreased in $sgk1^{+/+}$ (33.9±3.4 µmol/24h, n=12) and $sgk1^{-/-}$ mice (29.9±4.9 µmol/24h, n=12, Fig. 26).

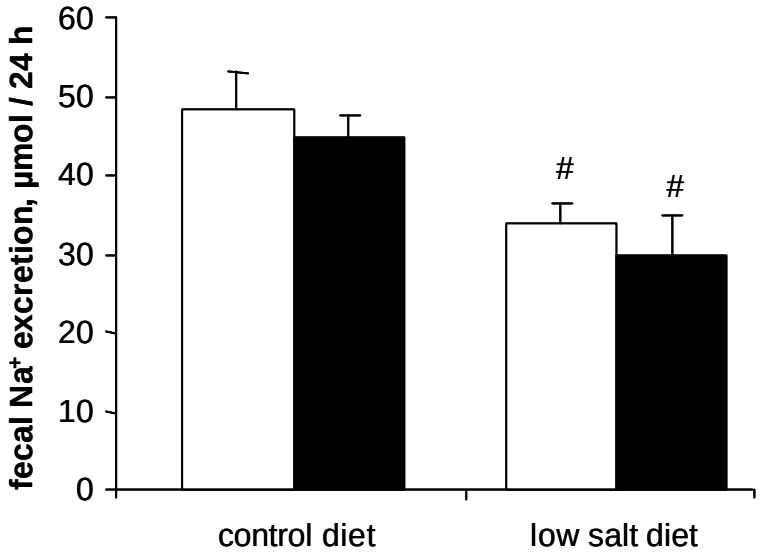

Figure 26. Fecal Na+ excretion
Arithmetic means ± SEM (n = 12 each) of fecal Na^+ excretion in *sgk1*$^{+/+}$ mice (open columns) and *sgk1*$^{-/-}$ mice (closed columns) under control diet (left) and low salt diet (right). # indicates statistically significant difference between control and low salt diet.

Fecal K^+ excretion was similarly increased in both genotypes. A 4 day treatment with dexamethasone decreased fecal Na^+ excretion in both sgk1$^{+/+}$ and sgk1$^{-/-}$ mice without increasing fecal K^+ excretion (Table8).

Table 8.Arithmetic means ± SEM of body weight, food and fluid intake, calculated Na^+ and K^+ intake

	Control		DEX treatment	
	sgk1$^{+/+}$	sgk1$^{-/-}$	sgk1$^{+/+}$	sgk1$^{-/-}$
Body Weight (g)	27.4 ± 1.3	28.0 ± 1.1	26.7 ± 1.2	27.4 ± 1.1
Food intake (g/24h)	3.3 ± 0.2	3.7 ± 0.1	4.0 ± 0.2 #	4.2 ± 0.2 #
Fluid Intake (ml/24h)	5.3 ± 0.4	6.1 ± 0.4	7.4 ± 1.0 #	6.9 ± 0.5 #
Calculated Na^+ intake (µmol/24h)	397 ± 19	437 ± 14	485 ± 18 #	501 ± 19 #
Fecal Na^+ excretion (µmol/24h)	87.0 ± 11.3	78.0 ± 9.0	40.3 ± 4.9 #	44.4 ± 4.0 #
Fecal Na^+ excretion / Na^+ intake (%)	22.2 ± 2.9	17.9 ± 2.1	8.5 ± 1.1 #	8.9 ± 0.7 #
Calculated K^+ intake (µmol/24h)	2119 ± 100	2334 ± 72	2586 ± 95 #	2673 ± 101 #
Fecal K^+ excretion (µmol/24h)	155 ± 19	157 ± 15	141 ± 14	146 ± 13

Fecal K^+ excretion / K^+ intake (%)	7.5 ± 0.9	6.8 ± 0.8	5.5 ± 0.5 #	5.5 ± 0.5

Arithmetic means ± SEM of body weight, food and fluid intake, calculated Na^+ and K^+ intake, fecal weight as well as fecal Na^+ and K^+ excretion in $sgk1^{+/+}$ and $sgk1^{-/-}$ mice treated with control diet and dexamethasone (DEX) for 4 days (n = 12 each).
# indicates significant difference between control and dexamethasone treatment.

4 Discussion

4.1 Effect of PI3 kinase inhibitors on electrogenic transepithelial transport of glucose

The present observations disclose the powerful influence of PI3 kinase inhibitors on electrogenic transepithelial transport of glucose and several amino acids.

Notably, the effect of PI3 kinase inhibitors occurs in the absence of any exogeneous hormonal stimulation of the tissue, such as IGF, further growth factors, insulin or glucocorticoids. Apparently, activation of the PI3 kinase is at least transiently maintained even in the absence of continued hormonal stimulation. Thus, the hormonal effect is maintained transiently even without continued presence of those hormones or PI3 kinase is activated by some other intramural mechanisms. Accordingly, PI3 kinase may not only be important for the stimulation of intestinal transport by hormones but may be required for the maintenance of transport even in the absence of hormones. Unlike glucose-induced currents, amino acid and forskolin-induced currents decreased substantially even in the absence of Wortmannin, which may point to relaxation of the effect or transport dependence on continuous exogenous stimulation. However forskolin and amino acid induced currents declined significantly faster in the presence of Wortmannin.

The present experiments did not address the mechanisms underlying the inhibition of electrogenic transport. Previous in vitro studies revealed the stimulating effect of the SGK isoforms and/or PKB on the electrogenic glucose transporter SGLT1 (13), the glutamine transporter SN1 (SLC38a3, SNAT3) (101) and the glutamate transporters EAAT1, (17), EAAT2 (18), EAAT3 (19), EAAT4 (20) and EAAT5 (21). Most likely, further amino acid transporters are targets of the SGK and PKB isoforms and thus dependent on PI3 kinase activity. Moreover, the kinases stimulate the voltage gated K^+ channel complex KCNE1/KCNQ1 (102). The channels contribute to the maintenance of the potential difference across the apical cell membrane (88;92) which is a critical driving force for electrogenic glucose and amino acid transport (44;103;104). The SGK isoforms have further been shown to stimulate the Na^+/K^+-ATPase (105-107), which is required for the maintenance of the Na^+ gradient, the second driving force for Na^+ coupled nutrient transport (104).

Inhibition of PI3- kinase may similarly affect the transport of electrolytes such as CFTR (108) or ClC-Ka/barttin (109)dependent Cl^- transport, ROMK dependent K^+ transport

(110-112), TRPV5 dependent Ca^{2+} transport (113;114)or Na^+ through the epithelial Na^+ channel ENaC, The latter is is regulated by insulin, and IGF-1 through the PI3 kinase pathway (62;63;115). ENaC is regulated by SGK1 (58;59), complete knockout of SGK1 leads, however, only to moderate impairment of renal Na^+ retention (64).

At least in theory, the decline of transport in the presence of Wortmannin could have been due to unspecific epithelial injury. However, the transepithelial resistance was not significantly affected by the presence of Wortmannin or LY294002. Moreover, TUNEL staining did not reveal evidence for apoptosis following a 15 minute treatment with Wortmannin. Nevertheless, we cannot rule out tissue damage by the PI3 kinase inhibitors which may eventually contribute to a decline of transport activity.

In conclusion, pharmacological inhibition of PI3 kinase markedly decreases the electrogenic transport of glucose and several amino acids. Thus, the PI3 kinase pathway is required to maintain intestinal transport function.

4.2 Intestinal and renal glucose transport

According to the Ussing chamber experiments and electrophysiology of proximal renal tubules, electrogenic glucose transport is significantly smaller in PDK1 hypomorphic mice ($pdk1^{hm}$) than in their wild type littermates ($pdk1^{wt}$). PDK1 could regulate SGLT1 through the downstream kinases PKB and SGK, which have previously been shown to stimulate the electrogenic glucose transporter SGLT1 expressed in Xenopus oocytes (13). Moreover, these kinases also stimulate the voltage gated K^+ channel complex KCNE1/KCNQ1 (109), which contributes to the maintenance of the potential difference across the apical cell membrane of the renal proximal tubule (92), a critical driving force for electrogenic glucose transport (44;103). K^+ channels similarly maintain the driving force of intestinal glucose transport (104). The kinases further stimulate the Na^+/K^+-ATPase (105;106), which is required to maintain the chemical driving force for Na^+ coupled nutrient transport (44;103;104). Thus, PDK1 may regulate SGLT1 activity both directly and by modifying the respective driving forces.

Decreased expression of PDK1 in the PDK1 hypomorphic mice does not only affect glucose transport but may affect a variety of other transport systems dependent on the SGK and PKB isoforms (7). Again, those transport systems may be affected by a direct regulation and/or by modification of the driving forces.

Deranged transport may contribute to the smaller size of the PDK1 hypomorphic mice

reported earlier (41). Interestingly, the animals excrete slightly less creatinine (see Table 2) pointing to some decrease of creatinine formation. Recent experiments have disclosed the ability of SGK isoforms to stimulate the creatine transporter (116). As formation of creatinine requires the cellular uptake of creatine (117), impaired function of the creatine transporter is expected to decrease the formation and renal excretion of creatinine. The increased ratio of glucose over creatinine concentration in urine is, however, largely due to marked glucosuria rather than slightly decreased creatinine excretion.

The protein abundance of SGLT1 in the brush border membrane of the jejunum, ileum and kidney was not significantly different between $pdk1^{hm}$ mice and $pdk1^{wt}$ mice. The scatter of the data does, however, not preclude effects of PDK1 on SGLT1 expression. Moreover, the residual PDK1 activity in the hypomorphic mice may be sufficient to maintain expression. Irrespective of the underlying mechanism, the observations disclose that SGLT1 activity in the brush border membrane is regulated by PDK1. The ß-adrenergic regulation of glucose transport in rat small intestine has previously been shown to involve phosphorylation dependent SGLT1 stimulation (118), whereas IGF mediated stimulation of intestinal glucose transport via SGLT1 has been reported to involve increase of mRNA and protein abundance (119).The effect of PDK1 deficiency is only moderate, but could be more profound at complete knockout of PDK1. Complete knockout of SGK3 leads to a moderate decrease of intestinal SGLT1 activity (120). Complete knockout of SGK1 abrogates the SGLT1-stimulating effect of dexamethasone without appreciably affecting the basal activity of SGLT1 (94). The defective intestinal and renal glucose transport did not appreciably alter basal plasma glucose concentration. The increase of plasma glucose concentration following intraperitoneal glucose administration tended to be slightly higher in pdk1hm mice than in pdk1wt mice. The difference, however, did not reach statistical significance. Thus, the ability of nonpolarized cells such as muscle or liver to accumulate glucose following an increase of plasma glucose concentration is not severely affected in the PDK1 hypomorphic mouse. This observation may be surprising in view of the substantial role of PKB (121-127) and SGK1 (128) in peripheral glucose uptake. Again, it should be kept in mind that the hyopomorphic mice do not completely lack PDK1, which would not be compatible with survival. Thus, the residual PDK1 activity may be able to maintain almost normal glucose uptake into peripheral tissues but may not be sufficient for full stimulation of intestinal and renal glucose transport.

In conclusion, the PDK1 hypomorphic mice display moderate impairment of electrogenic

epithelial glucose transport, an observation disclosing a novel player in the regulation of intestinal and renal nutrient transport.

In conclusion, the PDK-1 hypomorphic mice display moderate impairment of electrogenic epithelial glucose transport, an observation disclosing a novel player in the regulation of intestinal and renal nutrient transport.

4.3 Intestinal and renal transport of amino acids

As reported previously (41), PDK1 hypomorphic mice ($pdk1^{hm}$) are significantly smaller than their age and sex matched wild type littermates ($pdk1^{wt}$). Evidence suggested that the decrease of body mass is the result of smaller cell volumes and not due to a decrease in cell number (41). In theory, a decrease of cell volume could be due to lack of nutrients, as concentrative uptake of amino acids leads to cell swelling and subsequent stimulation of protein synthesis (42;43;129). Accordingly, the decreased cell volume could be due to impaired nutrient uptake.

Moreover, insufficient dietary supply or defective renal or intestinal uptake of amino acids is typically paralleled by delayed growth (130-134). Thus, the impaired intestinal uptake and renal retention of amino acids could contribute to the growth defect of the PDK1 deficient mice. On the other hand, food and water intake was not decreased in PDK1 deficient mice, further highlighting the significance of impaired intestinal absorption.

According to the Ussing chamber experiments, electrogenic transport of phenylalanine, cysteine, glutamine, proline, leucine and tryptophan is impaired. Previous *in vitro* studies revealed the stimulating effect of the SGK isoforms and/or PKB on the amino acid transporters SN1 (SLC38A3, SNAT3) (20), ASCT2 (SLC1A5) (135), EAAT1 (SLC1A3) (18), EAAT2 (SLC1A2) (21), EAAT3 (SLC1A1) (19), EAAT4 (SLC1A6) (17) and EAAT5 (SLC1A7) (101). Possibly, other transporters may also be targets of these kinases.

The profile of amino acids in urine and the observed reduction in transport induced currents for several amino acids point to the involvement of more than one amino acid transport system (45). Patients with mutations in either B^0AT1 (SLC6A19) or in $b^{0,+}AT$ (SLC7A9) and rBAT (SLC3A1) suffer from Hartnup disorder or cystinuria. Both diseases are characterized by the impaired renal and intestinal transport of neutral amino acids such as phenylalanine and leucine or cationic amino acids and cystine, respectively (51;136-138). Accordingly, the observed reduction in B^0AT1 (SLC6A19) expression correlates with the loss of leucine, phenylalanine and glutamine. Na-dependent leucine absorption

occurs in the kidney via several systems, including the low affinity system B^0 (B^0AT1, SLC6A19) in the initial part of the proximal tubule and probably related but unidentified members of the same gene family. XT2 (SLC6A18) and XT3, two related orphan transporters with no clearly established transport function (50) have been observed in the late proximal tubule. The electrophysiological measurements in the late proximal tubule indicated that amino acid induced currents were smaller in the $pdk1^{hm}$ mice suggesting that not only reduction of B^0AT1 (SLC6A19) expression in the initial proximal tubule but also reduced function (and/or expression) of these putative amino acid transporters may contribute to the observed aminoaciduria and reduced currents. The relatively high urinary loss of methionine and valine may result from the fact that no compensatory mechanisms exist. In contrast, the increased abundance of the SIT transporter may point to a compensatory mechanism. SIT (SLC6A20) is mainly expressed in the late proximal tubule, appears to transport particularly imino amino acids, and belongs to the same SLC6 family of amino acid transporters as B^0AT1 (SLC6A19) (48-50). Surprisingly, reduced abundance of the $b^{0,+}AT$ (SLC7A9) subunit of system $b^{0,+}$ did not induce urinary loss of its typical substrates arginine, lysine, and cystine. Again, the observed decrease in protein abundance may not adequately mirror the actual activity in the brush border membrane. Other transport systems that may compensate for loss of $b^{0,+}$ activity are presently not known. The increased abundance of SIT may indicate that regulation of amino acid transporters by PDK1 does not affect all amino acid transporters.

The SGK isoforms stimulate the voltage gated K^+ channel complex KCNE1/KCNQ1 (109), which contributes to the maintenance of the potential difference across the apical cell membrane of the renal proximal tubule (88;92), a critical driving force for electrogenic amino acid transport (44;103). K^+ channels similarly tune intestinal transport of amino acids (104). The SGK isoforms further stimulate the Na^+/K^+-ATPase (105-107;139), which is required to maintain the chemical driving force for Na^+ coupled nutrient transport (104). Thus, decreased PDK1 activity could modify nutrient transport indirectly, i,e by compromising the driving forces. The potential difference across the basolateral cell membrane of proximal renal tubules was, however, not significantly different between $pdk1^{hm}$ and $pdk1^{wt}$ mice. Moreover, a decreased K^+ channel activity should enhance and not decrease the depolarization following addition of substrates for Na^+ coupled transport. Thus, the blunted depolarisation in $pdk1^{hm}$ mice reflects decreased electrogenic amino acid transport rather than decreased K^+ channel activity.

PDK1 may not only stimulate the transport of amino acids, but may participate in the

regulation of further nutrients. SGK1 has been shown to stimulate the activity of the Na^+-glucose cotransporter SGLT1 (SLC5A1) (13) and the facilitative glucose transporter GLUT1 (SLC2A1) (140). It has further been shown to stimulate the Na^+,dicarboxylate cotransporter NaDC-1 (SLC13A2) (141), and the creatine transporter CreaT (SLC6A8) (116).

Any impairment of renal electrolyte excretion by blunted stimulation through PDK1 may be compensated by enhanced stimulation through other mechanisms. As a matter of fact, despite the powerful stimulating effect of SGK1 on the renal epithelial Na^+ channel EnaC (58;59), complete knockout of SGK1 leads only to moderate impairment of renal Na^+ retention which is only disclosed following exposure to a salt deficient diet (64).

The mild reduction in transport rates observed here may be explained by the only moderate decrease of transport function as compared to the loss of function mutations or knockout leading to severe loss of the respective amino acids (51;136-138;142). It should be kept in mind that the mice still express PDK1 and thus, PDK1 dependent regulation of amino acid transport is not completely disrupted in those mice.

The defective intestinal and renal transport of amino acids did not lead to gross alterations of plasma amino acid concentrations. Apparently, the enhanced food intake per body weight compensates for the renal loss of amino acids and maintains extracellular amino acid concentrations sufficient for cellular uptake. However, the availability of amino acids in extracellular fluid does not preclude impairment of cellular amino acid uptake in PDK1 deficient animals through modification of amino acid transport in nonpolarized cells.

In conclusion, the PDK1 hypomorphic mice display moderate impairment of amino acid transport which presumably contributes to the delayed growth of those mice. Therefore the present observations disclose a novel player in the regulation of intestinal and renal nutrient transport.

4.4 Role of Sgk 3 gene knock-outon glucose transport

The impaired intestinal absorption in the SGK3 knockout mouse may account for the enhanced fecal weight reflecting increased amounts of food escaping intestinal absorption. Considering the many transport systems apparently regulated by the SGK´s (15), several transport systems may be downregulated in the SGK3 knockout mouse. However, we found evidence only for impaired electrogenic glucose absorption while the transport of several amino acids appeared to be normal. This does, not of course, rule out the

impairment of further transport systems. The impaired intestinal absorption of glucose may account for the observed hypoglycaemia which in turn could stimulate food intake, which is significantly increased in the $sgk3^{-/-}$ mouse. The enhanced food intake contributes to the increase of fecal dry weight and would tend to compensate for the abnormal glucose absorption.

In any case, the present observations disclose the impaired ability of $sgk3^{-/-}$ mice to absorb glucose echoing the ability of SGK3 to up-regulate SGLT1 in the *Xenopus* oocyte expression system (13). Beyond impaired electrogenic glucose transport, the $sgk3^{-/-}$ mice excrete more K^+ potassium, which may point to some impairment of electrolyte absorption. On the other hand, the relative increase of K^+ excretion was similar to the relative increase of food intake and may thus simply be due to altered load.

The defect of Na^+ glucose cotransport in the SGK3 knockout mouse is only moderate indicating that functional expression of SGLT1 does not require the presence of SGK3. The activity of SGK3 could be partially replaced by SGK1 or the related protein kinase B which both have been shown to up-regulate SGLT1 activity (13). Protein kinase B has previously been shown to enhance the abundance of glucose transporters in the cell membrane (143-145). It is noteworthy that the in vivo functions of SGK1 and SGK3 may only partially overlap.

The different kinases do, however, not necessarily serve identical functions and the phenotypes of the SKG1 and SGK3 knockout mice display striking differences. The SGK3 mouse shows transient growth retardation and deranged hair growth but seemingly normal renal salt retention (57), while the SGK1 knockout mouse has seemingly normal growth and hair but suffers from reduced ability to maintain salt balance under dietary salt restriction (64). Unlike transcription of SGK3, the transcription of SGK1 is strongly regulated by a variety of hormones (4) including glucocorticoids (2;54;55), mineralocorticoids (58-60), gonadotropins (146-149), and TGFß (68;150). Moreover, SGK1 transcription is stimulated by cell shrinkage (61). Despite those differences, there is considerable overlap of regulation and function. Most importantly, all three SGK isoforms and protein kinase B require activation by insulin and growth factors including IGF1 (4). Thus, the kinases may participate in the known stimulating effect of insulin like growth factor on intestinal nutrient uptake (119;151;152).

In conclusion, SGK3 is expressed in enterocytes and is a modulator of intestinal glucose absorption. The slight impairment of intestinal glucose absorption may contribute to the delayed growth of mice lacking functional SGK3

4.5 Mineralocorticoids and glucocorticoids enhance the SGK1 transcript levels in distal colon

The present observations demonstrate that mineralocorticoids and glucocorticoids enhance the SGK1 transcript levels in distal colon, confirming and expanding earlier observations that SGK1 mRNA levels are increased by mineralocortioid treatment (62;72;81). However, lack of SGK1 does not decrease the transepithelial potential in the colonic epithelium and does not disrupt its increase following salt depletion. The transepithelial potential is even higher in gene-targeted mice lacking functional SGK1 ($sgk1^{-/-}$) than in their wild type littermates ($sgk1^{+/+}$) under both, normal and low salt diet. The increased transepithelial potential difference under low salt diet may partially result from stimulation of ENaC activity by steroid hormones. The particularly high values especially in $sgk1^{-/-}$ mice under salt deficient diet may, however, point to the involvement of additional mechanisms.

Treatment with the glucocorticoid dexamethasone or with the mineralocorticoid DOCA significantly enhanced the transepithelial potential difference only in the $sgk1^{+/+}$ mice which under the steroid treatment reached the values of the $sgk1^{-/-}$ mice. At first glance the blunted effect of steroid hormones on transepithelial potential in $sgk1^{-/-}$ mice could be taken as evidence for SGK1 sensitive stimulation of ENaC activity by steroid hormones. On the other hand, even under steroid treatment, the amiloride sensitive transepithelial potential difference is not higher in $sgk1^{+/+}$ mice than in $sgk1^{-/-}$ mice. Thus, it appears that due to enhanced plasma aldosterone concentrations in the untreated $sgk1^{-/-}$ mice the effect of steroid treatment may be limited in those mice.

The increased transepithelial potential difference in $sgk1^{-/-}$ mice may at least partially result from the increased plasma aldosterone concentrations in those mice. As reported earlier (61), the impaired renal ENaC activity leads to a moderate extracellular volume contraction in $sgk1^{-/-}$ mice, which in turn increases aldosterone release. The enhanced mineralocorticoid action partially compensates for the lack of renal ENaC activity leading to virtually normal renal salt excretion (61). The functional significance of SGK1 is unmasked by salt depletion which decreases renal salt elimination less rigorously in $sgk1^{-/-}$ mice than in $sgk1^{+/+}$ mice (61). In theory, expression of apical K^+ channels could partially short circuit the current generated by ENaC activity. If the expression of those putative K^+ channels were sensitive to SGK1, then lack of SGK1 would reduce the short circuiting

and thus increase the transepithelial potential difference. The transepithelial potential difference would remain fully amiloride sensitive, as following inhibition of the apical Na^+ channels with amiloride would hyperpolarize the apical membrane, thus dissipating the electrochemical gradient for K^+ flux through the K^+ channels. Thus, similar to the current through ENaC, the short circuiting K^+ current would disappear following inhibition of ENaC with amiloride. SGK1 stimulates the activity of a number of K^+ channels, including ROMK1 (55;59;77;153) KCNE1/KCNQ1 (58) Kv1.3 (74;94;154), Kv1.5 (155) and Kv4.3 (156). There is little doubt that further K^+ channels are under the control of SGK1. However, luminal application of the unspecific K^+ channel blocker barium had only little influence on the colonic transepithelial potential difference and at least under control conditions fecal K^+ excretion was not decreased in $sgk1^{-/-}$ mice. Thus, available experimental evidence does not point to a major contribution of SGK1-sensitive K^+ channels to the colonic transepithelial potential difference. Nevertheless, the present experiments do not rule out the possibility that SGK1 regulates K^+ channels in colonic epithelium.

The enhanced amiloride sensitive transepithelial potential difference in the $sgk1^{-/-}$ mice contrasts the expectation, that lack of SGK1 should compromize the stimulation of ENaC. The observation is at seeming variance to the powerful stimulating effect of SGK1 on ENaC in *Xenopus* oocytes (62;65;73;75;110;157), in cortical collecting duct cells (28;69) and in A6 cells (73;74;158). Those in vitro experiments parallel the SGK1 dependent regulation of ENaC in the renal collecting duct, where ENaC activity is indeed significantly decreased in $sgk1^{-/-}$ mice (61). Moreover, those in vitro experiments predicted a role of SGK1 in blood pressure regulation (67) and cardiac action potential (82), a prediction impressively confirmed by genetic studies (67;82). Thus, in vitro experiments are useful tools to disclose the potential of a signalling molecule to regulate channels or transporters but require animal experiments or investigations in humans to verify, where and under which conditions the observed regulations do occur in vivo.

In conclusion, gene-targeted mice lacking SGK1 exhibit higher ENaC activity under control and low salt conditions than their wild type littermates, a differene presumably due to higher aldosterone levels in the SGK1 knockout animals. Lack of SGK1 does not disrupt colonic ENaC activity and its regulation by salt depletion.

5 Summary

The phosphoinositide dependent kinase PDK1 activates the SGK isoforms SGK1, SGK2 and SGK3 and protein kinase B isoforms which in turn are known to stimulate a variety of sodium coupled transporters, such as the renal and intestinal Na^+-dependent glucose transporter SGLT1. SGK1 is known to be up-regulated by mineralocorticoids and to enhance ENaC activity in several expression systems. Moreover, the amiloride-sensitive transepithelial potential difference in collecting duct is lower in gene-targeted mice lacking SGK1 ($sgk1^{-/-}$) than in their wild type littermates ($sgk1^{+/+}$). Accordingly, the ability of $sgk1^{-/-}$ mice to decrease urinary sodium output during salt depletion is impaired. ENaC activity and thus transepithelial potential difference in the colon are similarly influenced by mineralocorticoids.

The first aim of the present study was to explore the role of PDK1 in in electrogenic glucose and amino-acid transport in small intestine and proximal renal tubules As mice completely lacking functional PDK1 are not viable, mice expressing 10-25% of PDK1 ($pdk1^{hm}$) were compared to their wild type littermates ($pdk1^{wt}$). Body weight was significantly smaller in $pdk1^{hm}$ than in $pdk1^{wt}$ mice. Despite lower body weight of $pdk1^{hm}$ mice, food and water intake were similar in $pdk1^{hm}$ and $pdk1^{wt}$ mice.

Ussing chamber experiments showed that electrogenic transport of glucose as well as phenylalanine, cysteine, glutamine, proline, leucine and tryptophan was significantly smaller in jejunum of $pdk1^{hm}$ mice compared to $pdk1^{wt}$ mice. Similarly, proximal tubular electrogenic glucose transport as well as phenylalanine, glutamine and proline transport in isolated perfused renal tubule segments was decreased. Intraperitoneal injection of 3 g/kg bw glucose resulted in a similar increase of plasma glucose concentration in $pdk1^{hm}$ and in $pdk1^{wt}$ mice but led to a higher increase of urinary glucose excretion in $pdk1^{hm}$ mice. The urinary excretion of proline, valine, guanidinoacetate, methionine, phenylalanine, citrulline, glutamine/glutamate and tryptophan was significantly larger in $pdk1^{hm}$ than in $pdk1^{wt}$ mice. According to immunoblotting of brush border membrane proteins prepared from kidney, expression of the Na^+-dependent neutral amino acid transporter B^0AT1 (SLC6A19), the glutamate transporter EAAC1/EAAT3 (SLC1A1) and the transporter for cationic amino acids and cystine $b^{0,+}AT$ (SLC7A9) was decreased but the Na^+/proline cotransporter SIT (SLC6A20) was increased in $pdk1^{hm}$ mice. In conclusion, reduction of functional PDK1 leads to impairment of intestinal absorption and renal reabsorption of amino acids of electrogenic intestinal glucose absorption and renal glucose reabsorption.

The combined intestinal and renal loss of amino acids may contribute to the growth defect of PDK1 deficient mice. The experiments disclose a novel element of glucose transport regulation in kidney and small intestine.

The next step was to look at the transepithelial potential (V_{te}) and the apparent amiloride-sensitive equivalent short circuit current (I_{amil}) in colon from $sgk1^{-/-}$ and $sgk1^{+/+}$ mice. Both V_{te} and I_{amil} were significantly ($p<0.05$) higher in untreated $sgk1^{-/-}$ than in untreated $sgk1^{+/+}$ mice under control diet. A 7 day exposure to low salt diet increased V_{te} and I_{amil} in both genotypes but did not abrogate the differences of V_{te} and I_{amil} between $sgk1^{-/-}$ and $sgk1^{+/+}$ mice. Plasma aldosterone levels were significantly higher in $sgk1^{-/-}$ than in $sgk1^{+/+}$ mice both under control conditions and under low salt diet. Treatment with dexamethasone (10µg/g BW) or with DOCA (1.5mg per day) significantly increased V_{te} and I_{amil} in $sgk1^{+/+}$ mice but not in $sgk1^{-/-}$ mice. Under treatment with dexamethasone or DOCA V_{te} and I_{amil} were similar in $sgk1^{-/-}$ and $sgk1^{+/+}$ mice. In conclusion, lack of SGK1 does not disrupt colonic ENaC activity and its regulation by salt depletion.

Finally the functional significance of SGK3-dependent regulation of intestinal transport were studied. *Xenopus* oocyte coexpression experiments revealed the capacity of SGK3 to up-regulate a variety of transport systems including the sodium-dependent glucose transporter SGLT1. To this end experiments were performed in gene targeted mice lacking functional sgk3 ($sgk3^{-/-}$) and their wild type littermates ($sgk3^{+/+}$). Oral food intake and fecal dry weight were significantly larger in $sgk3^{-/-}$ than in $sgk3^{+/+}$mice. Glucose-induced current (I_g) in Ussing chamber as a measure of Na^+ coupled glucose transport was significantly smaller in $sgk3^{-/-}$ than in $sgk3^{+/+}$mouse jejunal segments. Fasting plasma glucose concentrations were significantly lower in $sgk3^{-/-}$ than in $sgk3^{+/+}$mice. Intestinal electrogenic transport of phenylalanine, cysteine, glutamine and proline were not significantly different between $sgk3^{-/-}$ and $sgk3^{+/+}$ mice. In conclusion, SGK3 is required for adequate intestinal Na^+ coupled glucose transport and impaired glucose absorption may contribute to delayed growth and decreased plasma glucose concentrations of SGK3 deficient mice. The hypoglycemia might lead to enhanced food intake to compensate for impaired intestinal absorption.

6 Zusammenfassung

Die phosphoinositid-abhängige Kinase 1 (PDK1) aktiviert die SGK-Isoformen SGK1, SGK2 und SGK3 sowie die Isoformen der Proteinkinase B, die eine Vielzahl von Natrium-gekoppelten Transportern stimulieren wie z.B. den renalen und intestinalen glucose-Transporter SGLT1. SGK1 wird durch Mineralokortikoide hochreguliert und stimuliert die Aktivität des epithelialen Natrium-Kanals ENaC in verschiedenen Expressionssystemen. In SGK1 defizienten Mäusen ($sgk1^{-/-}$) ist die amilorid-hemmbare transepitheliale Potentialdifferenz niedriger als in Wildtyp-Mäusen, unter Niedrigsalz-Diät ist die Fähigkeit zur Na-Konservierung in den $sgk1^{-/-}$ Mäusen eingeschränkt. Die ENaC-Aktivität im Kolon ist ähnlich wie in der Niere mineralokortikoid-abhängig.

Das Ziel der ersten Studie war es, den Einfluss der PDK1 am elektrogenen Glukose- und Aminosäurentransport im Dünndarm und im proximalen Tubulus zu untersuchen. Da Mäuse mit vollständigem PDK1-Verlust nicht lebensfähig sind, wurden PDK1-hypomorphe Mäuse ($pdk1^{hm}$) mit einer PDK1-Restaktivität von 10-25% untersucht. Das Körpergewicht der PDK1-hypomorphen Mäuse war signifikant geringer als dasjenige der Wildtyp-Tiere, die Futter- und Flüssigkeitsaufnahme waren jedoch ähnlich hoch.

Ussing-Kammer-Experimente zeigten einen reduzierten elektrogenen Transport für Glukose sowie für die Aminosäuren Phenylalanin, Cystein, Glutamin, Prolin, Leucin und Tryptophan in $pdk1^{hm}$ -Mäusen verglichen mit $pdk1^{wt}$ Mäusen. Analog dazu war der elektrogene Transport im isolierten proximalen Tubulus für Glucose sowie für Phenylalanin, Glutamin und Prolin vermindert. Unter intraperitonealer Beladung mit 3 g/kg Glucose kam es zu einer Glukosurie in $pdk1^{hm}$ –Mäusen, trotz ähnlich hoher Glukose-Spiegel wie in Wildtyp-Mäusen. Die Urinausscheidung von Prolin, Valin, Guanidinoacetat, Methionin, Phenylalanin, Citrullin, Glutamine/Glutamat und Tryptophan war in $pdk1^{hm}$ –Mäusen signifikant höher als in Widltyp-Mäusen. Im Western Blot von renalen Bürstensaum-Membranen von $pdk1^{hm}$ Mäusen war die Expression der Na^+-abhängigen neutralen Aminosäuren-transporter B^0AT1 (SLC6A19), des Glutamat-Transporters EAAC1/EAAT3 (SLC1A1) sowie des Transporter für kationische Aminosäuren und Cystin $b^{0,+}AT$ (SLC7A9) erniedrigt, die Expression des Na^+-Prolin Cotransporters SIT (SLC6A20) erhöht. Zusammenfassend konnte gezeigt werden, dass eine Reduktion der PDK1 zu einer verminderten intestinalen Absorption sowie renalen Reabsorption von Glukose und Aminosäuren führte, was auf einen bisher nicht bekannten Regulationsweg hinweist. Der kombinierte intestinale und renale Verlust von

Aminosäuren und Glukose könnte zum Minderwuchs der PDK1 hypomorphen Mäuse beitragen.

In weiteren Untersuchungen wurde die transepitheliale Potentialdifferenz (V_{te}) und der amilorid-hemmbare Kurzschluss-Strom (I_{amil}) im Kolon von SGK1 defizienten ($sgk1^{-/-}$) und Wildtyp-Mäusen untersucht. Sowohl V_{te} und I_{amil} waren in unbehandelten $sgk1^{-/-}$-Mäusen unter Kontrolldiät signifikant höher als in $sgk1^{+/+}$ Mäusen. Eine 7-tägige Behandlung mit einer Niedrigsalz-Diät erhöhte V_{te} und I_{amil} in beiden Genotypen, konnte den Unterschied in V_{te} und I_{amil} zwischen $sgk1^{-/-}$- und Wildtyp-Mäusen jedoch nicht aufheben. Plasma-Aldosteron-Spiegel waren in $sgk1^{-/-}$ -Mäusen sowohl unter Kontroll- wie Niedrigsalz-Diät signifikant höher. Behandlung mit Dexamethason (10µg/g) oder mit DOCA (1.5mg/ die) erhöhte V_{te} und I_{amil} nur in Wildtyp-Mäusen, jedoch nicht in $sgk1^{-/-}$ Mäusen. Unter Behandlung mit Dexamethason oder DOCA waren sowohl V_{te} als auch I_{amil} in $sgk1^{-/-}$ und Wildtyp-Mäusen ähnlich hoch. Die Ergebnisse zeigen zusammengenommen, dass ein Fehlen der SGK1 nicht die Aktivität und Regulation des ENaCs im Kolon unterbricht.

Zuletzt wurde die funktionelle Bedeutung der SGK3 in der Regulation des intestinalen Transports untersucht. Zuvor hatten Experimente im Xenopus-Expressionssystem gezeigt, dass die SGK3 eine Vielzahl von Transportern beeinflussen kann, u.a. den Glucosetransporters SGLT1. In SGK3-defizienten Mäusen ($sgk3^{-/-}$) zeigte sich verglichen mit Wildtyp-Mäusen eine höhere Futteraufnahme und ein höheres Stuhltrockengewicht. Die Glukose-induzierten Ströme (I_{glc}) waren im Jejunum signifikant geringer in $sgk3^{-/-}$ -Mäusen als in Wildtyp-Tieren. Der Nüchtern-Blutzucker war in $sgk3^{-/-}$ -Mäusen signifikant niedriger. Der intestinale elektrogene Transport von Phenylalanin, Cystein, Glutamin und Prolin ware hingegen zwischen $sgk3^{-/-}$ und Wildtyp-Mäusen nicht verschieden. Daher kann gefolgert warden, dass die SGK3 für die intestinale Na^+-gekoppelte Glukoseaufnahme erforderlich ist und dass eine verminderte Glukoseaufnahme für die Wachstumsretardierung und die niedrigen Blutzuckerwerte verantwortlich sein könnte, was zu einer kompensatorischen Zunahme der Futteraufnahme führen könnte.

7 Abbreviations

AMP	Adenosine Mono Phosphate
ADP	Adenosine Di Phosphate
ATP	Adenosine Tri Phosphate
µA	Micro Amper
µg	Micro gram
µl	Micro liter
µM	Micro molar
Bw	Body weight
BSA	Bovine serum albumin
cAMP	Cyclic Adenosine Mono phosphate
Camp	Cyclic Adenosine Mono phosphate
cDNA	complementary Deoxyribonucleic Acid
cRNA	complementary Ribonucleic Acid
DMSO	Dimethylsulfoxide
DNA	Deoxyribonucleic Acid
dNTP	Deoxyribo-Nucleotidetriphosphate
DEX	Dexamethasone
DOCA	desoxycorticosterone acetate
dUTP	deoxyuridine-triphosphate
EDTA	Ethylenediamine tetraacetic acid
ELISA	Enzyme-Linked Immunoabsorbent Assay
ENaC	Epithelial sodium channel
GLUT1 / 4	Glucose Transporter isoforms 1 /4
HEPES	N-(2-Hydroxyethyl) piperazine-N-(2-ethanesulfonic acid)
IGF1	Insulin-like growth factor 1
I_{sc}	Shortcircuit current
Nedd4-2	Neuronal cell expressed developmentally down regulated 4-2
NHE3	The Na/H-exchanger isoform 3
NMDG	N-methyl-D-glucamine
^{o}C	Degree(s) Celsius (centigrade)
PBS	Phosphate Buffered Saline
PCR	Polymerase chain reaction

PDK1	Phosphoinositide-dependent kinase isoform 1
PFA	Paraformaldehyd
PI3K	Phosphatidyl-inositol-3-kinase
PKA	Protein Kinase A
PKB (Akt)	Protein Kinase B; oncogene from Akt mouse
PKC	Protein Kinase C
kDa	Kilo Dalton
Ringer	Buffer Solution
ROMK	Renal outer medullary K^+ channel
R_{te}	Transepithelial resistance
SE	Standard Error
SGKs	Serum and Glucocorticoid inducible protein Kinase isoforms
SGLT	Sodium-glucose cotransporter
TRIS	Tris (hydroxymethyl) aminomethane
TUNEL	Terminal uridine deoxynucleotidyl transferase
V_{te}	transepithelial potential difference

8 References

Reference List

1. Leevers,S.J., Vanhaesebroeck,B., and Waterfield,M.D. (1999) *Curr.Opin.Cell Biol.* **11**, 219-225.

2. Firestone,G.L., Giampaolo,J.R., and O'Keeffe,B.A. (2003) *Cell Physiol Biochem.* **13**, 1-12.

3. Kobayashi,T. and Cohen,P. (1999) *Biochem.J.* **339 (Pt 2)**, 319-328.

4. Lang,F. and Cohen,P. (2001) *Sci.STKE.* **2001**, RE17.

5. Perrotti,N., He,R.A., Phillips,S.A., Haft,C.R., and Taylor,S.I. (2001) *Journal of Biological Chemistry* **276**, 9406-9412.

6. Pearce,D. (2003) *Cell Physiol Biochem*. **13**, 13-20.

7. Lang,F., Bohmer,C., Palmada,M., Seebohm,G., Strutz-Seebohm,N., and Vallon,V. (2006) *Physiol Rev.* **86**, 1151-1178.

8. Brown,G.K. (2000) *J.Inherit.Metab Dis.* **23**, 237-246.

9. Scheepers,A., Joost,H.G., and Schurmann,A. (2004) *JPEN J.Parenter.Enteral Nutr.* **28**, 364-371.

10. Debonneville,C., Flores,S.Y., Kamynina,E., Plant,P.J., Tauxe,C., Thomas,M.A., Munster,C., Chraibi,A., Pratt,J.H., Horisberger,J.D., Pearce,D., Loffing,J., and Staub,O. (2001) *EMBO J* **20**, 7052-7059.

11. Coffer,P.J., Jin,J., and Woodgett,J.R. (1998) *Biochem J* **335 (Pt 1)**, 1-13.

12. Coffer,P.J. and Woodgett,J.R. (1991) *Eur.J Biochem* **201**, 475-481.

13. Dieter,M., Palmada,M., Rajamanickam,J., Aydin,A., Busjahn,A., Boehmer,C., Luft,F.C., and Lang,F. (2004) *Obes.Res.* **12**, 862-870.

14. Kobayashi,T., Deak,M., Morrice,N., and Cohen,P. (1999) *Biochem J.* **344**, 189-197.

15. Lang,F., Henke,G., Embark,H.M., Waldegger,S., Palmada,M., Bohmer,C., and Vallon,V. (2003) *Cell Physiol Biochem.* **13**, 41-50.

16. Loffing,J., Flores,S.Y., and Staub,O. (2005) *Annu.Rev Physiol*.

17. Bohmer,C., Philippin,M., Rajamanickam,J., Mack,A., Broer,S., Palmada,M., and Lang,F. (2004) *Biochem Biophys Res Commun.* **324**, 1242-1248.

18. Boehmer,C., Henke,G., Schniepp,R., Palmada,M., Rothstein,J.D., Broer,S., and Lang,F. (2003) *J Neurochem.* **86**, 1181-1188.

19. Schniepp,R., Kohler,K., Ladewig,T., Guenther,E., Henke,G., Palmada,M., Boehmer,C., Rothstein,J.D., Broer,S., and Lang,F. (2004) *Invest Ophthalmol.Vis.Sci* **45**, 1442-1449.

20. Boehmer,C., Okur,F., Setiawan,I., Broer,S., and Lang,F. (2003) *Biochem.Biophys.Res.Commun.* **306**, 156-162.

21. Boehmer,C., Palmada,M., Rajamanickam,J., Schniepp,R., Amara,S., and Lang,F. (2006) *J.Neurochem.* **97**, 911-921.

22. Alessi,D.R., Andjelkovic,M., Caudwell,B., Cron,P., Morrice,N., Cohen,P., and Hemmings,B.A. (1996) *EMBO J* **15**, 6541-6551.

23. Alessi,D.R. and Cohen,P. (1998) *Curr.Opin.Genet.Dev.* **8**, 55-62.

24. Divecha,N., Banfic,H., and Irvine,R.F. (1991) *EMBO J.* **10**, 3207-3214.

25. Gamper,N., Fillon,S., Feng,Y., Friedrich,B., Lang,P.A., Henke,G., Huber,S.M., Kobayashi,T., Cohen,P., and Lang,F. (2002) *Pflugers Arch.* **445**, 60-66.

26. Kotani,K., Yonezawa,K., Hara,K., Ueda,H., Kitamura,Y., Sakaue,H., Ando,A., Chavanieu,A., Calas,B., Grigorescu,F., and . (1994) *EMBO J.* **13**, 2313-2321.

27. Park,J., Leong,M.L., Buse,P., Maiyar,A.C., Firestone,G.L., and Hemmings,B.A. (1999) *EMBO J.* **18**, 3024-3033.

28. Gamper,N., Fillon,S., Huber,S.M., Feng,Y., Kobayashi,T., Cohen,P., and Lang,F. (2002) *Pflugers Arch.* **443**, 625-634.

29. Alessi,D.R. (2001) *Biochem.Soc.Trans.* **29**, 1-14.

30. Brunet,A., Bonni,A., Zigmond,M.J., Lin,M.Z., Juo,P., Hu,L.S., Anderson,M.J., Arden,K.C., Blenis,J., and Greenberg,M.E. (1999) *Cell* **96**, 857-868.

31. Liu,D., Yang,X., and Songyang,Z. (2000) *Curr.Biol.* **10**, 1233-1236.

32. Romashkova,J.A. and Makarov,S.S. (1999) *Nature* **401**, 86-90.

33. Segal,R.A. (2003) *Annu.Rev.Neurosci.* **26**, 299-330.

34. Grandage,V.L., Gale,R.E., Linch,D.C., and Khwaja,A. (2005) *Leukemia* **19**, 586-594.

35. Tapodi,A., Debreceni,B., Hanto,K., Bognar,Z., Wittmann,I., Gallyas,F., Jr., Varbiro,G., and Sumegi,B. (2005) *J.Biol.Chem.* **280**, 35767-35775.

36. Jung,F., Haendeler,J., Goebel,C., Zeiher,A.M., and Dimmeler,S. (2000) *Cardiovasc.Res.* **48**, 148-157.

37. Kim,A.H., Khursigara,G., Sun,X., Franke,T.F., and Chao,M.V. (2001) *Mol.Cell Biol.* **21**, 893-901.

38. Stokoe,D. (2005) *Expert.Rev.Mol.Med.* **7**, 1-22.

39. Zhu,Q.S., Xia,L., Mills,G.B., Lowell,C.A., Touw,I.P., and Corey,S.J. (2006) *Blood* **107**, 1847-1856.

40. Connor,K.M., Subbaram,S., Regan,K.J., Nelson,K.K., Mazurkiewicz,J.E., Bartholomew,P.J., Aplin,A.E., Tai,Y.T., Aguirre-Ghiso,J., Flores,S.C., and Melendez,J.A. (2005) *J.Biol.Chem.* **280**, 16916-16924.

41. Lawlor,M.A., Mora,A., Ashby,P.R., Williams,M.R., Murray-Tait,V., Malone,L., Prescott,A.R., Lucocq,J.M., and Alessi,D.R. (2002) *EMBO J* **21**, 3728-3738.

42. Haussinger,D. and Lang,F. (1992) *Trends Pharmacol.Sci.* **13**, 371-373.

43. Haussinger,D., Lang,F., and Gerok,W. (1994) *Am.J.Physiol* **267**, E343-E355.

44. Lang,F. and Rehwald,W. (1992) *Physiol Rev* **72**, 1-32.

45. Broer,S. (2002) *Pflugers Arch.* **444**, 457-466.

46. Palacin,M., Nunes,V., Font-Llitjos,M., Jimenez-Vidal,M., Fort,J., Gasol,E., Pineda,M., Feliubadalo,L., Chillaron,J., and Zorzano,A. (2005) *Physiology.(Bethesda.)* **20**, 112-124.

47. Verrey,F., Ristic,Z., Romeo,E., Ramadan,T., Makrides,V., Dave,M.H., Wagner,C.A., and Camargo,S.M. (2005) *Annu.Rev.Physiol* **67**, 557-572.

48. Broer,A., Klingel,K., Kowalczuk,S., Rasko,J.E., Cavanaugh,J., and Broer,S. (2004) *J.Biol.Chem.* **279**, 24467-24476.

49. Kowalczuk,S., Broer,A., Munzinger,M., Tietze,N., Klingel,K., and Broer,S. (2005) *Biochem.J.* **386**, 417-422.

50. Romeo,E., Dave,M.H., Bacic,D., Ristic,Z., Camargo,S.M., Loffing,J., Wagner,C.A., and Verrey,F. (2006) *Am.J.Physiol Renal Physiol* **290**, F376-F383.

51. Kleta,R., Romeo,E., Ristic,Z., Ohura,T., Stuart,C., Arcos-Burgos,M., Dave,M.H., Wagner,C.A., Camargo,S.R., Inoue,S., Matsuura,N., Helip-Wooley,A., Bockenhauer,D., Warth,R., Bernardini,I., Visser,G., Eggermann,T., Lee,P., Chairoungdua,A., Jutabha,P., Babu,E., Nilwarangkoon,S., Anzai,N., Kanai,Y., Verrey,F., Gahl,W.A., and Koizumi,A. (2004) *Nat.Genet.* **36**, 999-1002.

52. Seow,H.F., Broer,S., Broer,A., Bailey,C.G., Potter,S.J., Cavanaugh,J.A., and Rasko,J.E. (2004) *Nat.Genet.* **36**, 1003-1007.

53. Wagner,C.A., Lang,F., and Broer,S. (2001) *Am.J.Physiol Cell Physiol* **281**, C1077-C1093.

54. Webster,M.K., Goya,L., and Firestone,G.L. (1993) *J.Biol.Chem.* **268**, 11482-11485.

55. Webster,M.K., Goya,L., Ge,Y., Maiyar,A.C., and Firestone,G.L. (1993) *Mol.Cell Biol.* **13**, 2031-2040.

56. Dai,F., Yu,L., He,H., Zhao,Y., Yang,J., Zhang,X., and Zhao,S. (1999) *Genomics*

62, 95-97.

57. McCormick,J.A., Feng,Y., Dawson,K., Behne,M.J., Yu,B., Wang,J., Wyatt,A.W., Henke,G., Grahammer,F., Mauro,T.M., Lang,F., and Pearce,D. (2004) *Mol.Biol.Cell* **15**, 4278-4288.

58. Chen,S.Y., Bhargava,A., Mastroberardino,L., Meijer,O.C., Wang,J., Buse,P., Firestone,G.L., Verrey,F., and Pearce,D. (1999) *Proc.Natl.Acad.Sci.U.S.A* **96**, 2514-2519.

59. Naray-Fejes-Toth,A., Canessa,C., Cleaveland,E.S., Aldrich,G., and Fejes-Toth,G. (1999) *J.Biol.Chem.* **274**, 16973-16978.

60. Shigaev,A., Asher,C., Latter,H., Garty,H., and Reuveny,E. (2000) *Am.J.Physiol Renal Physiol* **278**, F613-F619.

61. Waldegger,S., Barth,P., Raber,G., and Lang,F. (1997) *Proc.Natl.Acad.Sci.U.S.A* **94**, 4440-4445.

62. Blazer-Yost,B.L., Liu,X., and Helman,S.I. (1998) *Am J Physiol* **274**, C1373-C1379.

63. Blazer-Yost,B.L., Paunescu,T.G., Helman,S.I., Lee,K.D., and Vlahos,C.J. (1999) *Am J Physiol* **277**, C531-C536.

64. Wulff,P., Vallon,V., Huang,D.Y., Volkl,H., Yu,F., Richter,K., Jansen,M., Schlunz,M., Klingel,K., Loffing,J., Kauselmann,G., Bosl,M.R., Lang,F., and Kuhl,D. (2002) *J Clin Invest* **110**, 1263-1268.

65. Huang,D.Y., Wulff,P., Volkl,H., Loffing,J., Richter,K., Kuhl,D., Lang,F., and Vallon,V. (2004) *J Am Soc.Nephrol* **15**, 885-891.

66. Alvarez de la Rosa,D., Zhang,P., Naray-Fejes-Toth,A., Fejes-Toth,G., and Canessa,C.M. (1999) *J.Biol.Chem.* **274**, 37834-37839.

67. Böhmer,C., Wagner,C.A., Beck,S., Moschen,I., Melzig,J., Werner,A., Lin,J.T., Lang,F., and Wehner,F. (2000) *Cell Physiol Biochem* **10**, 187-194.

68. Lang,F., Klingel,K., Wagner,C.A., Stegen,C., Warntges,S., Friedrich,B., Lanzendorfer,M., Melzig,J., Moschen,I., Steuer,S., Waldegger,S., Sauter,M., Paulmichl,M., Gerke,V., Risler,T., Gamba,G., Capasso,G., Kandolf,R., Hebert,S.C., Massry,S.G., and Broer,S. (2000) *Proc.Natl.Acad.Sci.U.S.A* **97**, 8157-8162.

69. Loffing,J., Zecevic,M., Feraille,E., Kaissling,B., Asher,C., Rossier,B.C., Firestone,G.L., Pearce,D., and Verrey,F. (2001) *Am.J.Physiol Renal Physiol* **280**, F675-F682.

70. Wagner,C.A., Ott,M., Klingel,K., Beck,S., Melzig,J., Friedrich,B., Wild,K.N., Broer,S., Moschen,I., Albers,A., Waldegger,S., Tummler,B., Egan,M.E., Geibel,J.P., Kandolf,R., and Lang,F. (2001) *Cell Physiol Biochem* **11**, 209-218.

71. Helms,M.N., Fejes-Toth,G., and Naray-Fejes-Toth,A. (2003) *Am J Physiol Renal*

Physiol **284**, F480-F487.

72. Naray-Fejes-Toth,A., Helms,M.N., Stokes,J.B., and Fejes-Toth,G. (2004) *Mol Cell Endocrinol.* **217**, 197-202.

73. Alvarez,d.l.R. and Canessa,C.M. (2003) *Am J Physiol Cell Physiol* **284**, C404-C414.

74. Faletti,C.J., Perrotti,N., Taylor,S.I., and Blazer-Yost,B.L. (2002) *Am J Physiol Cell Physiol* **282**, C494-C500.

75. Hummler,E., Barker,P., Gatzy,J., Beermann,F., Verdumo,C., Schmidt,A., Boucher,R., and Rossier,B.C. (1996) *Nat.Genet.* **12**, 325-328.

76. Hummler,E., Barker,P., Talbot,C., Wang,Q., Verdumo,C., Grubb,B., Gatzy,J., Burnier,M., Horisberger,J.D., Beermann,F., Boucher,R., and Rossier,B.C. (1997) *Proc.Natl.Acad.Sci.U.S.A* **94**, 11710-11715.

77. McDonald,F.J., Yang,B., Hrstka,R.F., Drummond,H.A., Tarr,D.E., McCray,P.B., Jr., Stokes,J.B., Welsh,M.J., and Williamson,R.A. (1999) *Proc.Natl.Acad.Sci.U.S.A* **96**, 1727-1731.

78. Barker,P.M., Nguyen,M.S., Gatzy,J.T., Grubb,B., Norman,H., Hummler,E., Rossier,B., Boucher,R.C., and Koller,B. (1998) *J Clin.Invest* **102**, 1634-1640.

79. Berger,S., Bleich,M., Schmid,W., Cole,T.J., Peters,J., Watanabe,H., Kriz,W., Warth,R., Greger,R., and Schutz,G. (1998) *Proc.Natl.Acad.Sci.U.S.A* **95**, 9424-9429.

80. Coric,T., Hernandez,N., Alvarez,d.l.R., Shao,D., Wang,T., and Canessa,C.M. (2004) *Am.J.Physiol Gastrointest.Liver Physiol* **286**, G663-G670.

81. Bhargava,A., Fullerton,M.J., Myles,K., Purdy,T.M., Funder,J.W., Pearce,D., and Cole,T.J. (2001) *Endocrinology* **142**, 1587-1594.

82. Brennan,F.E. and Fuller,P.J. (2000) *Mol.Cell Endocrinol.* **166**, 129-136.

83. Williams,M.R., Arthur,J.S., Balendran,A., van der,K.J., Poli,V., Cohen,P., and Alessi,D.R. (2000) *Curr.Biol.* **10**, 439-448.

84. McCormick,J.A., Feng,Y., Dawson,K., Behne,M.J., Yu,B., Wang,J., Wyatt,A.W., Henke,G., Grahammer,F., Mauro,T.M., Lang,F., and Pearce,D. (2004) *Mol Biol Cell* **15**, 4278-4288.

85. Mall,M., Bleich,M., Greger,R., Schreiber,R., and Kunzelmann,K. (1998) *J.Clin.Invest* **102**, 15-21.

86. Schulz-Baldes,A., Berger,S., Grahammer,F., Warth,R., Goldschmidt,I., Peters,J., Schutz,G., Greger,R., and Bleich,M. (2001) *Pflugers Arch.* **443**, 297-305.

87. Rexhepaj,R., Artunc,F., Grahammer,F., Nasir,O., Sandu,C., Friedrich,B., Kuhl,D., and Lang,F. (2006) *Pflugers Archiv European Journal of Physiology* **453**, 97-105.

88. Vallon,V., Grahammer,F., Volkl,H., Sandu,C.D., Richter,K., Rexhepaj,R., Gerlach,U., Rong,Q., Pfeifer,K., and Lang,F. (2005) *Proc Natl.Acad.Sci U.S.A* **102**, 17864-17869.

89. Burg,M., Grantham,J., Abramow,M., and Orloff,J. (1966) *Am J Physiol* **210**, 1293-1298.

90. Greger,R. (1981) *Pflugers Arch* **390**, 30-37.

91. Greger,R. and Hampel,W. (1981) *Pflugers Arch* **389**, 175-176.

92. Vallon,V., Grahammer,F., Richter,K., Bleich,M., Lang,F., Barhanin,J., Volkl,H., and Warth,R. (2001) *J Am Soc Nephrol* **12**, 2003-2011.

93. Biber,J., Stieger,B., Haase,W., and Murer,H. (1981) *Biochim.Biophys Acta* **647**, 169-176.

94. Grahammer,F., Henke,G., Sandu,C., Rexhepaj,R., Hussain,A., Friedrich,B., Risler,T., Metzger,M., Just,L., Skutella,T., Wulff,P., Kuhl,D., and Lang,F. (2006) *Am.J.Physiol Gastrointest.Liver Physiol* **290**, G1114-G1123.

95. Artunc,F., Amann,K., Nasir,O., Friedrich,B., Sandulache,D., Jahovic,N., Risler,T., Vallon,V., Wulff,P., Kuhl,D., and Lang,F. (2006) *J.Mol.Med.* **84**, 737-746.

96. Ganz,M.B., Boyarsky,G., Sterzel,R.B., and Boron,W.F. (1989) *Nature* **337**, 648-651.

97. Roos,A. and Boron,W.F. (1981) *Physiol Rev.* **61**, 296-434.

98. Boyarsky,G., Ganz,M.B., Sterzel,R.B., and Boron,W.F. (1988) *Am.J.Physiol* **255**, C857-C869.

99. Hirayama,B.A., Lostao,M.P., Panayotova-Heiermann,M., Loo,D.D., Turk,E., and Wright,E.M. (1996) *Am.J.Physiol* **270**, G919-G926.

100. Horiba,N., Masuda,S., Takeuchi,A., Takeuchi,D., Okuda,M., and Inui,K. (2003) *J.Biol.Chem.* **278**, 14669-14676.

101. Boehmer,C., Rajamanickam,J., Schniepp,R., Kohler,K., Wulff,P., Kuhl,D., Palmada,M., and Lang,F. (2005) *Biochem Biophys Res Commun.* **329**, 738-742.

102. Embark,H.M., Bohmer,C., Palmada,M., Rajamanickam,J., Wyatt,A.W., Wallisch,S., Capasso,G., Waldegger,P., Seyberth,H.W., Waldegger,S., and Lang,F. (2004) *Kidney Int* **66**, 1918-1925.

103. Lang,F., Messner,G., and Rehwald,W. (1986) *Am J Physiol* **250**, F953-F962.

104. Schultz,S.G. (1981) *Am J Physiol* **241**, F579-F590.

105. Henke,G., Maier,G., Wallisch,S., Boehmer,C., and Lang,F. (2004) *J.Cell Physiol* **199**, 194-199.

106. Setiawan,I., Henke,G., Feng,Y., Bohmer,C., Vasilets,L.A., Schwarz,W., and Lang,F. (2002) *Pflugers Arch.* **444**, 426-431.

107. Zecevic,M., Heitzmann,D., Camargo,S.M., and Verrey,F. (2004) *Pflugers Arch* **448**, 29-35.

108. Wärntges,S., Klingel,K., Weigert,C., Fillon,S., Buck,M., Schleicher,E., Rodemann,H.P., Knabbe,C., Kandolf,R., and Lang,F. (2002) *Cell Physiol Biochem* **12**, 135-142.

109. Embark,H.M., Bohmer,C., Vallon,V., Luft,F., and Lang,F. (2003) *Pflugers Arch* **445**, 601-606.

110. Palmada,M., Embark,H.M., Yun,C., Böhmer,C., and Lang,F. (2003) *Biochem.Biophys.Res.Commun.* **311**, 629-634.

111. Yoo,D., Kim,B.Y., Campo,C., Nance,L., King,A., Maouyo,D., and Welling,P.A. (2003) *J Biol Chem.* **278**, 23066-23075.

112. Yun,C.C., Palmada,M., Embark,H.M., Fedorenko,O., Feng,Y., Henke,G., Setiawan,I., Boehmer,C., Weinman,E.J., Sandrasagra,S., Korbmacher,C., Cohen,P., Pearce,D., and Lang,F. (2002) *J Am.Soc.Nephrol.* **13**, 2823-2830.

113. Embark,H.M., Setiawan,I., Poppendieck,S., van de Graaf,S.F., Boehmer,C., Palmada,M., Wieder,T., Gerstberger,R., Cohen,P., Yun,C.C., Bindels,R.J., and Lang,F. (2004) *Cell Physiol Biochem* **14**, 203-212.

114. Palmada,M., Poppendieck,S., Embark,H.M., van de Graaf,S.F., Boehmer,C., Bindels,R.J., and Lang,F. (2005) *Cell Physiol Biochem* **15**, 175-182.

115. Wang,J., Barbry,P., Maiyar,A.C., Rozansky,D.J., Bhargava,A., Leong,M., Firestone,G.L., and Pearce,D. (2001) *Am.J.Physiol Renal Physiol* **280**, F303-F313.

116. Shojaiefard,M., Christie,D.L., and Lang,F. (2005) *Biochem Biophys Res Commun.* **334**, 742-746.

117. Persky,A.M., Brazeau,G.A., and Hochhaus,G. (2003) *Clin.Pharmacokinet.* **42**, 557-574.

118. Ishikawa,Y., Eguchi,T., and Ishida,H. (1997) *Biochim.Biophys Acta* **1357**, 306-318.

119. Lane,R.H., Dvorak,B., MacLennan,N.K., Dvorakova,K., Halpern,M.D., Pham,T.D., and Philipps,A.F. (2002) *Am J Physiol Regul.Integr.Comp Physiol* **283**, R1450-R1460.

120. Sandu,C., Rexhepaj,R., Grahammer,F., McCormick,J.A., Henke,G., Palmada,M., Nammi,S., Lang,U., Metzger,M., Just,L., Skutella,T., Dawson,K., Wang,J., Pearce,D., and Lang,F. (2005) *Pflugers Arch* **451**, 437-444.

121. Bae,S.S., Cho,H., Mu,J., and Birnbaum,M.J. (2003) *J Biol Chem.* **278**, 49530-49536.

122. Foran,P.G., Fletcher,L.M., Oatey,P.B., Mohammed,N., Dolly,J.O., and Tavare,J.M. (1999) *J Biol Chem.* **274**, 28087-28095.

123. Jiang,Z.Y., Zhou,Q.L., Coleman,K.A., Chouinard,M., Boese,Q., and Czech,M.P. (2003) *Proc Natl.Acad.Sci U.S.A* **100**, 7569-7574.

124. Kohn,A.D., Summers,S.A., Birnbaum,M.J., and Roth,R.A. (1996) *J Biol Chem.* **271**, 31372-31378.

125. McCurdy,C.E. and Cartee,G.D. (2005) *Diabetes* **54**, 1349-1356.

126. Rathmell,J.C., Fox,C.J., Plas,D.R., Hammerman,P.S., Cinalli,R.M., and Thompson,C.B. (2003) *Mol Cell Biol* **23**, 7315-7328.

127. Taha,C., Liu,Z., Jin,J., Al Hasani,H., Sonenberg,N., and Klip,A. (1999) *J Biol Chem.* **274**, 33085-33091.

128. Palmada,M., Boehmer,C., Akel,A., Rajamanickam,J., Jeyaraj,S., Keller,K., and Lang,F. (2006) *Diabetes* **55**, 421-427.

129. Lang,F., Busch,G.L., Ritter,M., Volkl,H., Waldegger,S., Gulbins,E., and Haussinger,D. (1998) *Physiol Rev* **78**, 247-306.

130. Awrich,A.E., Stackhouse,W.J., Cantrell,J.E., Patterson,J.H., and Rudman,D. (1975) *J Pediatr.* **87**, 731-738.

131. Boulos,M., Boulat,O., Guignard,J.P., and Matthieu,J.M. (2001) *Rev Med Suisse Romande* **121**, 205-209.

132. Yeung,M.Y. and Smyth,J.P. (2003) *Biol.Neonate* **84**, 1-23.

133. Fellman,V., Rapola,J., Pihko,H., Varilo,T., and Raivio,K.O. (1998) *Lancet* **351**, 490-493.

134. Simell,O., Perheentupa,J., Rapola,J., Visakorpi,J.K., and Eskelin,L.E. (1975) *Am.J.Med.* **59**, 229-240.

135. Palmada,M., Speil,A., Jeyaraj,S., Bohmer,C., and Lang,F. (2005) *Biochem.Biophys.Res.Commun.* **331**, 272-277.

136. Font,M.A., Feliubadalo,L., Estivill,X., Nunes,V., Golomb,E., Kreiss,Y., Pras,E., Bisceglia,L., d'Adamo,A.P., Zelante,L., Gasparini,P., Bassi,M.T., George,A.L., Jr., Manzoni,M., Riboni,M., Ballabio,A., Borsani,G., Reig,N., Fernandez,E., Zorzano,A., Bertran,J., and Palacin,M. (2001) *Hum.Mol.Genet.* **10**, 305-316.

137. Seow,H.F., Broer,S., Broer,A., Bailey,C.G., Potter,S.J., Cavanaugh,J.A., and Rasko,J.E. (2004) *Nat.Genet.* **36**, 1003-1007.

138. Pineda,M., Wagner,C.A., Broer,A., Stehberger,P.A., Kaltenbach,S., Gelpi,J.L., Martin,D.R., Zorzano,A., Palacin,M., Lang,F., and Broer,S. (2004) *Biochem.J.* **377**, 665-674.

139. Verrey,F., Summa,V., Heitzmann,D., Mordasini,D., Vandewalle,A., Feraille,E., and Zecevic,M. (2003) *Ann.N.Y.Acad.Sci.* **986**, 554-561.

140. Palmada,M., Boehmer,C., Akel,A., Rajamanickam,J., Jeyaraj,S., Keller,K., and

Lang,F. (2006) *Diabetes* **55**, 421-427.

141. Boehmer,C., Embark,H.M., Bauer,A., Palmada,M., Yun,C.H., Weinman,E.J., Endou,H., Cohen,P., Lahme,S., Bichler,K.H., and Lang,F. (2004) *Biochem.Biophys.Res.Commun.* **313**, 998-1003.

142. Peghini,P., Janzen,J., and Stoffel,W. (1997) *EMBO J.* **16**, 3822-3832.

143. Hill,M.M., Clark,S.F., Tucker,D.F., Birnbaum,M.J., James,D.E., and Macaulay,S.L. (1999) *Mol.Cell Biol.* **19**, 7771-7781.

144. Kristiansen,S., Nielsen,J.N., Bourgoin,S., Klip,A., Franco,M., and Richter,E.A. (2001) *Am.J.Physiol Endocrinol.Metab* **281**, E608-E618.

145. von der Crone,S., Deppe,C., Barthel,A., Sasson,S., Joost,H.G., and Schurmann,A. (2000) *Eur.J.Cell Biol.* **79**, 943-949.

146. Alliston,T.N., Maiyar,A.C., Buse,P., Firestone,G.L., and Richards,J.S. (1997) *Mol.Endocrinol.* **11**, 1934-1949.

147. Alliston,T.N., Gonzalez-Robayna,I.J., Buse,P., Firestone,G.L., and Richards,J.S. (2000) *Endocrinology* **141**, 385-395.

148. Gonzalez-Robayna,I.J., Falender,A.E., Ochsner,S., Firestone,G.L., and Richards,J.S. (2000) *Mol.Endocrinol.* **14**, 1283-1300.

149. Richards,J.S., Fitzpatrick,S.L., Clemens,J.W., Morris,J.K., Alliston,T., and Sirois,J. (1995) *Recent Prog.Horm.Res* **50**, 223-254.

150. Waldegger,S., Klingel,K., Barth,P., Sauter,M., Rfer,M.L., Kandolf,R., and Lang,F. (1999) *Gastroenterology* **116**, 1081-1088.

151. Alexander,A.N. and Carey,H.V. (1999) *Am J Physiol* **277**, G619-G625.

152. Chung,B.M., Wallace,L.E., Hardin,J.A., and Gall,D.G. (2002) *Can.J Physiol Pharmacol.* **80**, 872-878.

153. Wärntges,S., Friedrich,B., Henke,G., Duranton,C., Lang,P.A., Waldegger,S., Meyermann,R., Kuhl,D., Speckmann,E.J., Obermuller,N., Witzgall,R., Mack,A.F., Wagner,H.J., Wagner,A., Broer,S., and Lang,F. (2002) *Pflugers Arch.* **443**, 617-624.

154. Ullrich,S., Berchtold,S., Ranta,F., Seebohm,G., Henke,G., Lupescu,A., Mack,A.F., Chao,C.M., Su,J., Nitschke,R., Alexander,D., Friedrich,B., Wulff,P., Kuhl,D., and Lang,F. (2005) *Diabetes* **54**, 1090-1099.

155. Palmada,M., Embark,H.M., Wyatt,A.W., Bohmer,C., and Lang,F. (2003) *Biochem Biophys Res Commun.* **307**, 967-972.

156. Baltaev,R., Strutz-Seebohm,N., Korniychuk,G., Myssina,S., Lang,F., and Seebohm,G. (2005) *Pflugers Arch* **450**, 26-33.

157. Busjahn,A., Aydin,A., Uhlmann,R., Krasko,C., Bahring,S., Szelestei,T., Feng,Y.,

Dahm,S., Sharma,A.M., Luft,F.C., and Lang,F. (2002) *Hypertension* **40**, 256-260.

158. Alvarez,d.l.R., Paunescu,T.G., Els,W.J., Helman,S.I., and Canessa,C.M. (2004) *J Gen.Physiol* **124**, 395-407.

9 Publications

1: Rexhepaj R, Artunc F, Metzger M, Skutella T, Lang F.
PI3-kinase-dependent electrogenic intestinal transport of glucose and amino acids.
Pflugers Arch. 2007 Mar;453(6):863-70. Epub 2006 Oct 19.
PMID: 17051390 [PubMed - indexed for MEDLINE]

2: Sandu C, Artunc F, Grahammer F, Rotte A, Boini KM, Friedrich B, Sandulache D, Metzger M, Just L, Mack A, Skutella T, Rexhepaj R, Risler T, Wulff P, Kuhl D, Lang F.
Role of the serum and glucocorticoid inducible kinase SGK1 in glucocorticoid stimulation of gastric acid secretion.
Pflugers Arch. 2007 Dec;455(3):493-503. Epub 2007 Jul 6.
PMID: 17618452 [PubMed - in process]

3: Rexhepaj R, Grahammer F, Volkl H, Remy C, Wagner CA, Sandulache D, Artunc F, Henke G, Nammi S, Capasso G, Alessi DR, Lang F.
Reduced intestinal and renal amino acid transport in PDK1 hypomorphic mice.
FASEB J. 2006 Nov;20(13):2214-22.
PMID: 17077298 [PubMed - indexed for MEDLINE]

4: Rexhepaj R, Artunc F, Grahammer F, Nasir O, Sandu C, Friedrich B, Kuhl D, Lang F.
Related Articles, Links
SGK1 is not required for regulation of colonic ENaC activity.
Pflugers Arch. 2006 Oct;453(1):97-105. Epub 2006 Aug 8.
PMID: 16897044 [PubMed - indexed for MEDLINE]

5: Sandu C, Artunc F, Palmada M, Rexhepaj R, Grahammer F, Hussain A, Yun C, Alessi DR, Lang F.
Impaired intestinal NHE3 activity in the PDK1 hypomorphic mouse.
Am J Physiol Gastrointest Liver Physiol. 2006 Nov;291(5):G868-76. Epub 2006 Jul 6.
PMID: 16825708 [PubMed - indexed for MEDLINE]

6: Artunc F, Rexhepaj R, Volkl H, Grahammer F, Remy C, Sandulache D, Nasir O, Wagner CA, Alessi DR, Lang F.
Impaired intestinal and renal glucose transport in PDK-1 hypomorphic mice.
Am J Physiol Regul Integr Comp Physiol. 2006 Nov;291(5):R1533-8. Epub 2006 Jun 1.
PMID: 16741145 [PubMed - indexed for MEDLINE]

7: Grahammer F, Artunc F, Sandulache D, Rexhepaj R, Friedrich B, Risler T, McCormick JA, Dawson K, Wang J, Pearce D, Wulff P, Kuhl D, Lang F.
Renal function of gene-targeted mice lacking both SGK1 and SGK3.
Am J Physiol Regul Integr Comp Physiol. 2006 Apr;290(4):R945-50.
PMID: 16537821 [PubMed - indexed for MEDLINE]

8: Grahammer F, Henke G, Sandu C, Rexhepaj R, Hussain A, Friedrich B, Risler T, Metzger M, Just L, Skutella T, Wulff P, Kuhl D, Lang F.
Intestinal function of gene-targeted mice lacking serum- and glucocorticoid-inducible kinase 1.Am J Physiol Gastrointest Liver Physiol. 2006 Jun;290(6):G1114-23. Epub 2006 Jan 12.

9: Vallon V, Grahammer F, Volkl H, Sandu CD, Richter K, Rexhepaj R, Gerlach U, Rong Q, Pfeifer K, Lang F.
KCNQ1-dependent transport in renal and gastrointestinal epithelia.
Proc Natl Acad Sci U S A. 2005 Dec 6;102(49):17864-9. Epub 2005 Nov 28.
PMID: 16314573 [PubMed - indexed for MEDLINE]

10: Sandu C, Rexhepaj R, Grahammer F, McCormick JA, Henke G, Palmada M, Nammi S, Lang U, Metzger M, Just L, Skutella T, Dawson K, Wang J, Pearce D, Lang F.
Decreased intestinal glucose transport in the sgk3-knockout mouse.
Pflugers Arch. 2005 Dec;451(3):437-44. Epub 2005 Jun 22.
PMID: 15971077 [PubMed - indexed for MEDLINE]

11: Gebhardt, R.; Rexhepaj, R.; Fausel, M.;
Antioxidative und hepatoprotektive Wirkung von Flavonoiden aus Blattextrakten der Artischocke.
Z. Phytother. 20 (1999) 97-98

Seminars and conferences

Poster presentation

Poster presentation at the German Physiological Society Congress 2007 in Hannover, Germany.

(P11-L1-02)

PI3-Kinase-dependent electrogenic intestinal transport of glucose and amino acids

R. Rexhepaj[1], F. Artunc[1], M. Metzger[2], T. Skutella[2] and F. Lang[1].

Depts. of Physiology[1] and Anatomy[2], University of Tübingen

Poster presentation in the The Federation of European Physiological Societies and German Society of Physiology 2006 in Munich, Germany

(PW03P-14)

Amiloride-sensitive transepithelial potential in gene-targeted mice lacking the Serum and Glucocorticoid inducible kinase SGK1

R. Rexhepaj[1], F. Artunc1, F. Grahammer[1], C. Sandu1, C. Korbmacher[2], P. Wulff[3], D. Kuhl[4], F. Lang[1]

Dpts. of Physiology, Universities of Tübingen[1] and Erlangen[2], Dpt. of Clinical Neurobiology[3], University of Heidelberg, Dpt. of Biology, Chemistry, and Pharmacy[4], Free University Berlin

Poster presentation at the German Physiological Society Congress 2005, in Gottingen, Germany

(P09-3)

Gastrointestinal function in the kcnq1 knockout mouse

Rexhepaj R, Grahammer F, Sandu C, Vallon V, Pfeifer K, Lang F

Institute of Physiology University Tübingen, University of California San Diego, NIH Bethe

10 Acknowledgements

An erster Stelle gilt mein Dank Herrn Prof. Dr. med. Florian Lang, der durch die Vergabe des interessanten Themas mir eine wissenschaftliche Laufbahn in Deutschland eröffnete. Er war mir stets ein guter Ratgeber und Mentor.

Ganz herzlich möchte ich mich bei meinem Doktorvater Herrn Prof. Dr. rer. nat. Michael Duszenko bedanken.

Herrn Dr. med. Florian Grahammer danke ich für die Einführung und ausführliche Einarbeitung in die Methode der Ussing-Kammer sowie für die Korrektur meiner Doktorarbeit. Seine Hilfestellungen haben wesentlich zum Gelingen dieser Arbeit beigetragen haben. Ebenso danke ich Herrn Dr. med. G. Henke und Herrn Dr. med. Ferruh Artunç für die Zusammenarbeit und ihre Mithilfe bei Fragen und Problemen sowie die Diskussion der Ergebnisse.

Mein besonderer Dank gilt den Kollegen des Mäusephänotypisierungs-Labors Omaima Nasir, Diana Sandulache, Dr.Nermina Jahovic, Krishna Boini, Anand Rotte und besonders Teresa Ackermann, und Frau Faber sowie Ciprian Sandu, der leider von uns gegangen ist.

Den Mitarbeitern in der Werkstatt Peter Dürr und Karl Schöntag danke ich für die hervorragende technische Hilfe bei den Versuchsapparaturen sowie Faruk Subasic für die zuverlässige Pflege der Tiere.

Uwe Schüler möchte ich für Tips und Hilfe bei Computer-Problemen herzlich danken.

Herrn Dr. Horst Apfel, Frau Tanja Loch und Frau Lejla Subasic haben bei organisatorischen Angelegenheiten geholfen, wofür ich ihnen sehr dankbar bin.

Bedanken möchte ich mich auch bei PD Thomas Wieder, PD Stefan Huber, Prof. Susanne Ullrich, PD Christoph Böhmer, PD Monica Palmada, Dr. Peter Dreischer, PD Guiscard Seebohm, Dr. Ekaterina Shumilina, Dr. Evgenia Koutsouki, Mentor Sopjani und Dr. Mehrdad Ghashghaenia für die konstruktiven Diskussionen und für die menschliche Art im Umgang miteinander.

Nicht zuletzt gilt auch mein ganz besonderer Dank meiner Familie, allen voran meiner Frau Lina und meinen Kindern Arianita und Arianit sowie Brüdern, Freunden und Bekannten, die Erfolg und Misserfolg mit mir geteilt haben und mich moralisch unterstützt haben.

11 Akademische Lehrer

Chemie

Prof. Dr. Xhavit Ahmeti

Prof. Dr. Bedri Kamberi

Physik

Prof. Dr. Mustaf Bytyqi

Qualitative Analytische Chemie

Prof. Dr. Mustaf Bacaj

Mathematik

Prof. Dr. Ruzhdi Kastrati

Anorganische Chemie

Prof. Dr. Merita Shehdula

Physikalische Chemie

Prof. Dr. Sali Gashi

Prof. Dr. Mujë Rugova

Quantitative Analytische Chemie

Prof. Dr. Mandushe Berisha

Organische Chemie

Prof. Dr. Nexhat Daci

Prof. Dr. Osman Leci

Prof. Dr. Muhamet Bicaj

Stereochemie

Prof. Dr.Vuksan Kalaj

Chemische Technologie – Toxikologie

Prof. Dr. Selim Jusufi

Instrumentelle Analytische Chemie:

Prof. Dr. Rexhep Mehmeti

Biochemie:

Prof. Dr. Nevzat Aliaga

Prof. Dr. Myrtezan Ismaili

Prof. Dr. Dieter H. Wolf

Prof. Dr. Rolf Gebhardt

Prof. Dr. Michael Duszenko

Prof. Dr. Helmut Heinle

Physiologie und Elektrophysiologie:

Prof. Dr. S. Gruender

Prof. Dr. R. Guelch

Prof. Dr. H. Heinle

PD Dr. S. M. Huber

Prof. Dr. F. Lang

Prof. Dr. S. Ullrich

PD Dr. T. Wieder

12 Lebenslauf

Zur Person

Name: Rexhep Rexhepaj

Geburtsdatum: 22.01.1967

Geburtsort: Hereq - Gjakovë Kosova

Familienstand: Verheiratet -2 Kinder

Anschrift : Markus-Schleicher-Strasse 4 70565 Stuttgart

Telefon: 0711 / 5496 469

E-Mail: RRexhepaj@aol.com

rexhep.rexhepaj@unituebingen.de

Schulausbildung:

1973 – 1981 Grundschule in Gramoçel (Kosova)

1981 – 1985 Gymnasium in Gjakovë (Kosova)

Abitur- Juni 1985

Hochschulstudium:

1986 - 1991 An der Universität Prishtina – Kosova FSHMN

Fakultät für Mathematik und Naturwissenschaften

Studium der Chemie

Diplom- September 1991

In BRD:

September 1993 An der Universität Stuttgart – Gast Studium

04. - 05. 1995 Biochemie Praktikum Universität Stuttgart

Diplomarbeit:

1997 - 2002 Physiologisch-chemisches Institut der Eberhardt-Karls - Universität Tübingen

Thema: >>Untersuchungen zu antitumoriellen und antifibrotischen Wirkungen pflanzlicher Flavonoide in tierischen Zellkulturen<<.

Promotion : Ab Oktober 2003 Physiologisches Institut PHD- der Eberhardt-Karls - Universität Tübingen

Thema: >>Die Rolle von Serin-Threonin-Kinasen für epitheliale Transportvorgänge<<.